Valorization of Bio-oil from Maple Sawdust for Transportation Fuels

A thesis submitted to the College of Graduate Studies & Research in partial fulfillment of the requirements for the Master of Science Degree in the Department of Chemical and Biologicial Engineering, University of Saskatchewan, Saskatoon, SK

By Kathlene Laurie Jacobson

Copyright

Abstract

Fuels from biomass (biofuels) are used to mitigate the greenhouse gases produced through the utilization of fossil fuels. Non-edible or waste biomass can be pyrolized to produce bio-oil. The oil (an unstable and low energy product) can be further upgraded through hydrodeoxygenation to produce gas and/or diesel range hydrocarbons and value added chemicals. In this research, the valorization of fast pyrolysis bio-oil from maple sawdust was explored in two steps. Primarily, solvent extraction was carried out to remove water from the bio-oil (35% water, 55% oxygen and a heating value of 21.6 MJ/kg). The solvents explored were benzene, ethanol, and chloroform. Chloroform reduced the amount of high molecular oxygenates from 58 to 30%, increased the amount of hydrocarbons from 20 to 41%, and reduced the moisture content to <0.2%. The modified bio-oil was comprised almost entirely of phenol and phenol derivatives. It possessed 42% oxygen and a heating value of 44.0 MJ/kg. Then, the objective was to remove oxygen while obtaining a high yield of hydrocarbons suitable for use as transportation fuels through hydrodeoxygenation. Hydrodeoxygenation of the modified bio-oil was studied with different metal catalysts impregnated on H-ZSM-5 in a batch reactor. H-ZSM-5 was chosen based on results from model compound testing and it's use in industry. 8.5-13% Mo, 1-5% Ni, 2.5-5% Sr, 5-10% W, CoMo and NiMo were loaded onto H-ZSM-5 (average pore size, 0.54 nm). The experiments were carried out over a temperature range of 250-350°C, pressure range of 2-5 MPa, stirring speed of 500 rpm, catalyst loading 2-10wt%, and a tetralin to oil ratio of 2-10:1. Tetralin was

added as a hydrogen donor solvent and lignin dilutant to prevent polymerization of the feed. The products were coke/tar, gas, water, and an organic liquid. 2.5% Ni/ZSM-5 proved to be the most effective catalyst with 95% oxygen removal and 89.0% yield of hydrocarbons (20% of which were aliphatic). The least effective was 2.5% Sr/ZSM-5 with 87% oxygen removal and 24.5% hydrocarbon yield. The liquid products obtained via 2.5% Ni had a heating value of 47.0 MJ/kg, a moisture content of 0.07%, and a crystallization point of -81.3°C. The products were fully miscible with diesel fuel.

Optimization of the process utilizing statistical design software and 2.5% Ni/ZSM-5 catalyst yielded an experimental hydrocarbon yield of 94.3% (predicted value of 95.3%). The optimum conditions were found to be T=350°C, P=3 MPa, catalyst loading=3.5 g (7 wt%), solvent to oil ratio of 10, rpm=500, and a reaction time of 45 min. The liquid products obtained under optimum conditions contained 22wt% aliphatic hydrocarbons. The physical properties of the liquid product included a high heating value of 47.3 MJ/kg, a low moisture content of 0.07wt%, a close-to-neutral pH of 6.4, and a crystallization temperature of -88.4°C. This data suggests these liquid hydrocarbons could be used as a transportation fuel.

Acknowledgement

I would first like to thank my supervisor, Dr. Ajay Dalai, for his valued guidance and supervision throughout the planning, execution, and communication of my thesis work. I greatly appreciate the time taken to organize my study abroad and his willingness to answer my many questions. I would also like to thank the other two members of my advisory committee, Dr. Hui Wang and Dr. Gordon Hill, for their contributions to my graduate studies and the time taken to review and critique my written materials.

Secondly, I would also like to thank Dr. José María Arandes Esteban and all of my colleagues at the Universidad del Pais Vasco for all their assistance and guidance during my stay in Bilbao, Spain. I had a wonderful experience and can't thank them enough for tolerating my terrible Spanish during the first months of my stay. I have to thank Mr. Richard Blondin, Miss Heli Eunike and Mr. Dragan Cekic and my colleagues in the laboratory for their assistance in the laboratory work that contributed to my project.

My appreciation must also be given to the Natural Sciences and Engineering Research Council of Canada, Agriculture and Biomass Innovation Program, Auto21, Canadian Research Chair Program, and the University of Saskatchewan for their much-appreciated financial assistance. I also must thank the Study Abroad Assistant Fund for providing financial support to students who study abroad and Mr. and Mrs. Lindsay Milne for making the Bruce J. Milne Memorial Scholarship available. Without either of these award opportunities, my exchange in Spain would not be possible and I will be forever grateful for receiving them.

I would like to thank my Mom and Dad for their constant support and belief in me. Most of all, I would like to thank my husband, Stu, for always proof reading my work, supporting me no matter how much I complained about unsuccessful results or paper writing, and his infinite patience in continuing to support me during the many years of my university career.

Table of contents

List of Tables

List of Figures

Nomenclature

β	Beta as referring to glucosidal bonds within sugars or the zeolite
γ-Al_2O_3	Gamma alumina catalyst support
Å	Angstroms
ASTM	American society for testing and materials
BET	Brunauer-Emmett-Teller nitrogen adsorption analysis
b.p.	Boiling point
C_n	Molecules that contain n number of carbons
CHNSO	Carbon, hydrogen, nitrogen, sulfur and oxygen analysis
DSC	Differential scanning calorimeter
DTA	Differential thermal analysis
FCC	Fluid catalytic cracker
FTIR	Fourier transform infrared spectroscopy
GC	Gas chromatogram
GC-FID	Gas chromatogram with flame ionization detector
GC-MS	Gas chromatogram with mass spectrometer
H/C	Hydrogen to carbon ratio
HDM	Hydrodemetallation
HDN	Hydrodenitrification
HDO	Hydrodeoxygenation
HDS	Hydrodesulphurization
HDY	Hydrogenation
H-NMR	Hydrogen spectrum of nuclear magnetic resonance analysis
HPLC	Hewlitt Packard liquid chromatography
HV	Heating value, MJ/kg
ICP-MS	Induced coupled plasma with mass spectroscopy

KBr	Potassium bromide
LHSV	Liquid hourly space velocity, h^{-1}
MS	Mass spectrometer
MTG	Methanol to gasoline
NREL	National Renewable Energy Laboratory
O/C	Oxygen to carbon ratio
P	Pressure, MPa
PNNL	Pacific Northwest National Laboratory
RI	Refractive Index
T	Temperature, °C
TEM	Transmission electron microscopy
TGA	Thermogravimetric analysis
WHSV	Weight hourly space velocity, h^{-1}
wt%	Weight percent
XRD	X-ray diffraction

1 Introduction

Hydrocarbons, especially liquid and gaseous fuels, are vital to the transportation industry. Traditionally, desirable hydrocarbons are produced from fossil fuel sources. However, the continuous use of fossil fuels for hydrocarbon and energy sources has created severe global problems.

Of primary concern, is the current availability of such sources; fossil fuels are being consumed without replacement, creating a volatile market with ever increasing prices. Companies are failing to find new reserves of oil sufficient to meet the future need. Most oil producers are investing in more capital-intensive projects, needing to drill in remote places and deeper to obtain oil. The second problem, which has generated a lot of public and political concern, is the global warming effect of carbon dioxide (CO_2) and other greenhouse gased on the environment. The utilization of fossil fuels and related chemicals introduces gases such as carbon dioxide, chlorofluorocarbons and methane into the atmosphere causing the "greenhouse gas effect".

Renewable energy resources can provide solutions to these problems. They have become a large focus of research in the energy sector due to their reduced environmental risks and greenhouse gas emissions; they are favorable alternatives to fossil fuels and their derivatives. In addition to their sustainable favorability, they are, in general, more evenly distributed over earth's surface than fossil fuels and may be exploited using less capital-intensive technologies. Hence, they increase the scope for diversification and decentralization of energy supplies and the achievement of energy

self-sufficiency at a local, regional, and national level [Jones, 1989].

Biomass is one such promising alternative. It has a worldwide abundance and is considered a renewable feed. Despite the complexity associated with biomass as a feed for bio-oils, the use of biomass is rapidly expanding. Several industries have commercialized the production of so-called first generation bio-fuels, bio-ethanol from sugar-like products (sugar, starch, etc.) and bio-diesel (from rapeseed, sunflowers etc) [Forson et al, 2004]. However, the scale of production of these first generation biofuels appears to be several times lower than typical unit operations in refineries (few barrels a day compared to thousands of barrels per day in conventional refineries) [Wildschut, 2009]. Besides, these feeds are in competition with the food industry, which may raise ethical questions as well.

Thus, there is a demand for a second generation of biofuels. These biofuels would preferably be derived from non-edible biomass resources. Options are woody biomass, such as forest residues, straw, aquatic biomass, industrial residues such as bagasse and the like. Possible conversion technologies of said biomass are: fermentation processes (conversion of the cellulosic materials to low molecular weight sugars through chemical and/or physical processes; then, subsequent conversion to ethanol via fermentation), gasification to produce bio-syngas for further upgrading to methanol or gas/diesel, or liquefaction with further upgrading either through gasification or through deoxygenation, hydrogenation etc. to produce gas and/or diesel range hydrocarbons and value added chemicals.

Nevertheless, biomass is still not widely used for biofuel production. The main

reasons are the presence of contaminants (including ash, water, and oxygen), the variation in chemical composition, and its low energy density. To overcome these issues, an indirect approach seems advantageous. A possible indirect approach would be the conversion of biomass into a more uniform and stable structure, after which secondary conversion processes would transform the intermediates to transportation fuels and value added chemicals. The primary conversion process referred to in this introduction is the (fast) pyrolysis of biomass. Here, the biomass is subjected to rapid heating to temperatures in the range of 450-650°C with a residence time of <2s in an oxygen free atmosphere. Incomplete degradations occur, which yield three major products: char (mostly carbon which can be employed to enrich soil, as a source for activated carbon, or as a solid fuel additive), fuel gas (usable in any combustor or syngas feed), and liquid oil to be further upgraded to a bio-fuel.

In recent years, the liquid products obtained from pyrolysis of biomass have received considerable attention. However, the important consideration is that these liquids from biomass are not useful as fuels other than direct boiler applications and possibly for some types of turbine and large diesel applications after significant engine modifications [Elliot, 2007]. In order for the bio-oil to be useful as transportation fuel, it requires chemical transformation to reduce volatility, increase thermal stability and reduce viscosity through oxygen removal and molecular weight reduction. Recent upgrading techniques are hydrotreating (hydrodeoxygenation), hydrocracking, catalytic cracking, and emulsification [Junming et al, 2008; Lopez et al, 2000; Michio et al, 2003]. Emulsification of bio-oil with diesel provides a short-term approach to the use of bio-oil in diesel engines, however, fuel properties such as heating value, cetane value and

corrosivity are unsatisfied. This leaves two feasible avenues for bio-oil upgrading: atmospheric pressure upgrading (catalytic cracking) and high pressure upgrading (hydrotreating and hydrocracking).

Catalytic cracking is a conventional petroleum reforming process capable of decomposing heavy fractions into medium and light distillates to produce H_2O, CO_2 or CO under atmospheric pressure in the presence of an acidic and preferably hydrophobic catalyst, typically ZSM-5. The same technology can be applied to the reforming of highly oxygenated, and bulky bio-oil. The high temperatures associated with this process, are able to cleave bonds in the larger molecules as well as deoxygenate compounds present in the pyrolysis oil, and produce desirable (generally aromatic) fuel-range hydrocarbons.

Hydrotreating is another conventional form of petroleum hydroprocessing technology. Commonly in industry, hydrotreating utilizes bi-metallic acid catalysts such as CoMo/γ-Al_2O_3 and NiMo/γ-Al_2O_3 to remove sulfur and/or nitrogen from heavy gas oil through hydrodesulphurization (HDS) and hydrodenitrification (HDN), respectively. In the case of bio-oils, neither sulfur nor nitrogen is present in significant quantities, but oxygen is abundant. Therefore, hydrotreatment of bio-oils requires the removal of oxygen through hydrodeoxygenation (HDO). HDO and HDN are very similar due to the overlapping nature of nitrogen and oxygen molecules. Thus, hydrotreating of bio-oil incorporates the same principles and process technology as hydrotreating of conventional petroleum feeds. Hydrocracking is a similar process with higher temperatures utilizing noble metal catalysts such as Pt/γ-Al_2O_3 or Pd/γ-Al_2O_3.

The most common obstacle when utilizing either hydrodeoxygenation/ hydrocracking or catalytic cracking as the upgrading method is that the yield of desirable upgraded oils is generally low due to the high yields of char, coke and tar [Junming et al, 2008]. The coking can be so severe that it plugs fixed-bed reactor systems resulting in termination of experimentation [Baker et al, 1988]. Desirable product yield can be increased while decreasing the undesirable carbon deposition by co-feeding hydrogen donors as well as modifying reactor systems. The most common co-feeds are methanol, tetralin, and decalin.

2 Literature review

2.1 Introduction

A variety of biomass was examined in order to further understand the scope of the project as well as to find a reliable basis for comparison of results found. The following are the literature findings.

2.2 Characterization of Canadian biomass

2.2.1 Biomass availability

The availability of biomass in the world is 220 billion dry tonnes per year [Anon, 2004]. It is the world's largest and most sustainable energy resource. Furthermore, residues of this biomass are abundant and do not compete with existing industries or food distribution.

The two most abundant types of biomass residues, forest residue (hardwood sawdust) and agricultural residue (wheat straw, barley straw, and flax), are easily found

across Canada. Forest biomass can be found from coast to coast in Canada's boreal forest. Canada's average annual round wood cut has been estimated at 167.5 million m^3 creating over 60 million tonnes of residues [Anon, 2008 and Mohan, 2006]. These annual harvests are taken from approximately 1 million ha, constituting only about 0.25% of the total forestland in Canada [Anon, 2008]. Therefore, more could be harvested to replace bio-fuels without exceeding Canada's sustainable forestation limits.

The potential for agricultural biomass derived energy is less than that of forest-derived biomass in Canada. Most agricultural residues have alternative uses as animal fodder or soil conditioners and typically have a lower energy intensity than wood (i.e., 1 m^3 of wood contains as much energy as 50 m^3 of baled field residues) [Anon, 2008]. Also, agricultural biomass is usually only available at one time of year, while forests can be harvested year-round.

2.2.2 Biomass properties

Biomass is composed of three main components; cellulose, hemicellulose, and lignin. Cellulose (25-45 %) is composed of monomers of glucose, a six-C sugar linked by β (1-4) glycoside bonds. Hemicellulose (20-40 %) is a highly branched carbohydrate and is composed of both hexose and pentose sugar. Lignin (10-30 %) is a macromolecule in nature with phenolic character; it is helical and contains ether and carbon-carbon linkages. It is a source of aromatics or valuable phenolic by-products, and combustion of lignin contributes to energy [Biagina et al, 2004].

2.2.3 Characterization techniques

Fundamental characterization of biomass is imperative as the chemical composition of biomass affects conversion processes differently. Currently, there is limited literature on comprehensive biomass characterization. A few papers have explored near-infrared spectroscopy after extraction to identify sugars, lignins, and inorganics [Sanderson et al, 1996; Ye et al, 2008], while others have explored thermo gravimetric analysis (TGA) to identify and quantify cellulose in biomass [Biagina et al, 2004; Chen et al, 2003]. The National Renewable Energy Laboratory (NREL) has the most extensive library on biomass and bio-oil characterization techniques.

Rout et al [2009] proposed characterization of biomass through chemical and physical means for the determination of the heating value, ash content, volatile matter, elemental composition and amounts of key components (cellulose, hemicellulose, and lignin). The key components are determined through solvent extraction and subsequent acid treatment. A schematic of the proposed techniques used in this dissertation is shown in Figure 1.

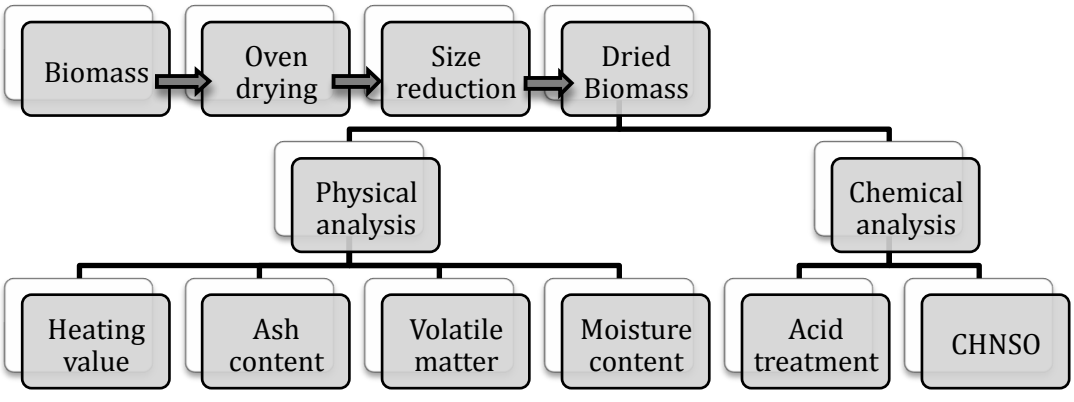

Figure 2.1: Schematic diagram of biomass characterization techniques [Rout et al, 2009]

2.3 Characterization of oil derived from pyrolysis of biomass

2.3.1 Fast pyrolysis for bio-oil production

Fast pyrolysis is the most common method of converting biomass into bio-oil. It is defined as the thermochemical decomposition of organic material at elevated temperatures in the absence of oxygen. Pilot or large scale biomass pyrolysis operations such as Dynamotive, Advanced Biorefinery Inc, and Ensyn utilize Waterloo Fast Pyrolysis Process technology. In this system, the biomass is fed into the fluidized bed using a variable twin speed screw feeder. It allows recycled product gas to be used as the fluidizing gas. It operates at temperatures of 450°C+, atmospheric pressure, and low residence times of 0.3-1.5s in the presence of a carrier gas, N_2. Pyrolysis yields three main products; a hydrogen-enriched gas, a hydrogen-deficient oil (thick dark-brown liquid also known as bio-oil), and a carbon-rich solid known as char. Optimum yields (total liquids) from the Waterloo Fast Pyrolysis Process have been reported at 75wt% of dry feed at a heating rate of 105°C/s and short residence times [Scott et al, 1985]. The present discussion will focus solely on the oil obtained.

2.3.2 Bio-oil properties

Bio-oil produced from fast pyrolysis possesses undesirable properties of high viscosity, thermal instability and corrosiveness; all are obstacles to the substitution of fossil fuels by bio-oils. Furthermore, any variations in the pyrolysis process can yield very different bio-oils. Several studies reported that feedstock chemical composition, particle size, moisture content, pyrolysis temperature, and heating rate significantly affect the bio-oil yield and properties [Demirbas, 1998; Bonelli et al., 2001; Debdoubi et

al., Boateng et al., 2006; Onay, 2007; He et al., 2009]. Furthermore, according to Huber et al [2006] the exact composition of the bio-oil is dependent on the feedstock (including dirt and moisture content), organic nitrogen or protein of the feedstock, heat transfer rate and final char temperature during pyrolysis, time and temperature of vapours in the reaction, efficiency of the char removal system, and efficiency of the condensation equipment to recover the volatile components from the noncondensable gas stream. Therefore, characterization of bio-oil is beneficial in understanding what measures need to be taken in order to upgrade bio-oil to produce quality transportation fuels and chemicals.

Because of the original biomass' complexity (and variation in cellulose, hemicellulose and lignin content), the composition of the bio-oil is slightly unpredictable and contains a plethora of constituents. Huber et al [2006] reported bio-oil from any source to contain acids (including acetic and propanoic), alcohols (methanol, ethylene glycol, ethanol), ketones (acetone), aldehydes (acetaldehyde, formaldehyde, ethanedial), miscellaneous oxygenates (glycolaldehyde, acetol), sugars (1,6-anhydroglucose, acetol), furans (furfurol, furfural), phenols (phenol, methyl phenol, dimethyl phenol), and guaiacols (isoeugenol, eugenol, 4-methyl propyl syringol). The general liquid products produced during certain pyrolysis processes are further explored in the following section.

The multicomponent bio-oil mixtures are derived primarily from depolymerization and fragmentation reactions of the three building blocks of lignocellulose: cellulose, hemicellulose, and lignin. The phenols, guaiacols, and syringols are formed from the lignin fraction, whereas the miscellaneous oxygenates, sugars, and

furans are produced from the cellulose and hemicellulose. The esters, acids, alcohols, ketones, and aldehydes probably form from decomposition of the miscellaneous oxygenates, sugars, and furans [Huber et al, 2006].

2.3.3 Characterization techniques

Current literature on bio-oil characterization focuses on determination of chemical composition and fuel characteristics [Dermibas, 2007; Garcia-Perez et al, 2007; Oasmaa et al, 1991; Scholze et al, 2001; Sensoz et al, 2008; Zhang et al, 2007]. Different fuel characteristics such as kinematic viscosity, flash point, density, water content, and pH were documented [Oasmaa et al, 1991; Scholze et al, 2001; Sensoz et al, 2008]. Several attempts have been well documented in literature to characterize bio-oil, derive its composition, and compare its fuel characteristics with conventional petroleum derived fuel. The most notable differences between the two types of fuels are the higher oxygen and water content associated with bio-oil, as well as the acidic pH. Bio-oil contains 15-30wt% water (although, up to 60wt% has been reported [Rout et al, 2009]), which is derived from the original moisture in the feedstock and forms as a product through dehydration during the pyrolysis reaction as well as during storage [Dermibas, 2007; Garcia-Perez et al, 2007; Oasmaa et al, 1991; Scholze et al, 2001; Sensoz et al, 2008; Zhang et al, 2007]. The presence of water lowers the heating value and viscosity.

The oxygen content in bio-oil is typically 35-40% [Oasmaa et al, 1991; Scholze et al, 2001] and is distributed in more than 300 compounds depending on the source of biomass and conditions under which pyrolysis is carried out (temperature, heating rate,

etc). The presence of oxygen creates the primary issue for the differences between bio-oils and hydrocarbon fuels. The high oxygen content leads to the lower energy density and immiscibility with hydrocarbon fuels [Garcia-Perez et al, 2007]. Additionally, the strong acidity (attributed to the high concentration of organic acids present and thus carboxyl groups present) of bio-oils makes them extremely unstable. The typical properties of bio-oil obtained by fast pyrolysis of wood are compared with heavy fuel oil in Table 2.1 below.

Table 2.1: Typical properties of wood pyrolysis bio-oil and of heavy fuel oil [Oasmaa et al, 1991]

Physical Property	**Bio-oil**	**Heavy Fuel Oil**
Moisture content (wt%)	15-30	0.1
pH	2.5	-
Specific gravity	1.2	0.94
Elemental composition (wt%)		
C	54-58	85
H	5.5-7.0	11
O	35-40	1
N	0-0.2	0.3
Ash	0-0.2	0.1
Heating Value (MJ/kg)	16-19	40
Viscosity (at 50 C) (cP)	40-100	180
Solids (wt%)	0.2-1	1

The chemical composition of bio-oils is commonly identified through chromatographic techniques such as GC, GC-MS, and other spectroscopic techniques including H NMR, FT-IR, and CHNS [Dermibas, 2007; Sensoz et al, 2008]. An example of

chemical compound identification, using coupled GC and GC-MS spectroscopic techniques, for flax derived bio-oil is shown in Table 2.2. In this case, only the most plentiful compounds were identified using GC-MS and quantified using GC. Table 2.3 is an example chemical group classification carried out through GC, GC-MS, FT-IR, and NMR for bio-oil derived from a mixture of wheat and hemlock (a hard wood). A summary of both the physical and chemical bio-oil characterization techniques can be seen below in Table 2.4.

2.4 Removal of water from crude bio-oil

Water removal, as a means of pretreatment, will improve the bio-oil's properties (e.g. viscosity, heating value, density) and reduce the risk of catalyst poisoning in bio-oil upgrading, especially in the case of a noble metal catalyst. In literature, water removal from bio-oil has been attempted in four methods: distillation, dehydration, reactive rectification, and physiochemical separation.

2.4.1 Distillation and dehydration

The bio-oil is heat sensitive and subject to re-polymerization, so it cannot be fractionated by distillation [Sheu et al, 1988]. Water removal from bio-oil via dehydrated Na_2SO_4 was attempted with a ratio of Na_2SO_4 to bio-oil of 3:1. This method only partially removed the water from bio-oil and the ultimate analysis of Na_2SO_4 treated bio-oil showed high sulfur (1.6%) content [Rout et al, 2009].

Table 2.2: GC-MS Liquid pyrolysis products from Flax Straw [Tushar et al, 2010]

Compound	Retention time (min)	Area (%)
1-hydroxy-2-butanone	6.47	1.93
2,3-butanedione	1.86	1.34
2,3-pentanedione	2.52	0.51
2-cyclopenten-1-one	6.11	0.57
2-cyclopenten-1-one, 2-hydroxy-3-methyl	11.70	1.25
2-cyclopenten-1-one, 2-methyl	6.23	0.57
2-cyclopenten-1-one, 3-methyl	8.17	0.74
2-furfanol, tetrahydro-2-methyl	18.71	3.29
2-methoxy-4-vinylphenol	19.34	0.73
2-propanone, 1-(acetyloxy)	7.53	0.85
2-propanone, 1-hydroxy	5.60	4.07
2-furanmethanol	9.87	1.87
3-pyridinol	32.76	0.86
Acetaldehyde	0.97	1.00
Acetic acid	6.95	20.87
Acetic acid, methyl ester	1.18	1.63
Acetone	1.15	1.06
Butyrolacetone	9.48	1.07
Cyclopropyl carbinol	16.08	1.62
Formic acid, ethyl ester	1.44	5.41
Furan, tetrahydro-2-(methoxymethyl)	8.02	2.01
Furfural	7.47	1.42
Phenol	14.35	nd
Phenol, 2.6-dimethoxy	22.30	1.25
Phenol, 2-methoxy	12.05	2.71
Phenol, 2-methoxy-4-methyl	13.38	1.17
Phenol, 4-ethyl-2-methoxy	14.70	0.73
Propanoic acid	8.28	1.97

[a] nd: not detected

Table 2.3: Chemical classification of bio-oil produced from the fast pyrolysis of wheat-hemlock mixture [Rout et al, 2009]

Chemical Classes	Amount present in bio-oil (%)
Hydrocarbons	2.6
Low molecular wt. Fatty acids/esters	13.7
Hexodecanoic acid	23.6
Furanoids	3.2
Pyranoids	1.2
Benzenoid hydrocarbons	2.6
Oxygenated benzenoids	14.6
Low molecular wt. alcohols/aldehydes/ketones	1.7
High molecular wt. alcohols	19.5
High molecular wt. waxy components	2.1

Table 2.4: Summary of bio-oil characterization methods

Characterization Technique	Purpose of technique
Bomb Calorimetry	To calculate the calorific or heating value
FTIR	To identify functional groups
C,H,N,S,O analysis	To quantify the elemental composition and derive an approximate empirical formula
H NMR	To determine chemical bonding within molecules
GC-MS	To identify and quantify chemical compounds present

2.4.2 Reactive rectification

Junming et al. [2008] reported that esters (e.g. ethyl formate, b.p. 327.8 K) had a lower boiling point than their corresponding acids (e.g. formic acid, b.p. 373.7 K); hence it was possible to convert low-molecular-weight acids with alcohol into esters and separate them from original bio-oil by reactive rectification. Surprisingly, with the separation of volatile organic acids, it was found that the remaining H_2O and nonvolatile compounds form a phase separation (creating fractions of 'light oil' and 'heavy oil')

[Junming et al, 2008]. Reactive rectification capitalizes on water and organic acids having higher polarity than the other major constituents in bio-oil. Their results showed that this method was able to reduce the water content in the bio-oil from 33wt% to 11wt%.

2.4.3 Additional water for fractionation

Bio-oil from pyrolysis is composed of phenolic lignin decomposition products together with water and a plethora of compounds of many classes. This makes fractional distillation of bio-oil impossible. Therefore, bio-oil solvent fractionation seems to be a very important topic to consider. The most common solvent utilized in literature is water. When an excess of water is added to bio-oil, two layers form. The top layer is the aqueous fraction where the highly polar compounds of bio-oil (acid, esters, etc) settle as well as many carbohydrate-derived compounds. Through the addition of excess water, an organic fraction with approximately 2% water may be obtained. The bottom layer is a viscous, oligomeric, lignin-containing fraction. Upgrading work on the aqueous fraction has been well documented [Adjaye, 1993; Mohan et al, 1996; Rout et al, 2009]. Because it is rich with carbohydrates, it serves as an excellent feed for the fermentation of alcohols. However, the commercialization of the lignin-rich fraction has not been explored, but applications such as the use of the lignin as a phenol replacement in phenol formaldehyde resins have been studied.

2.4.4 Supercritical CO_2 extraction

Rout et al [2009] attempted separation of valuable components from bio-oil by supercritical CO_2. A wheat-hemlock biomass mixture was converted to bio-oil through

pyrolysis at the Advanced Biorefinery Inc. in Ottawa, Canada. The yields of the supercritical CO_2 extracts were 4.3%, 13.2% and 15.2% corresponding to 10, 25 and 30 MPa respectively. The remaining bio-oil was a waxy residue. Characteristics of the biomass, crude bio-oil, and the three fractions obtained through supercritical CO_2 are summarized in Table 2.5. It was observed that the calorific value of the bio-oil supercritical CO_2 fractions was higher than the calorific value of the original biomass. Similarly, the ultimate analysis of CO_2 fractions indicated that the carbon percentage was increased with decreased percentage of oxygen as presented in the empirical formulae. Therefore, the supercritical CO_2 extraction process was successful as a pretreatment method. The extracts contained a low percentage of moisture along with high percentage of carbon.

2.5 Catalysts

Hydroprocessing catalysts are quite versatile, exhibiting activity for a number of important reactions. Those of major interest in hydroprocessing are removal of heteroatoms via hydrodesulphurization (HDS), hydrodenitrification (HDN), hydrodemetallation (HDM), and for coal or biomass-derived liquids, hydrodeoxygenation (HDO).

Table 2.5: Proximate analysis, ultimate analysis, calorific value and pH of wheat-hemlock biomass, bio-oil and supercritical CO_2 fractions of bio-oil [Rout et al, 2009]

samples	Proximate analysis (%)				Ultimate analysis (%)								Calorific value (MJ/Kg)	pH
	moisture	Ash	volatile matter	fixed carbon[1]	C	H	N	S	O_2[2]	H/C molar ratio	O/C molar ratio	empirical formulae[3]		
Wheat-hemlock biomass	8.3±0.2	1.8±0.1	83.0±0.2	6.9±0.2	46.7±0.2	6.4±0.2	0.05±0.02	0.01	46.8±0.3	1.64	0.75	$CH_{1.64}O_{0.75}N_{0.0009}$	18.6±0.2	-
Crude bio-oil	59.1±0.9	0.03±0.1	-	-	19.3±0.1	9.2±0.1	0.74±0.02	0.17	70.6±0.2	5.72	2.74	$CH_{5.72}O_{2.74}N_{0.033}$	nd	2.8±0.2
10 MPa fraction	0.5±0.1	-	-	-	75.8±0.2	11.9±0.1	0.01	nd	12.3±0.2	1.88	0.12	$CH_{1.88}O_{0.12}N_{0.0001}$	45.0±0.4	4.5±0.1
25 MPa fraction	1.5±0.2	-	-	-	74.6±0.3	11.5±0.2	0.02±0.01	0.01	13.8±0.3	1.85	0.14	$CH_{1.85}O_{0.14}N_{0.0002}$	43.2±0.2	4.3±0.1
30 MPa fraction	3.1±0.3	-	-	-	76.0±0.2	11.7±0.1	0.09±0.01	0.02	11.9±0.4	1.85	0.12	$CH_{1.85}O_{0.12}N_{0.001}$	38.8±0.5	4.0±0.1

nd - not detected; 1-% of fixed carbon calculated from difference of moisture, ash and volatile matter content; 2 - % of O calculated from the difference of C; H, N and S; 3-S not taken into consideration

2.5.1 Deactivation by water

Hydroprocessing reactions occur on the active sites of the catalysts. These active sites are available on the surface as well as within the pores of the catalyst. A suitable pore size distribution is required to ensure the access of reactant molecules to the active sites. The main reason for deactivation of the catalysts involves loss of active sites [Furimsky et al, 1999]. Basic causes include blocking of pore mouths (rendering still active sites unavailable to reactants), irreversible site poisoning (reducing the number of sites available for reaction), and sintering of the active sites (reducing the total number of surface sites available). In commercial operation, hydroprocessing catalysts invariably experience some degree of deactivation, depending on the feed source. Initial deactivation is caused by coke and water formation [Furimsky, 1999]. Continued deactivation over a longer time period is due to metal deposits, whose rate of deactivation depends on the metals level in the feed. The final, catastrophic loss in activity is attributed to pore constriction and ultimate pore blockage. At this stage, the temperature cannot be raised sufficiently to keep up with deactivation, and the run has to be terminated.

Although the oxygen content in conventional feeds is low, in the case of coal-derived liquids and biomass-derived feeds, water derived from these feeds may have an inhibiting effect on HDO reactions. H_2O may modify the catalyst surface during operation and contribute to loss in catalyst activity [Vogelzang et al, 1983]. Krishnamurthy and Shah [1982] reported that the addition of 0.75wt% of dibenzofuran to 1wt% of dibenzothiophene reduced the HDS rate by 25%. However, addition of 1wt% of cyclohexylphenol resulted in a 50% reduction in

HDS. This was attributed to inhibition by water, which was rapidly formed from the cyclohexylphenol, although polymer formation on the catalyst surface cannot be ruled out.

Lipsch and Schuit [Lipsch et al, 1969] observed a poisoning effect of water on HDS of thiophene, and Krishnamurthy and Shah [1982] found that the pseudo-first-order rate constant for hydrogenation of biphenyl to cyclohexylbenzene decreased by an order of magnitude when 1 wt.% water was added to the feed. Vogelzang et al. [1983] observed a weak inhibition of naphthol HDO by water. On the other hand, Satterfield et al. [1985] reported a promoting effect of water on the HDN of quinoline. The enhancing effect of water was increased in the presence of H_2S. Laurent and Delmon [1993, 1994a] reported that water caused only very weak inhibition in the HDO of phenols, ketones and carboxylic compounds, compared to H_2S and NH_3. These authors expanded their studies [1994b] to include the HDO of bio-oils under high water pressure in a batch reactor with a sulphided NiMo catalyst. For the blank run (dodecane solvent), little change in the catalyst activity was noted. However, with the addition of water, about two-thirds of the activity was lost. The poisoning effect of water was evident also with H_2S present, whereas the selectivity of methylcyclohexanol and toluene was hardly affected. The surface changes signify a modification of the catalyst structure by water. In summary, it is apparent that the effect of water gains importance with increasing concentration in the feed, and after certain level is exceeded, the poisoning effect of water may be quite significant. Almost certainly, poisoning by water will be present during hydroprocessing of the biomass derived feeds.

The effect of water on hydroprocessing metal catalysts has widely been investigated in other processes as well. It is well known that water may reoxidize metal catalysts during synthesis [Hilmen et al, 1990]. Hilmen and co-workers [Schanke et al, 1999; Adnanes, 1995] studied the effect of water on Co/Al_2O_3 and $Co\text{-}Re/Al_2O_3$ catalysts by adding water to the synthesis gas feed during Fischer Tropsch synthesis. It was found that the catalysts were deactivated when water was added during Fischer–Tropsch synthesis. Li et al. [Li et al, 2000] found that water decreased CO conversion of a $Co\text{-}TiO_2$ catalyst. An explanation for this is that water decreases and/or destroys the strong metal–support interaction effect for metal supported catalysts.

2.5.2 Deactivation by metal components

During hydroprocessing, part of the metals present in the feed will deposit on the catalyst surface and cause deactivation. As indicated previously, species which poison active sites on the catalyst contribute to the overall deactivation, as well as changes in the catalyst structure which may occur during the operation. The nature of the metals deposited depends on the origin of the feed. V and Ni are the predominant metals in petroleum crudes, heavy oils and oil shale- derived liquids, Fe and Ti are the main metals in coal-derived liquids and Mg and P are the main metals in biomass-derived liquids. Biofeeds, usually prepared by a thermal treatment of biomass (such as pyrolysis), are the least contaminated by metals.

Deactivation by metals always occurs simultaneously along with deactivation by coke. Deactivation by metals is irreversible. Kinetic data have

shown that the rate of metal deposition varies from metal to metal. For example, in the case of V and Ni, the initial deposition occurs at much higher rate for V than for Ni, and increases with increasing pore diameter [Kobayashi et al, 1987]. This suggests that the formation of V deposits may have an adverse effect on the rate of Ni deposit formation. While the initial coke deposition is rapid before the pseudo-equilibrium level is reached, metal deposits continually increase with time [Myers et al, 1989]. During the entire period, metals deposition occurs on the catalyst, which has already lost a substantial portion of its original porosity and surface area due to coke formation [Fonseca et al, 1996]. This is generally true for petroleum-derived feeds and coal-derived feeds as well as other feeds. In order to maintain design activity, temperature is raised to offset deactivation. Hence, the deposition of metals affects the lifetime of the catalyst.

2.5.3 Deactivation by nitrogen compounds

Due to the presence of proteins in the biomass, bio-oils can contain certain nitrogen containing compounds. The amount ranges from 0.1 wt% (wood) up to 3-4 wt% (grass). These nitrogen components are present or are converted during hydrotreatment to ammonia, methyl amine, pyridine, and methyl pyridine [Weiksner et al, 2005]. In the case of hydroprocessing catalysts, deactivation by nitrogen compounds may occur due to adsorption on the active acid sites [Chiaramonti et al, 2003].

2.5.4 Advantages of zeolites

γ–Alumina is the most commonly used support for hydroprocessing catalysts in the petroleum industry. Its desirable properties include strong mechanical and textural properties, ability to provide great dispersion for active transition metals, and low cost [Euzen et al, 2002]. However, γ–Alumina suffers from some shortcomings. One negative aspect of γ–alumina is the strong chemical interaction between the alumina and the transition metal in their oxide phase. This can make transition of the catalyst metal to its active phase a difficult procedure and can prevent the catalyst from reaching its maximum potential activity [Topsoe et al, 1981]. The quest for a superior support system that avoids this disadvantage has led researchers to explore alternative support materials. In the past couple decades, use of porous materials such as carbon and zeolites of different topologies and mesoporous materials have received considerable attention [Farag et al, 1998; Erica et al, 2006] for use as a catalyst support. There has especially been a growing interest to use porous materials as support for hydrotreating processes due to the many unique attributes linked with zeolites: high surface area, large variety of pore sizes, variable surface functional groups, easy metal recovery by the burning of the support, reduced coking propensity, and resistance to nitrogen poisoning. Zeolites are among the most popular of these porous materials.

2.5.4.1 Zeolite shape selectivity and acidity

Zeolites are crystalline microporous silica based materials, which are extensively used as heterogeneous catalysts in industry. They offer a well-defined, ordered pore structure on a molecular level and provide a tunable acidity. Traditionally, zeolites (aluminosilicates) are defined as crystalline materials in which Si and Al are tetrahedrally coordinated by oxygen atoms in a three-dimensional network creating uniformly sized pores of molecular dimensions.

Furthermore, zeolites have been proven effective as catalysts in many refining and hydroprocessing processes [Adjaye, 1993]. These reactions have been postulated to proceed through intermediate compounds called carbenium ions which are created on the surface of zeolites through interaction of reaction molecules with active sites. Zeolites then act as "solid acids" which are capable of converting the adsorbed molecule into various forms. This is accomplished by either transferring a proton from the solid acid to the adsorbed molecule (Bronsted acid site) or by transferring electron pairs from the adsorbed molecule to the solid surface (Lewis acid site). Zeolite acidity arises from the imbalance in charge between silicon and aluminum atoms within the framework so that each aluminum atom is capable of inducing a potential active site.

The following main characteristics of the zeolites have contributed significantly to the commercial success of zeolites:

- High surface area and adsorption capacity.
- Active sites, for example acid sites, can be generated in the framework and their strength and concentration can be tailored for a particular application.

- The sizes of their channels and cavities match with the dimensions of most of the molecules involved in various chemical processes (i.e. 0.55-1.2 nm)
- The complex channel structure in the zeolites allows different kinds of shape selectivities, i.e. product, reactant, and transition state.

2.5.4.2 H-ZSM-5 catalyst

Among the different zeolites, ZSM-5 (Zeolite Socony Mobil-5) is a very stable zeolite with a variable content of alumina and uniform pores of 5.5 Å diameter. It is widely used in hydroprocessing due to its unique structure. The relatively small size of the pores allow only narrow (~4 Å dia) molecules enter its pores and undergo rapid hydrogenolysis [Sivasanker, 2002]. The framework type of the high silica zeolite ZSM-5 can be described in terms of pentasil units (one honeycomb-shaped ring in figure 2.2a) [Maeson et al, 2001]. These units are linked to form pentasil chains, and mirror images of these chains are connected via oxygen bridges to form corrugated sheets with 10-ring holes [Maeson et al, 2001]. Each sheet is then linked by oxygen bridges to form a 3-dimensional structure. The overall structure can be viewed below in Figure 2.2b.

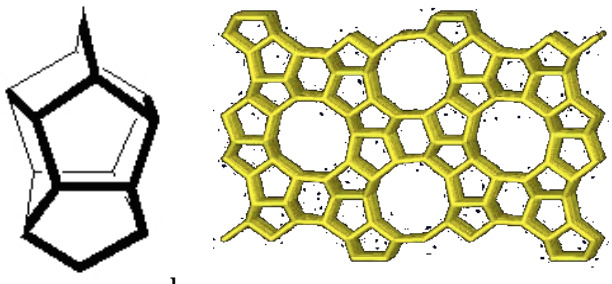

a. b.

Figure 2.2: a. Pentasil Unit [Imamura et al, 1994], b. ZSM-5 structure [Roy et al, 1999]

2.5.4.3 Other zeolites of interest

HZMS-5 is only one example of a zeolite that is commonly used. It is of smaller pore diameter as it has 10-member-ring openings and thus is more ideal for petroleum selectivity. Nonetheless, bio-oil contains many bulky molecules with side chains. Therefore, other zeolites with larger ring openings should be mentioned. Y zeolites have a 12-membered ring and have been proven to be an effective catalyst in hydrodesulphurization. They are commonly used in FCC catalysts (cracking catalysts) as part of a diluted framework. Furthermore, β-zeolites (a 14-membered ring zeolite) are commonly used in hydrocracking reactions before Mobil's discovery of pentasil zeolites (ZSMs).

2.5.5 Incorporating metal onto the catalyst

The functionality of zeolites can be changed through post synthesis modification to incorporate metals. Although the catalytic activity is heavily dependent on the kind of zeolite and its SiO_2/Al_2O_3 ratio, addition of metal promotes added functionality in the hydrogenation and deoxygenation reactions.

2.5.5.1 Metal supported catalysts for hydrotreating

Metals from the VIII group, such as nickel, are well known for their hydrogenation activity and usefulness in hydrotreating processes. The hydrogenation activity of the group VIII metals increases across the transition series in the order of Fe < Co < Ni [Satterfield, 1991]. Thus nickel, palladium, and platinum have the highest hydrogenation activity of group VIII metals.

Furthermore, nickel and platinum make ideal catalyst as they adsorb reactants strongly enough and activate them, but not so strongly that the product are unable to break away [Satterfield, 1991]. Nonetheless, nickel is more abundant and less expensive than palladium and platinum.

VIB group metals, such as tungsten, have also been proven effective in hydrotreating processes and may prove to be effective in oxygen removal. Tungsten is a well-known hydrotreating catalyst and in some studies has proven more effective than molybdenum [Mauchausse et al, 1992]. It is highly effective in HDN and HDS, thus it should also be active in HDO. Furthermore, elemental tungsten resists attack by oxygen, acids, and alkalis making it a promising catalyst for the resistance of poisoning from water present in bio-oil, organic acids, and high level of oxygenates [Mauchausse et al, 192]. W/ZSM-5 has proven effective in conversion of oxygenates through the MTG (methanol to gasoline) process where only a 3.2 wt% tungsten was capable of an optimum methane conversion of 29.4% corresponding to a C_5+ selectivity of 57.2% [Saidina et al, 2004].

Sr-ZSM-5 was explored in a study by Okado et al. [1988] where the authors tested Mg, Ca, and Sr containing ZSM-5-type zeolite for oxygenate-to-gasoline reactions. It was found that all modified zeolites had increased selectivity to olefins at temperature above 500°C [Mauchausse et al, 1992]. In a long term testing of ZSM-5 containing alkaline earth metals, the strontium containing zeolite showed the most stable activity [Okado et al, 1988].

Furthermore, commercial hydrotreating catalysts such as NiMo and CoMo have been proven effective not only in conventional petroleum hydrotreating, but also in the hydrotreatment of bio-oil [Grange et al, 1996; Elliot et al, 1984; Elliot, 2007; Baldauf et al, 1997]. However, these metals have normally been studied on a γ-alumina support. Alumina has a tendency to interact with transition metals which in turn lowers the life of the catalyst whereas zeolites are a thermally stable, robust support. Thus, CoMo and NiMo on ZSM-5 will display multi-functional characteristics as the acidic, hydrophobic and high activity functions of the support will help to crack and hydrogenate large molecules in the bio-oil while the noble metals will aid in removing oxygen.

2.5.5.2 Synthesis of various metal catalysts

Metals are more commonly introduced onto aluminosilicate supports through incipient wetness technique. For example, nickel is impregnated by mixing a hydrous nickel nitrate solution with the support. This solution is then dried overnight at 110°C and then calcined at 550°C [Luengnaruemitchai et al, 2008]. Similar methods are used for other metal impregnations [Kumaran et al, 2006; Guo et al, 2003; Bataille et al, 2001; Sundaramurthy et al, 2007; Ferdous et al, 2006].

Metal loading plays an important role in catalyst preparation. Too much metal can clog the pores of the support or damage the catalyst structure. However, too little metal will elude an optimum conversion that could be achieved. Each metal has an optimum or recommended range of metal loading. Suggested nickel loading is in the range of 1-8wt% [Masalaka et al, 2005]. For tungsten, it was found

that a 3-30wt% metal doping was optimum for MTG processing [Amin et al, 2003]. A strontium loading of 2.5wt% was suggested by Guo et al [2003]. In industry, a common CoMo catalyst consists of 8.5 wt.% Mo and 2.2 wt.% Co whereas NiMo [Bataille et al, 2001] is composed of 2.5-3wt% Ni and 13-14wt% Mo [Ferdous et al, 2006; Sundarmurthy et al, 2007].

2.6 Model compound upgrading

Because of the complicated nature of bio-oil, many researchers have chosen to work with model compounds or synthetic bio-oil to develop successful techniques in upgrading. Because most bio-oils are highly phenolic in nature, a large amount of research in this area has concentrated on deoxygenation of phenols.

2.6.1 Upgrading phenols at high pressure

Senol et al. [2007] carried out a thorough investigation on HDO of phenol. A tubular flow reactor made of stainless steel was utilized. 1-3 mm of either commercial NiMo/γ-Al_2O_3 or CoMo/γ-Al_2O_3 was packed between two layers of silicon carbide and activated at 400°C under atmospheric pressure. Experiments were carried out at 250°C under 15 bar with H_2S/H_2 mixture.

Reaction products of phenol detected in the liquid samples included aromatic and alicyclic hydrocarbons and a few oxygen-containing compounds. The HDO products of phenol were benzene, cyclohexane and cyclohexene, while oxygen-containing compounds were cyclohexanone and diphenyl ether. In addition, due to the presence of H_2S, a sulphur containing compound, cyclohexanethiol, was

detected. The oxygen- and sulphur- containing compounds were formed in trace amount.

In their study, Senol et al [2007] explored the effect of H_2S on the reactions with phenol. When no H_2S was added, the HDO conversions of phenol were 19% on the NiMo catalyst and 28% on the CoMo catalyst. When 60 ppm of H_2S was added, the conversion dropped to 16% for NiMo and 20% for CoMo. The decrease continued as higher amounts of H_2S were added.

They also compared the industrial catalyst's activity in phenol conversion to aliphatic oxygenates conversion. It was concluded that, under identical conditions, phenol is less reactive on the sulphided catalyst than are aliphatic oxygen-containing compounds such as ester, alcohol, and carboxylic acid. Further, contrary to the activity for the HDO of phenol, the activity for the HDO of aliphatic oxygenates was higher with the NiMo catalyst than with CoMo catalyst. The effect of the sulphiding agent on the HDO of phenol was opposite to its effect on the HDO of the aliphatic oxygenates. The addition of sulphiding agent enhanced the acid-catalyzed reactions of aliphatic oxygenates such as dehydration and hydrolysis, while it suppressed the direct hydrogenolysis reaction of phenol due to it's competitive adsorption. Thus, the opposite effects can be explained in terms of the different reaction mechanisms for the elimination of oxygen, a difference that is related to the different molecular and electron structures of aromatic and aliphatic oxygenates.

This work indicates that the performance of the HDO process under the effect of the sulphiding agent added to the HDO feed to maintain catalyst activity and stability are dependent on the composition of the bio-oil feed. Addition of a sulphiding agent to a wood-based HDO feed, which contains mainly phenolic compounds, will probably affect the total HDO negatively. In contrast, a promoting effect is likely for vegetable oils and animal fats, which contain mainly aliphatic oxygenates.

Elliot [1983] at the Pacific Northwest National Laboratory (PNNL) did extensive work on heterogeneous catalytic processing of bio-oil. Initial work involved batch reactor tests of model phenolic compounds with various catalysts. Commercial samples of catalysts were used representing CoMo, NiMo, NiW, Ni, Co, Pd, and CuCrO to hydrogenate phenol at 300°C or 400°C and 140 bar (1 h at temperature). Of the catalysts tested, the sulphided form of CoMo was the most active producing a product containing 33.8% benzene and 3.6% cyclohexane at 400°C. The Ni catalyst was also active, producing a product with 16.9% benzene and 7.6% cyclohexane at 400°C. A Pd catalyst produced a 7.8% benzene product with 2.7% cyclohexane but 5.5% cyclohexanone. At a lower temperature of 300°C, cyclohexanone was the primary product at 8.1% and benzene and cyclohexane were nearly equal at 2.0% and 2.5%, respectively.

In 2009, Yang et al [2008] published work investigating hydrodeoxygenation of crude bio-oil using phenol as a model compound in supercritical hexane. Reactions were carried out at temperature of 300-450°C and hydrogen pressure of

5 MPa with MgO-supported sulphided CoMo with and without phosphorus as a catalyst promoter (CoMoP and CoMo). In this study, it was concluded that both MgO-supported catalysts proved to be effective for HDO of phenol in supercritical hexane at temperatures greater than 350°C. The HDO activity of the catalyst was greatly promoted by addition of a small amount of phosphorus. Further, the HDO of phenol may proceed with direct hydrogenolysis reaction and hydrogenation reaction involving cyclohexanol as an intermediate/precursor, resulting in conversion of phenol into benzene, cyclohexyl-aromatics and C_{12}-products. Hydrogenolysis of phenol to benzene (direct elimination of the hydroxyl group) is the dominant reaction and it becomes much more favorable at a higher temperature.

The HDO activity of CoMoP/MgO increased drastically with increasing reaction temperature. The hydrotreatment of phenol at 450°C with CoMoP/MgO catalyst led to a liquid product containing 10.2% phenol and 64% benzene. Furthermore, very little coke formation was detected. This superior resistance to coke formation was attributed to the basic character of the MgO support.

Kallury et al [1984] explored HDO of phenol over MoO_3-NiO-Al_2O_3 catalyst in an autoclave batch reactor at a temperature of 350-450°C and pressure of 2.8-9.8 MPa. The reaction of phenol using the MoO_3-NiO catalyst at 450°C and 2.8 MPa gave essentially complete conversion of the reactant after 45 min reaction time, with formation of benzene (60%), cyclohexane (16%), and methylcyclopentane (7%) as the major products. In addition, a group of products were formed that were

presumably derived from coupling of two phenol-derived units, namely, cyclohexylcyclohexane (2%), diphenyl (3%), and cyclohexylbenzene (2%). These results indicate that benzene is essentially inert to these reaction conditions.

At lower temperatures of 350°C or 400°C, the conversion of phenol is not complete even after 2 h, and the proportion of saturated products had increased at the expense of the benzene. Evidently the reaction mechanism for the hydrogenolysis of phenol to benzene and the ring saturation to cyclohexanol are quite different, and the former process becomes much more favorable at higher temperatures.

Fisk et al [2009] explored model compound upgrading through a synthetic bio-oil. The oil consisted of a mixture of methanol (5wt%), acetaldehyde (12wt%), acetic acid (14wt%), glyoxal (4wt%), acetol (8wt%), glucose (8wt%), guaiacol (17wt%), furfural (4wt%), vanillin (8wt%), and de-ionized water (20wt%). Upgrading of the synthetic oil was carried out in a stainless steel autoclave at 0.7 MPa and 350°C over a series of supported Pt catalysts. Of the catalysts tested, Pt/Al_2O_3 showed the highest activity for oxygen removal, the oxygen content of the model oil decreasing from an initial value of 41.4wt% to 2.8wt% after upgrading. Analysis of the product oil showed it to be highly aromatic, the major components corresponding to alkyl-substituted benzenes and alkylcyclohexanes. CO_2 was formed as the major gaseous product, together with lower yields of H_2 and C_1-C_6 hydrocarbons.

Based on the products obtained in these experiments, bio-oil upgrading is suggested to proceed via two main pathways. The first of these corresponds to reforming of the light oxygenates, resulting in H_2 generation and O_2 rejection as CO_2. Simultaneously, the aromatics present undergo C-O bond cleavage; in the presence of H_2, this leads to the formation of benzenes and their hydrogenated products. The highly alkylated nature of the products appears to be a consequence of the acidic nature of the reaction medium, favoring the occurrence of aromatic electrophillic substitution reactions. The formation of coke was also observed, believed to be due to both thermal and catalyzed reactions. This suggests that for prolonged operation, regular burn-off of the coke would be necessary to maintain the catalyst in an active state.

Table 2.6 presents a summary of model compound upgrading that has been completed over the past few decades. All studies examined oxygen removal through hydrodeoxygenation using moderate to high temperatures and pressures as well as a traditional hydroprocessing metal catalyst such as CoMo, NiMo or Pt on alumina. In all cases, benzene and cyclohexane were the main products.

Table 2.6: Summarization of model compound upgrading via hydrotreating

Reference	feedstock	diluent	Catalyst	T (°C)	P (MPa)	conversion [a]	reaction system
Senol et al, 2008	Phenol	m-xylene	CoMo/ Al_2O_3	250	1.5	28%	fixed-bed
Elliot, 1983	Phenol	n-octane	CoMo/ Al_2O_3	400	14	34%	batch
Yang et al, 2009	Phenol	n-hexane	CoMo/ MgO	380	5.0	51%	batch
Kallury et al, 1984	Phenol	n-octane	NiMo/ Al_2O_3	450	2.8	60%	batch
Fisk et al, 2009	Synthetic bio-oil[b]	-	Pt/ Al_2O_3	350	0.7	60%	batch

a HDO conversion %

b a mixture containing methanol (5wt%), acetaldehyde (12wt%), acetic acid (14wt%), glyoxal (4wt%), acetol (8wt%), glucose (8wt%), guaiacol (17wt%), furfural (4wt%), vanillin (8wt%), de-ionized water (20wt%)

2.6.1.1 REACTION MECHANISM

Another notable discovery made through model compound studies was the prediction of reaction mechanisms. Hydrodeoxygenation (HDO) can be defined as the removal of the heteroatom, oxygen, in the form of water in the presence of hydrogen. More specifically, HDO of phenolic compounds proceeds through hydrogenolysis and hydrogenation reactions [Yang et al, 2008]. Hydrogenolysis removes the oxygen yielding a benzene ring; then, subsequent hydrogenation yields cyclohexene and cyclohexane. However, it is possible for the reaction to proceed primarily through hydrogenation of the aromatic ring to yield cyclohexanol with subsequent hydrogenolysis to rapidly dehydrate the alcohol to yield cyclohexane [Yang at al, 2008]. Figure 2.3 depicts these proposed pathways. HDO products of phenol are commonly benzene, cyclohexane and cyclohexene. This mechanism was proposed by both Satterfield [1991] and Senol et al [2008].

Kallury et al [1984] presented an alternative reaction where a group of products (C_{12} products) were formed. These were presumably derived from the coupling of two phenol-derived units, namely, cyclohexenecyclohexane, cyclohexenebenzene, and diphenyl. This alternative is presented in Figure 2.4.

It should be noted that $NiMo/Al_2O_3$ promotes hydrogenolysis (the upper pathway in figure 2.4) over Co, where $CoMo/Al_2O_3$ promotes hydrogenation (the lower pathways in figure 2.4) over Ni. This suggests that the metal provides acid sites that are shared by both reaction pathways. A bifunctional catalyst that provides separate sites for both reactions is desired.

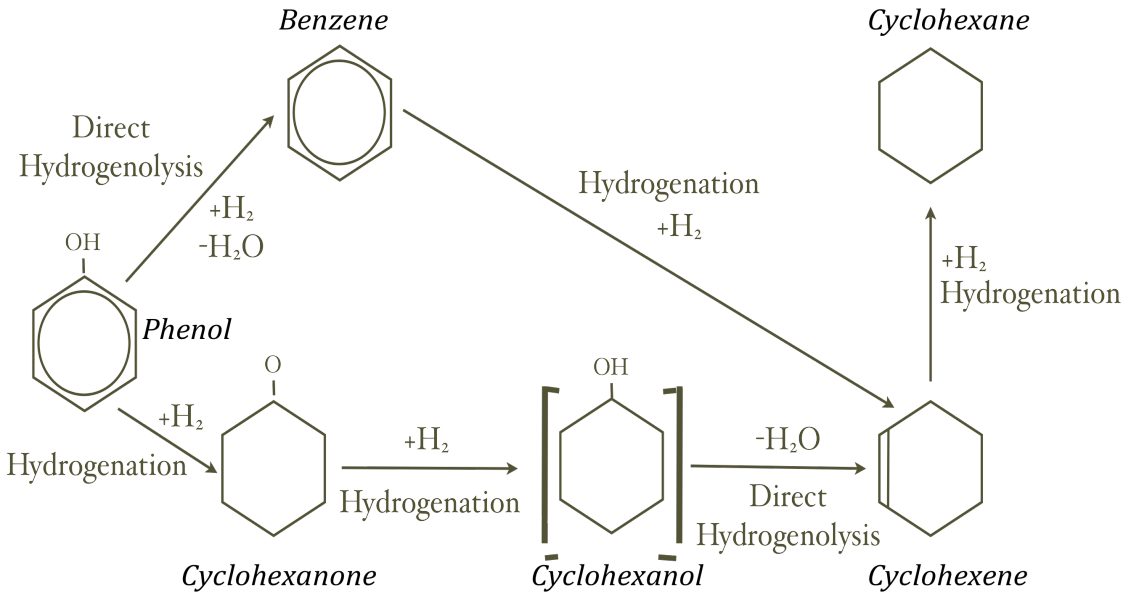

Figure 2.3: Reaction scheme for the HDO of phenol on sulphided catalysts [Satterfield, 1991]

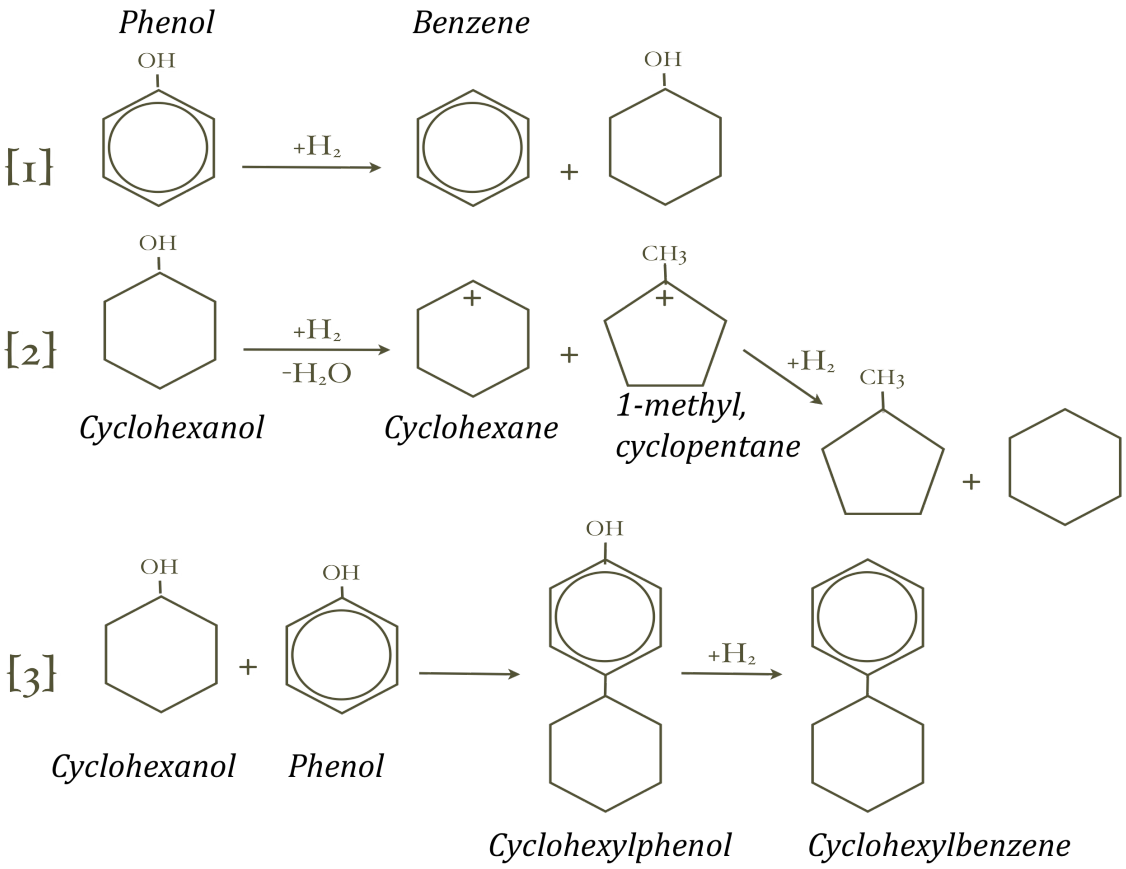

Figure 2.4: Reaction scheme for the hydrodeoxygenation of phenol as proposed by Kallury et al [1984]

2.6.2 Upgrading phenols and bio-oil at low pressure with zeolites

Adjaye [1993] utilized a fixed-bed reactor at a temperature of 330°C, atmospheric pressure, and 3.6 WHSV. HZSM-5 activity was explored on a mixture of model compounds representing bio-oil (propanoic acid, methyl ester of acetic acid, 4-methylcyclohexanol, cyclopentanone, 2-methylcyclopentanone, methoxybenzene, ethoxybenzene, phenol and 2-methoxy-4-(2-propenyl)phenol). The mixture of model compounds contained 14.6wt% phenol which produced 5.1% conversion to benzene. Their low phenol conversions were contributed to phenol's stable nature.

It was predicted that isomerization of the original molecule was the main reaction route in their studies.

Sharma et al [1991] used a fixed bed reactor and tetralin as a hydrogen-donor solvent to upgrade an oil produced by the Waterloo fast pyrolysis process. About 66wt% conversion of the non-volatile matter, a maximum of 60wt% organic liquid product and coke fractions between 11 and 17wt% were obtained.

Chen et al [1988] achieved 68wt% conversion of a pyrolytic oil using helium as a carrier gas in a fluidized bed. Upon processing with methanol as a co-feed in a 1:1 weight ratio, the conversion increased to 85wt%. Also, the methanol resulted in reduced coke formation from 9 to 4 wt%. However, they obtained very low yields of hydrocarbons (6wt% in the absence of methanol, and 11wt% with methanol) probably due to the high flow rates (850 mL/min) employed.

Gayubo et al [2009] explored bio-oil upgrading at atmospheric pressure in a "two-step" process. Crude bio-oil was continuously fed through a u-shaped reactor which can be viewed in Figure 2.5. The first part of the "u", the feed preheating zone, is filled with glass spheres where the carbonaceous matter produced by polymerization of bio-oil lignin derivates is deposited. This is thought to attenuate the catalyst life and reduce coking drastically. In the second part of the "u", the reaction is carried out. The catalyst is placed on a glass wool layer, which is supported by the bed of glass spheres. Typical reactions were carried out at 400°C, feed rate of 0.20 cm^3/min, and a reaction time of 1 h. It was observed that at

temperatures above 400°C, there was only a minimal increase of lignin deposition on the glass beads.

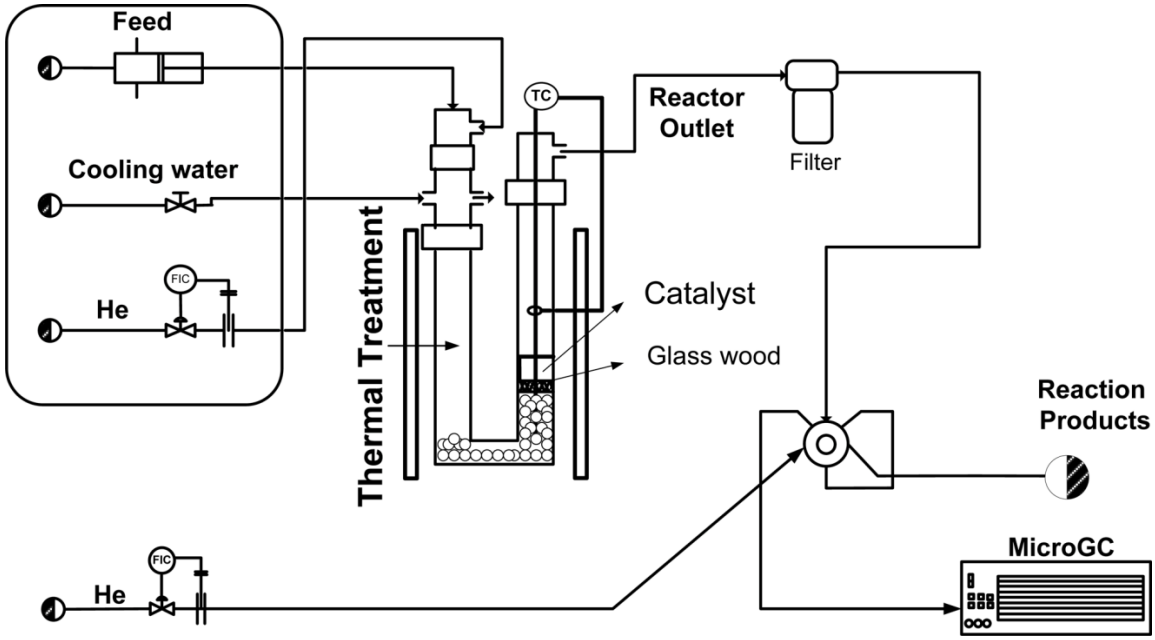

Figure 2.5: Reaction equipment utilized for "two-step" upgrading by Gayubo et al [2009]

Furthermore, Gayubo et al [2009] observed that water addition treatments and dilution of bio-oil with methanol considerably reduce pyrolytic lignin deposition. In the case of water addition treatments, it appeared that water had a positive effect on the reaction due to the fact that the undesirable phenolis/lignin fraction of the bio-oil was diluted. Methanol co-feeding attenuates the thermal degradation of biooil and this result is not only due to dilution. It is observed that as the methanol content in the mixture increased, there was a steady and almost linear decrease in the percentage of bio-oil degraded. For a methanol content higher than 70wt% in the feed, the fraction of biooil deposited is constant. This result indicates

that methanol addition has a beneficial effect, not only due to feed dilution, but also due to its ability to inhibit condensation reactions of biooil phenolic components.

Methanol cofeeding by 70 wt% with crude biooil gives way to the maximum attenuation of pyrolytic lignin deposition and a considerable decrease in catalyst deactivation, with an initial bio-oil conversion similar to that achieved by feeding crude biooil. With a moderate space-time and temperature above 400°C, the conversion of the bio-oil in the mixture is higher than 92 wt%, with a hydrocarbon yield higher than 80 wt%.

2.6.2.1 REACTION MECHANISM

When using a zeolite to upgrade bio-oil, phenol, or other oxygenates under atmospheric pressure, the reaction is hydrogen limited [Bridgewater, 1996]. Zeolites are known to deoxygenate through carboxylation and dehydration [Adjaye, 1993]. As mentioned earlier, Adjaye examined phenol and substituted phenols under the conditions previously stated. As mentioned above, the major products were isomers of the phenol showing that isomerization of the original molecule was the main reaction route. Isomerizations of substituted phenols have been mentioned to be one of the major reactions over zeolite catalysts [Renaud et al., 1996; Chen et al., 1989].

The second reaction route occurring to a far lesser extent involves condensation-type reactions, which result in an aqueous fraction and high boiling molecules, mainly ethers. It has been mentioned [Chantal et al., 1985] that the dehydration of phenol leads to an intermediate ether formation. Successive

condensation may result in non-volatile residue or coking. This intermediate could be the cause of severe coking and reactor plugging that occurs when upgrading lignin-rich bio-oil fractions at high temperatures. The proposed pathway for upgrading phenol over ZSM-5 at atmospheric pressure is given in Figure 2.6.

A notable conclusion from Adjaye's thesis work was how effectively ZSM-5 converted ethers and ketones even though it's conversion of phenol and its derivatives were low under the same conditions. This occurred because ethers as well as ketones are less stable than phenols and can give up oxygen more easily by forming or breaking double bonds where the oxygen was attached. This is not possible with phenol as the attached benzene ring is completely stable. Ethers (furans) and ketones (cyclopentanone, etc.) are abundant in bio-oil and must be deoxygenated in order to obtain a quality product. Therefore, these reactions are also important and make upgrading bio-oil via ZSM-5 more appealing.

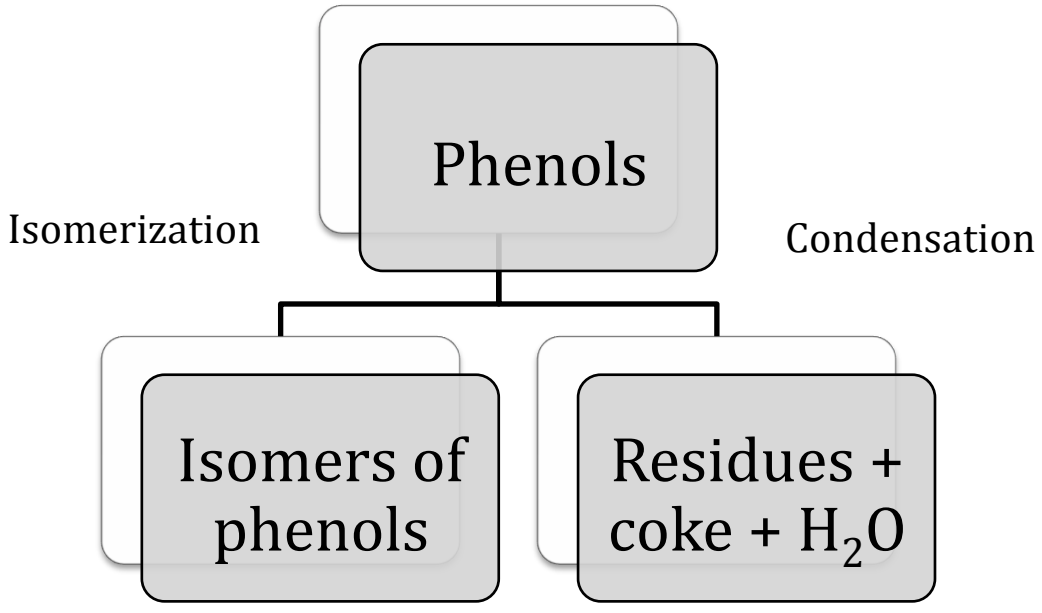

Figure 2.6: Reaction pathway for the conversion of phenols [Adjaye, 1993]

2.7 Hydrotreatment of bio-oil to obtain chemicals and fuels

Bio-oil is disadvantageous as a fuel in its crude form mainly due to its high oxygen content. The oxygen content contributes to negative attributes such as: high viscosity, instability, corrosiveness, and a low heating value. Therefore, it is essential to upgrade the bio-oil in order to reduce/remove the oxygen. This can be accomplished through hydrodeoxygenation. If the bio-oil is mostly phenolic (which typical pyrolysis oil is), then HDO can proceed through the reaction mechanism proposed in Figures 2.3 and 2.4 as the model compound studies would accurately represent the true feedstock.

2.7.1 Common problems with polymerization

The most common obstacle when utilizing either hydrodeoxygenation/ hydrocracking or catalytic cracking as the upgrading method is the yield of desirable upgraded oils is generally low due to the high yields of char, coke and tar [Junming et al, 2008]. The coking can be so severe that it plugs fixed-bed reactor systems resulting in termination of experimentation [Baker et al, 1988]. Co-feeding hydrogen donors as well as utilizing a two-step reaction procedure can increase desirable product yield while decreasing the undesirable carbon deposition. The most common co-feeds are methanol, tetralin, and decalin.

2.7.2 Successful upgrading of bio-oil via hydrotreatment

Soltes and coworkers (Soltes et al, 1987) conducted studies on the hydroprocessing of tars produced from the pyrolysis of biomass (a very phenolic

substance). The tests were carried out under hydrotreating conditions (high pressure and temperature) in a batch reactor with decalin as a hydrogen donor. Various catalysts were screened and hydrocarbon conversion varied from 56% over a Pd/alumina catalyst to 3% over silica-alumina.

Zhang et al. [2005] studied bio-oil conversion into liquid fuels via hydrotreatment with sulphided CoMo-P/Al_2O_3 in an autoclave with tetralin as a solvent. The optimum conditions were: temperature of 360°C, reaction time of 30 min, and a cold hydrogen pressure of 2 MPa. These optimum conditions yielded 75.8% conversion with 59.6 wt% hydrocarbon-rich product.

Baldauf et al. [1992] studied the hydrotreatment of bio-oil both thermally and catalytically in a fixed-bed reactor over hydrotreating catalysts, CoMo/Al_2O_3 and NiMo/Al_2O_3 at 350°C and 18 MPa. Thermal hydrotreatment resulted in 70-80wt% reductions in oxygen content in the final product whereas >90% deoxygenation was achieved when using catalysts. Depending on the severity and the water content of the feedstock, a product yield of 30-50% could be achieved. The product was fractionated by distillation and it was shown that the product properties of the heavy fraction are close to those of a fluid catalytic cracking (FCC) feedstock. The light fraction had properties close to that of gasoline.

Churin et al. [1990] used a fixed bed reactor loaded with CoMo and NiMo catalysts for upgrading of pyrolysis oil. Upgrading was carried out in the presence of hydrogen at 5-12 MPa and 270-400°C. The oil initially contained 10-20wt% hydrocarbons and 40wt% phenols. After upgrading the hydrocarbon fraction

increased to 70wt% while the phenols decreased to 18wt%. In the presence of tetralin, the fraction increased further to 75wt% and 20wt%, respectively. However, the role of tetralin or its recovery was not studied.

Baker and Elliot [1988] upgraded a fast pyrolysis oil produced at Georgia Tech. Upgrading was carried out in a reactor with two temperature stages using $CoMo/Al_2O_3$ catalyst at 13 MPa. The first and second zones were maintained at 274 and 353°C, respectively. The yield of hydrocarbons was 31wt% of the oil. Rapid catalyst coking was also observed and was considered a major problem.

Oasmaa [1992] studied bio-oil upgrading via batchwise hydrotreatment at 21.5 MPa, 390°C, reaction time of 2 h and a catalyst loading of 10wt%. The catalyst explored was 4% CoO/15.5% MoO_3/Al_2O_3. Through this procedure, the oxygen content was lowered from 22% to 3%. Nitrogen and sulfur contents of the product were 4.3% and 0.10 %, respectively. Straight-chain material predominated in the upgraded product and C_{14}-C_{29} n-alkanes were identified along with some phenols.

Wildschut [2009] carried out a catalyst screening study using noble metal catalysts for the hydrotreatment of fast pyrolysis oil. The reactions were carried out in an autoclave batch reactor at two conditions relevant for the process, a mild hydrotreatment at 250°C (100 bar hydrogen) and a more severe hydrotreatment at 350°C (200 bar hydrogen). Distinct differences in catalyst performance, product yield and product properties were observed for mild and deep hydrotreatment. Ru/C catalyst was found to be superior.

With the Ru/C catalyst in mild HDO conditions, product oil with an oxygen content between 18 and 27wt% was obtained in yields between 21 and 55wt% (dry basis). The yields as well as the level of deoxygenation for the noble metal catalysts were higher than for the classical hydrotreatment catalysts. At deep HDO conditions, two product liquids were obtained with the noble metal catalysts, one with a density higher and one with a density lower than water. The composition of the top oil differs from that of the bottom oil. The top oil has a higher H/C and O/C ratio. The weight average oxygen level of the product oils ranged from 5-11wt%, which was considerably lower than for the mild HDO process.

Relevant product properties and the chemical composition of the top oil produced at deep HDO conditions (350°C, 200 bar, 4 h) using the Ru/C catalyst were determined. The heating value was approximately 43 MJ/kg which was considerably higher than for the feed pyrolysis oil (20 MJ/kg). The acidity of the hydrotreated oil was considerably lower than the original feed as expressed by an increase in the pH from 2.5 to a 5.8.

Mahfud [1975] conducted an experimental study on the hydrodeoxygenation of pyrolysis oil using heterogeneous catalysts with the objective to produce oil with product properties in the range of conventional liquid transportation fuels. Catalyst screening studies were carried out at temperatures in the range of 350-425°C. Mahfud concluded that of the classical hydrotreating catalysts, pre-sulphided NiMo on alumina was a more active catalyst than pre-sulphided CoMo on alumina and Ru on alumina. Furthermore, the results indicated that no sulphur is required in the feed.

Process studies on NiMo catalysts indicated that HDO oil with an oxygen content of 10 wt% could be obtained. Additionally, there is a strong indication for excessive catalyst deactivation, either due to the presence of water, the absence of sulphur or pore blocking by char formation. 100 g of crude pyrolysis was converted to 34 g of HDO oil, 42 g of an aqueous phase, 13 g of gas and about 4 g of char using the NiMo catalyst. The energy efficiency of the process is approximately 62%. The HDO oil produced with the NiMo catalyst has a heating value of 39 MJ/kg, which is about twice that of a crude pyrolysis oil.

A summary of hydrodeoxygenation studies with pyrolysis products to date is presented in Table 2.7 below. Two interesting observations can be made from this summary table. The first is the low conversion that Soltes et al [1987] observed when using a metal-free catalyst (SiO_2/Al_2O_3) vs. a Pd catalyst. Without the metal present, conversion was as low as 5% where as with palladium present, conversion reached 56%. The second is that a batch reactor seems to yield a higher conversion. This could be due to excessive polymerization in the lines of a continuous system. In all cases, hydrocarbons were the main products.

Table 2.7: Summary of bio-oil hydrotreating studies to date

Reference	Feedstock	Catalysts	T (°C)	P (MPa)	Conversion[a]	Reaction system
Soltes et al, 1987	Tars from pyrolysis (phenolic)	Pd/Al_2O_3	400	0.7	56%	batch
Soltes et al, 1987	Tars from pyrolysis (phenolic)	SiO_2/Al_2O_3	400	0.7	5%	batch
Zhang et al, 2005	Oil phase after water separation	$CoMoP/Al_2O_3$	360	0.2	38%	batch
Baldauf et al, 1992	Crude pyrolysis oil	$CoMo/Al_2O_3$ $NiMo/Al_2O_3$	350	1.8	30-50%	Fixed bed
Churin et al, 1988	Crude pyrolysis oil	$CoMo/Al_2O_3$ $NiMo/Al_2O_3$	350	1.2	64-70%	batch
Baker and Elliot, 1988	Crude pyrolysis oil	$CoMo/Al_2O_3$	353	1.3	31%	Fixed bed
Oasmaa, 1992	Crude pyrolysis oil	$CoMo/Al_2O_3$	390	2.2	N.R.	batch
Wildshut, 2009	Crude pyrolysis oil	Ru/C	350	2.0	55%	batch
Mahfud, 2009	Crude pyrolysis oil	$NiMo/Al_2O_3$	400	2.0	40%	batch

[a] HDO conversion; N.R. – Not reported

2.7.3 Hydrogen donor solvents

Hydrogen donor products are termed liquefaction "solvents". These are reactive solvents act on the hydrogen donor principle: i.e., they are capable of taking on hydrogen very easily and can also readily give up hydrogen to form their

respective condensed aromatic hydrocarbons [Grainger, 1981; Bockrath, 1983]. Examples of such solvents are tetralin (1,2,3,4-tetrahydronaphthalene), indoline, 1,2,3,4-tetrahydroquinoline.

Hydrogen donor solvents have been used extensively in the processing of coal. In coal liquefaction this has often resulted in the stabilization of reactive fragments such as free-radicals and in dissolution of such fragments during the initial stages of liquefaction. In the upgrading of coal liquids, hydrogen donor solvents have been used to effect hydrogenation, removal of heteroatoms and reduction in molecular weight [Kang, 1976; Bockrath, 1983].

Excessive coking and charring (and the associated problems) of wood-derived pyrolysis oils in a fixed bed operation as a result of low H/C ratios and the phenolic nature of the feedstock has been mentioned in the previous sections. Various attempts have been made to process bio-oils with hydrogen donor solvents [Soltes et al 1987; Sharma et al, 1991; Zhang et al, 2005] with the aim of reducing the coke formation by improving the stability of the oil to temperature effects. In addition, the solvation property of hydrogen donor solvents enhances the effective transport of these feeds, thus preventing pore blockage in the catalyst, a common problem with bio-oil feeds. Increased yields of hydrocarbons have also been observed [Soltes et al 1987; Sharma et al, 1991; Zhang et al, 2005].

Most of the processing of bio-oils by hydrotreatment have been carried out in the presence of hydrogen. These processes employ high pressures. The main advantage of using hydrogen donor solvents over hydrogen is the much lower

operating pressures that can be employed in its use. In addition, hydrogen donor solvents have better effectiveness in stabilizing the primary thermal decomposition products, thus preventing charring and coking in upgrading work [Adjaye, 1993] with resulting higher yields for upgraded liquids than hydrogen.

The selection of a solvent can have a profound effect on the yield of liquids products. A number of compounds are available as hydrogen donor solvents as long as they contain mobile carbon-hydrogen bonds [Adjaye, 1993]. A good solvent readily dehydrogenates and enhances solvation capabilities [Kang, 1976; Grainger, 1981; Bockrath, 1983]. Furthermore, it possesses acceptable physical properties such as reasonable viscosity. High liquefaction yields and reduction in char and coke formation are also expected of a good hydrogen donor solvent. Tetralin (1,2,3,4-tetrahydronaphthalene) compared with similar solvents has proven to possess these exceptional properties in both coal and biomass processing to liquid products.

2.7.4 Product properties

Product properties of HDO oil reported in the literature are scarce, despite the necessity to compare it with crude oil standards. In fact, there is currently no standard for the analysis of bio-oils and HDO oils.

To be used as a transportation fuel, the HDO products should fulfill a number of properties. After oxygen removal and thus, hydrocarbon synthesis, product properties have to fulfill those of typical gasoline and diesel products [Wildshut, 2009]. However, products with a certain oxygen content may still be attractive

biofuels, as oxygen can reduce sooting in diesel engines. For these, no standards are available yet. Properties of particular interest to be considered are:

- Elemental analysis (content of O_2, H, C, N, S)
- Water content
- Heating Value
- Boiling point range
- Viscosity
- Organic acid content
- Solids content
- Flash points
- Cold flow properties (pour and cloud point)
- Storage stability

These properties may be measured using standardized procedures. Some relations between these properties have been observed. For instance, the viscosity of the product is a function of oxygen content [Elliott et al, 1996]. At high oxygen contents, the oil contains substantial amounts of water, rendering the oil in to a relatively low viscosity product (20–50 cps at 20°C). However, upon oxygen removal, the viscosity increases drastically (up to 100,000 cps at 20°C). The highest viscosity is observed at an oxygen content between 20-30 %.

Currently, there is a large interest in identification of individual components or classes of components by dedicated analytical techniques. However, this work is seriously hampered by the diversity of components with a broad range of molecular weights in the (upgraded) oils. One technique is often not sufficient to characterize the full matrix and a combination of techniques is required to get insights in the molecular composition.

Oasmaa et al [2003a and b] characterized oils using a solvent fractionation scheme. This method successfully enables the observation of major chemical changes in the oils. The fractions are labeled extractives, the ether solubles and insolubles, dichloromethane solubles and dichloromethane insolubles. All fractions are enriched in certain component classes. For the components present in these individual fractions, the reader is referred to Oasmaa et al. [2003a and b].

Suping et al [2003] studied bio-oil and it's upgrading and concluded that it was very difficult to determine how the chemical compounds convert during deoxygenation. However, from the Fourier transform infrared (FTIR) spectra in 3200-3500 cm^{-1} a significant diminishing of the –OH group in the upgraded oil can be seen.

3 Research Motivation

3.1 Knowledge Gap

Currently in literature, there are many gaps within the field of bio-oil processing. The diverse composition of the bio-oil lends itself to many potential obstacles when designing a process to feasibly convert bio-oil into useable transportation fuels and/or value-added chemicals. After reviewing open literature pertaining to bio-oil upgrading, an opportunity was presented to explore various avenues to determine the salient route in obtaining transportation fuels from bio-oil (pyrolysis oil). Firstly, a need to characterize the crude bio-oil was identified to

provide insight into potential product formation. As literature on characterization of bio-oil alone is limited, this presented the first obstacle that required attention.

Furthermore, from literature, it appeared that many researchers were unsuccessfully attempting to upgrade bio-oil. One common problem was poor product quality and catalyst poisoning due to the high moisture content. Thus, another avenue was presented; water should be removed prior to upgrading. This concept had been explored minimally within the literature. Full removal had never occurred and therefore, there was a need for a new method or modification of an existing method for water removal. As water addition appeared to be the most successful technique to date, solvent extraction appeared to be the most promising route for this endeavor. Because the compounds within bio-oil have varying polarity, it would be prudent to explore solvents of different polarities.

An additional problem researchers in bio-oil upgrading seemed to encounter was excessive coking and polymerization during hydroprocessing. Therefore, not only was it important to identify appropriate operating conditions, and reactor design, it was also crucial to attenuate the amount of coke and tar formed during the reaction. Furthermore, it was of utmost importance to identify an appropriate catalyst capable of extensive oxygen removal and high hydrocarbon yield. Based on similarities between conventional petroleum hydroprocessing and the necessary requirements for bio-oil upgrading (removal of heteroatom and reduction in molecular size), it was predicted that similar catalysts and operating conditions would be successful in bio-oil hydroprocessing

What makes this study unique is that no studies have explored;

- Upgrading of a moisture-free bio-oil (a bio-oil pre-treated via solvent extraction to remove virtually all water)
- A comparison study of a variety of catalysts for identification of salient features required for hydrodeoxygenation of bio-oil. Nickel, cobalt-molybdenum, and nickel-molybdenum have been explored in individual bio-oil upgrading studies. Tungsten, strontium and molybdenum catalysts have not been explored.

3.2 Research Objectives

The overall objective of this research is to treat bio-oil via solvent extraction followed by hydrotreating to produce an environmentally friendly transportation fuel. To accomplish this task the following sub-objectives were formed:

1. Extensively characterize hardwood maple biomass and its derived bio-oil via fast pyrolysis.
2. Pretreat the pyrolysis oil via solvent extraction (chloroform) to remove water and consequently improve the viscosity of the oil as well decrease risks of catalyst poisoning for further upgrading.
3. Reform bio-oil through deoxygenation to obtain transportation fuels and value-added products.
    a. Find a suitable aluminosilicate support for various metals for the hydrodeoxygenation of treated bio-oil.

b. Develop and characterize a variety of multifunction metal catalysts capable of both hydrogenation and hydrogenolysis reactions.
c. Screen the products in a batch reactor system using identical conditions to compare catalysts activity for oxygen removal and hydrocarbon formation.
d. Optimize the process through parameter variation with the best catalyst to determine the settings that provide the optimum bio-oil hydroprocessing catalyst activity. Temperature, catalyst loading, and solvent to oil ratio will be varied.

4 Experimental methods

4.1 Characterization of biomass (maple sawdust)

Hardwood maple sawdust biomass was obtained from Dynamotive's West Lorne Bio-oil Plant. It was characterized following the methods reported by Naik et al [2009] and ASTM and NREL standards as illustrated in Figure 2.1. Biomass was subjected to both thermal and chemical analysis. These methods included bomb calorimetry to determine heating value, oven/furnace use for moisture content, ash content and volatile matter content determination, x-ray diffraction (XRD) to determine cellulosic structure, inductively couple plasma mass spectroscopy (ICP-MS) to determine metal content, thermogravimetric analysis (TGA) to understand the decomposition and quantity of compositional elements (cellulose, hemicellulose, and lignin), Fourier transform infrared spectroscopy (FT-IR) to further understand functional groups present, elemental analysis using CHNSO, and acid treatment (H_2SO_4) followed by Hewlett Packard liquid chromatography (HPLC) to quantify cellulose, hemicellulose, and lignin in the maple sawdust.

After the dried biomass samples were ground in a Wiley Mill (0.5mm), the physical and chemical characteristics of biomass samples were identified through various methods. The moisture content of the biomass was determined using the procedure given in ASTM 3173-87 [2003]. 3.0 g of biomass was placed in an oven set to 105±5°C for 4h and then cooled in a desiccator. This procedure was repeated until constant weight was observed. The ash content was determined in laboratory muffle furnace (Holpack, USA) as per ASTM 3174-04 [2004]. 1.0 g of biomass

sample was taken in crucible and placed in muffle furnace maintained at 575±10°C for 4 h. Then, the crucible was removed from the furnace and placed in a desiccator. The above process of heating and cooling was repeated until constant weight was obtained. The volatile matter in the biomass was determined by the procedure given in ASTM D 3175-07 [2007]. 1.0 g of sample was taken and placed in a muffle furnace maintained at 950±10oC for 7 min. Then the crucible was removed from the furnace and placed in the desiccator. The loss of weight accounted for the volatile matter in the biomass.

The calorific values were determined in a static bomb calorimeter; a sealed Parr 1108, using NREL method [Anon, 2005] and detail procedure described by Hubbard et al [1956]. Sample pellets of 1.0 g were used for each analysis. The bomb was filled with oxygen at 25°C with 1.0 cm^3 of water added to the bomb. The calorimeter was placed in an isothermal jacket with an air gap separation of 10 mm between all surfaces. The electrical energy for ignition was determined from the change of potential across a 1256 or 2900 mF capacitor when discharged from about 40 V through a platinum wire. The bomb calorimeter was submerged in a 10 calorimeter cane filled with distilled water. The calorimeter jacket was maintained at constant temperature by circulating water at 25 °C.

The XRD analysis was performed using Rigaku diffractometer (Rigaku, Tokyo, Japan) using Cu Ka radiation at 40 kV and 130 mA in the scanning angle of 5-45° at a scanning speed of 5° min^{-1}. Samples were mounted on quartz.

TG analysis of the biomass samples was performed using PerkinElmer

instrument, Pyris Diamond TG/DTA. The purpose of TGA is to understand the devolatilization characteristics of the biomass samples with temperature. 0.5 mg of sample was submitted to a temperature ramp from 20-650 °C at the rate of 10 °C/ minute. The rate of purge gas (Nitrogen) flow was 60 mL/min.

The chemical analysis of biomass samples was performed using CHNSO, FTIR and ICP-MS test methods. Furthermore, sugar composition was determined through NREL methods. The common organic elements such as C, H, N, S and O were analyzed in PerkinElmer Elementar CHNSO analyzer. C, H, N and S values were determined for each sample (4.0-6.0 mg) through combustion and detection of combustion products such as carbon dioxide, water, and nitric oxide within the apparatus. The percentage of oxygen was determined by means of difference.

The analysis of some common elements present in the ash was determined through ICP-MS. A standard sample contained metals such as Mg, Al, Ca, P, Mn, Fe, Cu, Zn and Sr. It was used for calibration (signal intensity vs. mass to charge ratio). A full scan m/z 40-250 was carried out for quantification study.

The FT-IR spectra of biomass were obtained through the KBr pelleting method using PerkinElmer, FT-IR spectrum GX to identify the functional groups present. The biomass (10 mg) was well mixed with 150 mg of KBr and the mixture was compressed into thin disc-like pellets. Each spectrum was the average of 64 co-addition of scans with a total scan time of 15 s in the IR range of 600 to 4000 cm^{-1} at 2 cm^{-1}.

For structural sugar analysis, the biomass was acid hydrolyzed for conversion of hemicellulose and cellulose to sugars following NREL method (2005). Then, the sugar solution was neutralized with calcium carbide and analyzed using a Hewlett-Packard HPLC equipped with an RI detector and an Aminex HPX 87P column (BioRad, Hercules, CA) with a deashig guard cartridge (BioRad). Degassed HPLC grade water was used as the mobile phase at the rate of 0.6 mL/min with an ambient column temperature (35^{o}C). The injection volume was 20 μl with a run time of 20 min. Calibration was carried out using mixed sugar standards of cellulobiose, glucose, xylose, galactose, arabinose and mannose. These standards were also used for quantification analysis by comparison of weight percentages. The acid insoluble part of the biomass was considered lignin.

4.2 Characterization of crude, extracted, and upgraded bio-oil

Whole bio-oil was obtained from Dynamotive in Weste Lorne, Ontario, Canada. The sample obtained was from fast pyrolysis of waste Maplewood sawdust at 450-500 °C in a bubbling-fluid bed reactor. The bio-oil was analyzed through both chemical and physical techniques to determine the moisture content, solid content, pH, ash content, CHNSO content, heating value, kinematic viscosity, and elemental analysis.

The moisture content was determined by Karl Fischer titration performed by the POS pilot plant. The solid content was determined through filtration where 100g of bio-oil was filtered through gravity and the remaining solids content was determined on a weight percent basis. The pH was determined through both litmus paper and verified by a pH meter. The ash content was determined through

incineration in our laboratory furnaces at 575±10°C for 4 h. The ash was also analyzed through ICP-MS in order to determine inorganic compounds present. Calorific value was determined through bomb calorimetry similar to the method described above for biomass characterization. The viscosity was determined using a low viscosity (LV) cone and plate viscometer. A range of readings was taken at varying rotating speeds to extrapolate a viscosity for the liquid. The upgraded products were also analyzed using differential scanning calorimetry (DSC) to identify the crystallization point of the fuel. During DSC analysis, both the sample (8-12mg) and a reference were cooled to -110°C using liquid nitrogen. When the sample undergoes a phase change, the DSC detects its change in enthalpy in the form of the peak. It is at these temperatures that the melting and crystallization temperatures can be identified.

CHNSO analysis was performed by an Elementar analysis system. GC analysis was carried out on a HP 5980 Gas Chromatograph equipped with a flame ionization detector (FID) and a 30 m x 0.25 mm WCOT column coated with 0.25 mm film thickness of 5 % diphenyl dimethyl siloxane supplied by J &W (DB-5). Helium was used as the carrier gas at a flow rate of 1.5 mL/ min at a column pressure of 22 KPa. 0.2 μL of each sample was injected into the injection port of the GC using a split ratio of 50:1. Compound separation was achieved following a linear temperature program of 50^{o}-250^{o}C (5^{o}C/min), 250^{o}C (20 min), so the total run time was 1 h. Percentage composition was calculated using a peak normalization method with response factors used to correct detector response for oxygenated compounds. Each sample was analyzed twice in the GC and results were calculated as averages. The GC/MS analysis was carried out on a

Varian Saturn 2200 GC/MS fitted with the same column and temperature programmed as the GC-FID. MS parameters: ionization voltage (EI) 70 eV, peak width 2 sec, mass range 40-500 amu and detector voltage 1.5 volts. Peak identification was carried out by comparison of the mass spectra with mass spectra available on NIST-1 and NIST-II libraries. The compound identification was finally confirmed by comparison of their relative retention indices (RRI) with literature values [Vichi et al, 2007].

4.3 Solvent extraction for water removal

The whole bio-oil (50mL) was extracted separately with chloroform (CHCl3), benzene, and ethanol. For extraction purposes, 50mL of the solvent was added and this process was repeated three times to ensure that maximum extracts had been recovered. The effluent (soluble in the solvent) was concentrated in a rotary evaporator under vacuum and then tested following the procedures outline in section 4.2.

4.4 Catalyst preparation

4.4.1 Aluminosilicate Preparation

All catalysts were obtained from commercial catalyst providers. ZSM-5 (CBV 5524G, SiO_2:Al_2O_3 = 50), HY (CBV 712, SiO_2:Al_2O_3 = 5.2), and Beta (CP 814E, SiO_2:Al_2O_3 = 25), zeolites were obtained in their ammonia form from Zeolyst International, Conshohocken, Pennsylvania, USA. The γ-alumina was obtained from Derivados del Fluor, Spain and the fluid catalytic cracking (FCC) catalyst was obtained in a coke-deactivated state from Refinería la Pampilla, Callao, Spain. All

three zeolites were activated into their acid forms using a 7-step calcination program shown in Figure 4.1, following a procedure given in the literature [Villanueva Lopez, 2007]. This procedure was proven successful in removing all ammonia from the zeolites without causing structural damage or sintering. The FCC catalyst regenerated was performed in a furnace at 550°C for 2h to burn off the coke.

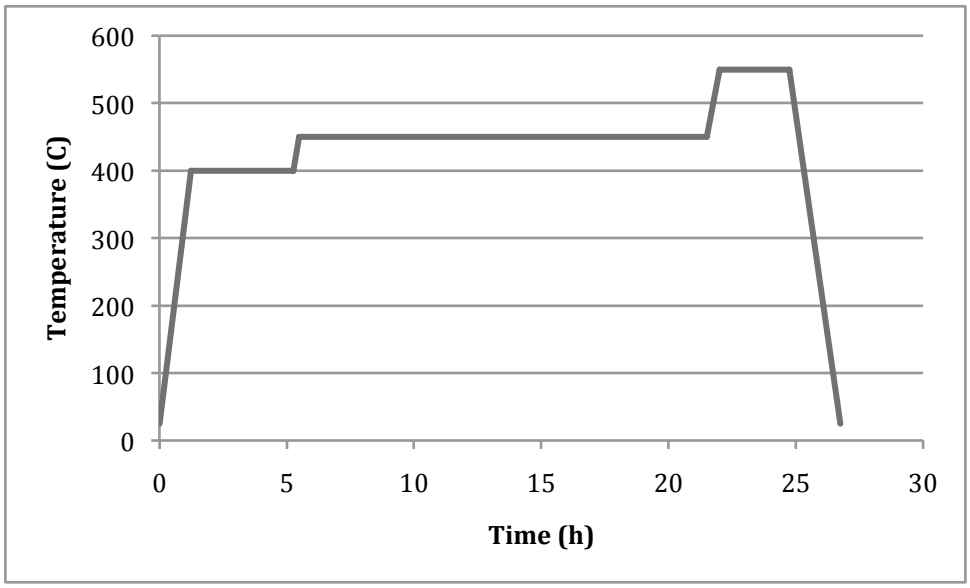

Figure 4.1: Temperature program used to obtain zeolites in acid-form.

4.4.2 Metal Catalyst Preparation

Incipient wetness technique was used to impregnate the desired active aluminosilicate support, ZSM-5 (in its ammonia form) using a rotary evaporator shown in Figure 4.2. The desired support was placed in the rotavapour's bulb, and vacuum was obtained via vacuum pump. The aqueous metal solution was fed through a burette into the bulb with the support (approximately 20mL at a time until all the solution was consumed). The water evaporates via the condenser

leaving behind a metal-impregnated support. This catalyst was then activated through the temperature ramp displayed in Figure 4.1.

Impregnations were as follows: 8 and 13 wt% Mo, 2.5 and 5 wt% Ni, 2.5 and 5 wt% Sr, 5 and 10 wt% W, CoMo (2.2 wt% Co and 8.5wt Mo) and NiMo (2.5wt% Ni and 13 wt% Mo).

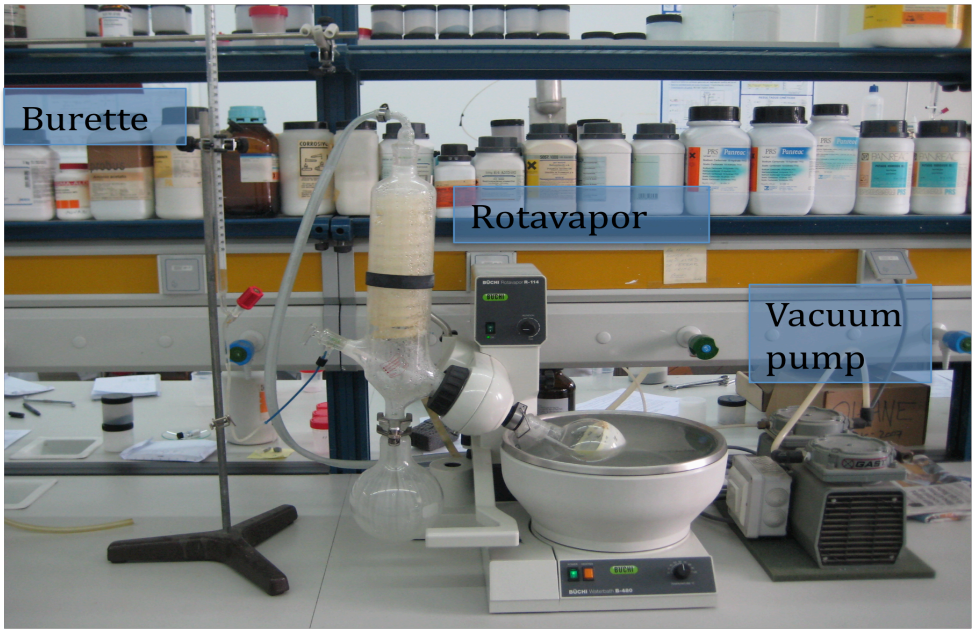

Figure 4.2: Rotary evaporator apparatus used for incipient wetness impregnation

4.5 Catalyst characterization

Several characterization techniques were applied to both the aluminosilicates and the metal-impregnated ZSM-5. These methods were used to define the morphology and structure of the catalysts, as well as to explain the exhibited behaviour of the catalysts.

4.5.1 X-ray powder diffraction (XRD)

The crystal structure of the fresh and activated catalysts were monitored by comparing the X-ray powder diffraction patterns of the catalysts with those corresponding to the literature. The diffractograms were collected by using a PHILIPS X'PERT PRO automatic diffractometer operating at 40 kV and 40 mA, in theta-theta configuration (sample is stationary in x-ray tube while the detector is rotated around the sample), secondary monochromator with Cu radiation (λ = 1.5418 Å) and a PIXcel solid state detector. The samples were mounted on a zero background silicon wafer fixed in a generic sample holder. Data was collected from 7 to 70° 2θ (step size = 0.026 and time per step = 98 s) at room temperature. A fixed divergence and antiscattering slit giving a constant volume of sample illumination were used.

4.5.2 Thermogravimetric Analysis (TGA)

The phase of the aluminosilicate was further monitored by thermogravimetric analysis (TGA) by heating a 5 mg sample of the catalyst to 650°C for 30 min at 10°C/min under nitrogen flow of 60 mL/min. Using a Perkin-Elmer (Pyris Diamond) TGA instrument, data was collected at 0.5 s intervals. Through this analysis it was obvious whether the zeolites were in ammonium or hydrogen form. For example, if ammonia was present, the release of the ammonia would be detected as a peak during analysis.

4.5.3 N_2 Adsorption/Desorption

The Brunauer-Emmett-Teller (BET) surface area, pore volume, and pore diameter of the aluminosilicates and metal-impregnated catalysts were analyzed by adsorption-desorption of N_2 at 77 K in a Micrometrics 2000 ASAP analyzer. A 0.05 gram quantity of each sample was degassed for 2 h under vacuum conditions and a temperature of 200°C. The physical characteristics of each sample were determined using the procedure developed by BET [Gregg et al, 1977].

4.5.4 Ammonia Temperature Programmed Desorption (TPD)

The total acidity and acid strength distribution was determined by calorimetric measurements of differential adsorption of ammonia and temperature programmed desorption (TPD) of ammonia. The NH_3 adsorption-desorption experiments were carried out in a simultaneous thermobalance, SDT 2960 (TA Instruments) connected on-line to a mass spectrometer, Thermostar (Balzars Instruments).

Approximately 30 mg of catalyst was loaded in a vial and placed within the SCT 2960 apparatus. The catalyst impurities were removed by heating the sample to 500°C in the presence of helium for one hour. Once the sample was cooled and stable at 150°C, adsorption began by injecting ammonia through a syringe. The sample remained at 150°C for 1 h to ensure full adsorption. Finally, the temperature was ramped to 850°C and the ammonia desorbed was quantified through mass spectroscopy.

4.5.5 Fourier Transform Infrared (FT-IR) Spectroscopy

The nature of the active sites, Brønsted type (proton donor) or Lewis type (coordinate base) was determined by diffuse reflectance Fourier transform infrared spectroscopy (FT-IR) of adsorbed pyridine [Aguayo, 2005]. The spectrophotometer used was a Nicolet 740 provided with a Spectra Tech vacuum catalytic chamber. Each catalyst was prepared in pellet form with potassium bromide (KBr). After inserting the pellet into the chamber of the FT-IR apparatus, the body was heated to 150°C. Once the body was stable at 150°C, the sample was heated to 300°C for 30 minutes, and then cooled to 150°C to remove impurities. Pyridine was injected via a septum (~120 ml of pyridine gas), and left to adsorb for 5-10 minutes.

The nature of the active sites was determined by FT-IR spectrometry of adsorbed pyridine. The band at 1545 cm^{-1} is assigned to the vibrational tension of the C-C bond of pyridinium ion and indicates the presence of Brønsted sites. The band at 1455 cm^{-1} is assigned to the vibrational tension of C-C coordinate bond of pyridine complex, which is an indication of Lewis acidity [Aguayo, 2005]. The Brønsted/Lewis site ratio was determined from the ratio of the areas corresponding to the respective bands.

4.5.6 Transmission Electron Microscopy (TEM)

Transmission electron microscopy, allowed for the measurement of the distribution of the metal particles on the support. The TEM images were retrieved using a Phillips CM200 apparatus. Each sample was prepared by sonification in ethanol for 10 minutes. The sample was then placed on a 200 mesh Cu grid coated

with a porous carbon film and allowed to dry overnight. The sample images ranged from 20k to 500k times magnification.

4.5.7 Inductively Coupled Plasma Mass Spectroscopy (ICP-MS)

The elemental compositions of the fresh metal-impregnated catalysts were analyzed with a Thermo Xseries 2 ICP-MS instrument. This method identified exact metal content by applying ICP to produce ions from the sample and MS to separate and detect ions. It is a useful instrument as the actual and desired metal contents can differ.

50mg of sample was prepared by mixing with a 1:2 HNO_3:HF. This solution was kept at 90°C for 24hrs. Hypochlorous acid (HClO) was then added and the solution was placed on heat until the acid had evaporated. Next, HCl was added and again the solution was placed at 90°C for 24hrs. Finally, the sample was diluted with milli-Q water to reach a final volume of 25 mL.

4.5.8 Summary of Characterization techniques

All characterization techniques are summarized in Table 4.1.

Table 4.1: Summary of catalyst characterization techniques and their objectives.

Characterization Technique	**Objectives**
Powder X-ray diffraction (XRD)	Monitor structure and phase purity
Thermogravimetric Analysis (TGA)	Monitor phase purity
Surface area and porosity measurement by nitrogen adsorption (BET)	Determine pore size distribution, pore volume and surface area. The sorption properties of molecular sieves also provides information on hydrophobic/hydrophilic character
Temperature programmed desorption (TPD)	Quantify and identify acid sites by adsorption of NH_3
Fourier transform infrared (FTIR) spectroscopy	Aid in determination of structural details and acid sites presence by identifying function groups present
Transmission electron microscope (TEM)	Observation of exterior surface of catalyst
Inductively Coupled Plasma Mass Spectroscopy (ICP-MS)	Quantification of actual metal content impregnated on catalyst.

4.6 Upgrading of model phenol compounds with aluminosilicates

The reaction equipment, PID Eng&Tech Microactivity Reference V3.0 reactor model MAPXXM4, is provided with a cylindrical reactor of 7.9 mm internal diameter and 300 mm length. This reactor operates in an isothermal fixed bed regime and is placed within a stainless steel chamber heated by electrical resistance. The reactor temperature is controlled and monitored by a temperature controller. Temperature is noted by means of two thermocouples, one located in the middle of the catalytic bed and the other one at the wall of the chamber used for heating the reactor. The reactor process flow diagram is shown in Figure 4.3.

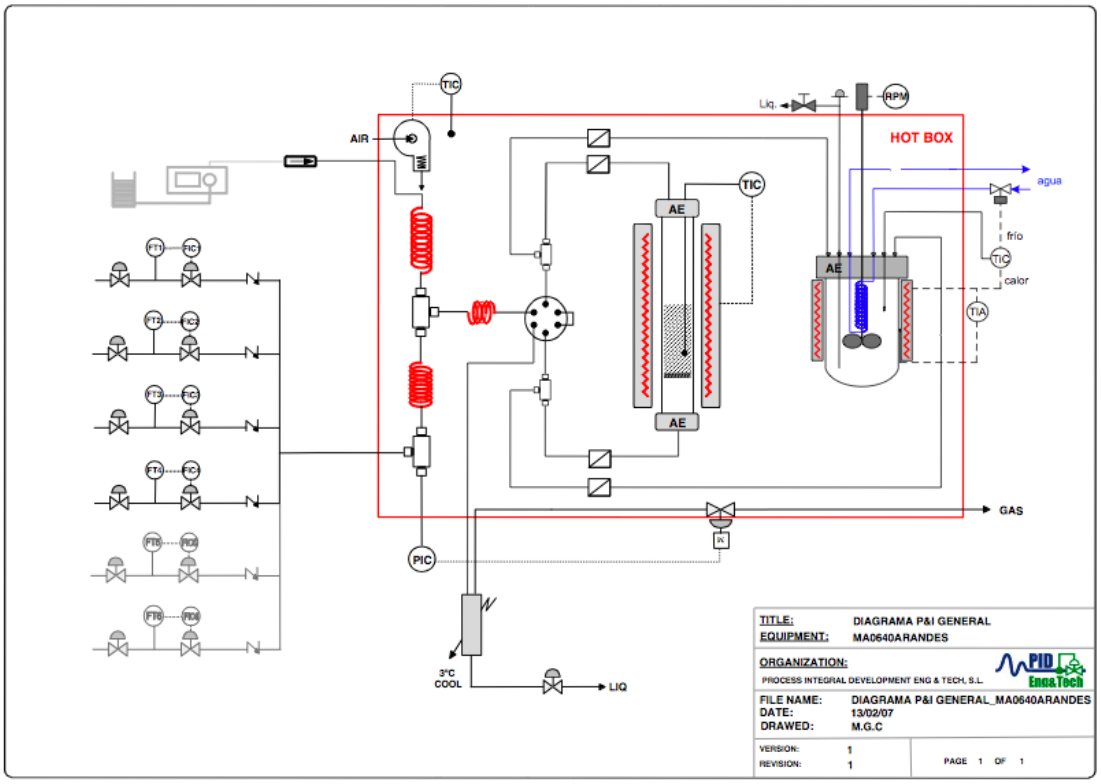

Figure 4.3: PFD of reactor set-up utilized in research

Experiments were conducted with an aluminosilicate catalyst (dried at 105°C overnight in an oven) layered with silica carbite in the reactor on top of glass wool. The reactor and catalyst were heated to 350°C in the presence of 30 mL/min of nitrogen. The gas was then switched to hydrogen where the reactor was kept isothermal for 30 minutes in the presence of 35 mL/min H_2. The feed (a 1:1 mixture of phenol and xylenes) was fed into the heated reactor using a high pressure Harvard syringe at a constant flowrate of 0.035 mL/min. Reaction was then conducted at 350°C, a hydrogen partial pressure of 50 bar, a hydrogen:oil ratio of 1000 (based on volumetric flow), and a LHSV (based on catalyst volume of 1 mL) of 2.1 h^{-1}. Gases were controlled by a Bronkhurst mass flow meter.

Liquid and gas samples were collected and separated at the outlet stream by means of A Peltier condenser. The gas samples were analyzed by a Micrometrics MicroGC-MSD. The microGC was equipped with 4 columns and injections were taken every 5 minutes. The liquid samples were analyzed in a Hewlett-Packard 5890 series II gas chromatograph provided with a FID (flame ionization detector). A capillary column (PONA Crosslinked Methyl Silicone, 50 m x 0.2 mm x 0.5 μm with a flowrate of the carrier gas ((He) of 1 cm^3 min^{-1}) is used for the analysis with an injection volume of 0.2 μL. Mass balances were carried out for each experiment. The retention times of the relevant products are set out in Table 4.2. Furthermore, response factors (size of spectral peak proportional to the amount of the substance that reaches the detector in the GC instrument) of oxygenated and aromatic compounds were calculated through methods described by Dietz [1968]. 1:1 mixtures of compound with a known response factor (hexane with a known response factor of 1) and a compound with an unknown response factor were injected into the GC and the response factor of the unknown was calculated based on peak area differences. This was necessary as no detector responds equally to different compounds. These are also listed in Table 4.2. The remainder of the liquid characterization methods can be viewed in section 4.2.

Table 4.2: Production and retention times for products in the chromatographic analysis

	Retention time (min)	Product	Calculated response factor
1	5.5-8.5	Hydrocarbons	1.0
2	14.98	2,5-dimethyl naphthalene	1.05
3	17.03	Benzaldehyde	0.79
4	18.99	Phenol	0.76
5	21.91	1,3 dimethoxy benzene	0.72
6	22.68	naphthalene	1.04
7	25.33	2-methyl naphthalene	1.05
8	26.75	vanillin	0.71
9	29.08	phenol-2,6-dimethoxy-4-(2-propenyl)	0.81
10	29.83	Benzaldehyde, 4-hydroxy 3,5-dimethoxyphenol	0.72
11	31.36	Ethanone, 1-4 hydroxy 3,5 dimethoxyphenol	0.78

4.7 Upgrading of moisture-free bio-oil with various metal-impregnated zeolites

4.7.1 Metal catalyst screening reactions

Hydrotreatment was carried out in a Parr batch reactor model 4567 (Figure 4.4). The metal impregnated catalysts were dried in an oven overnight at 105°C and then reduced in a fixed-bed reactor. Reduction was carried out in the presence of hydrogen and a heating rate of 2°C/min to 600°C. The catalyst was then cooled in the presence of He. Once cooled, the catalyst was passivated with a mixture of 1% O_2 and 99% He for 2 h. The passivated catalyst was then transferred to the Parr batch reactor where 20 g of tetralin was added. The catalyst was re-reduced in the

presence of the tetralin, a hydrogen pressure of 60 bar, a temperature of 300°C, and stirring rate of 200 rpm for 2hr.

Figure 4.4: Parr batch reactor model 4567

Next, the reactor was quenched to cool and the reactants were added: 10 g of moisture-free bio-oil, 20 g of tetralin, and 1 g of catalyst. After sealing of the reactor, 0.5 MPa of hydrogen was used to flush out the oxygen present. Flushing was repeated a total of 3 times. Stabilization of the moisture free bio-oil was carried next to react the most volatile components in order to reduce excessive polymerization and coking. The conditions for this step were 120°C, 3 MPa of hydrogen pressure at ambient temperature, and a stirring rate of 500 rpm for 30 min. After stabilization, reaction commenced at 330°C, 3 MPa, tetralin:oil of 4:1 and a stirring speed of 500 rpm for 45 min. The reactor was quenched to cool and depressurized.

The liquid products and spent catalyst were separated using gravity filtration. Liquid products were characterized using the methods described in section 4.2. Spent catalysts were washed with methanol and were analyzed using CHNS to determine extent of coking. It was not possible to re-use the catalyst or characterize them further due to excessive coking and tar build-up on the catalyst. No solvent was capable of recovering the catalyst.

The experimental conditions for screening reactions are summarized using schematic in Figure 4.5.

4.7.2 Optimization of Pressure and Reaction Time

Optimization of both pressure and time were carried out similarly to the screening of the metal catalysts. However, a commercial $NiMO/Al_2O_3$ catalyst was used. For pressure optimization, reactions were carried out at T=330°C, rpm=500, a tetralin:oil ratio of 4:1 and a reaction time of 1 h. Five experiments were carried out at five different pressures ranging from 1-5 MPa. Reaction time optimization experiments were carried out at T=330°C, P=3MPa, rpm=500, and a tetralin:oil ratio of 4:1. One experiment was carried out under these conditions and samples were taken after the stabilization step and then after 15, 30, 45, 60, 75, and 90 min. Both reaction schemes used the same procedure presented in Figure 4.5 with adjustments to reaction parameters.

The liquid products and spent catalyst were separated using gravity filtration. Liquid products were characterized using the methods described in section 4.2. Spent catalysts were washed with methanol and were analyzed using

CHNS to determine extent of coking. It was not possible to re-use the catalyst or characterize them further due to the excessive coking and tar build-up on the catalyst. No solvent was capable of recovering the catalyst.

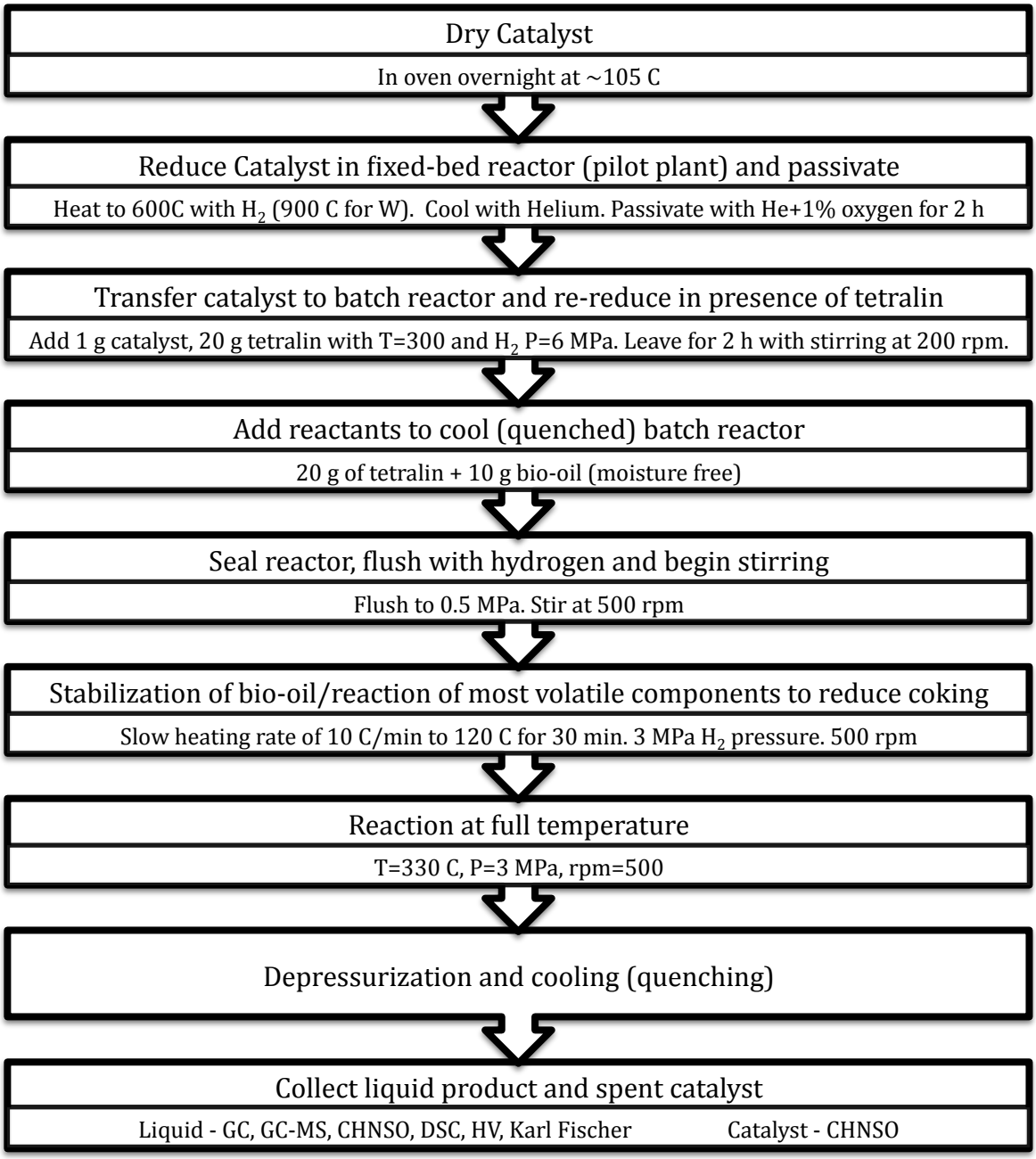

Figure 4.5: Experimental scheme for screening various metal-impregnated zeolites for activity in hydrodeoxygenation of bio-oil in a batch reactor.

4.7.3 Optimization of Temperature, Catalyst Loading and Solvent:Oil

The optimization of temperature, catalyst loading and solvent:oil was carried out in 17 experiments using 2.5% Ni/ZSM-5. The conditions for these reactions were generated by statistical design software, Design Expert 6.0 and are shown in Table 4.3. Each experiment used the procedure presented in Figure 4.5. However, reaction parameters were adjusted accordingly.

The liquid products and spent catalyst were separated using gravity filtration. Liquid products were characterized using the methods described in section 4.2. Spent catalysts were washed with methanol and were analyzed using CHNS to determine extent of coking. It was not possible to re-use the catalyst or characterize it further due to the excessive coking and tar build-up on the catalyst. No solvent was capable of recovering the catalyst.

Table 4.3: Planned experiments for the optimization of moisture-free bio-oil upgrading over 2.5%Ni/ZSM-5 in a batch reactor system as generated by statistical design software.

Run	Temperature ºC	Catalyst loading (g)	Solvent:oil
1	350	1.0	10
2	250	5.0	2
3	216	3.0	6
4	350	1.0	2
5	250	1.0	2
6	350	5.0	10
7	250	1.0	10
8	300	3.0	12.7
9	250	5.0	10
10*	300	3.0	6
11*	300	3.0	6
12	350	5.0	2
13	300	0.0	6
14	384	3.0	6
15*	300	3.0	6
16	300	6.4	6
17	300	3.0	1

*Repeat experiments

5 Results and discussion

5.1 Characterization of biomass

The maple sawdust pyrolysis feed obtained from Dynamotive was characterized to determine both its physical and chemical properties. The maple sawdust was also compared to pinewood to determine if hardwood species are similar in composition. Physical analysis included bomb calorimetry to determine heating value, oven and furnace heating to determine moisture, volatile, ash, and fixed carbon contents, CHNSO analysis to determine it's overall empirical formula, ICP-MS to identify metals present with the ash, and XRD to identify structural cellulose. Chemical analysis included TG analysis to evaluate devolatization of the key components, FT-IR to understand the chemical groups present, and HPLC of acid-soluble sugars to identify the monomers comprising cellulose and hemicellulose within the biomass.

5.1.1 Physical properties

The proximate and ultimate analysis of both maple sawdust and pinewood can be seen in Tables 5.1 and 5.2 below. From these tables it can be observed that both hardwoods possess very similar properties with minute differences. The moisture content for the maple sawdust was slightly higher than that of the pinewood as was the volatile matter and hydrogen to carbon ratio. However, the calorific value of the pinewood was marginally higher than the maple sawdust. Moreover the calorific value of pinewood in present study i.e. 19.6 ± 0.2 MJ/Kg

closely resembles the value (20 MJ/Kg) reported by Demirbas [74]. Therefore, these results follow closely with those reported by others.

Table 5.1: Proximate analysis of biomass

Plant Material	Proximate analysis (%)			
	moisture	**ash**	**volatile matter**	**fixed carbon**
Maple sawdust	6.6±0.2%	1.0±0.2%	88.3±0.2	4.1±0.2
pinewood	5.8±0.4	1.5±0.2	82.4±0.1	10.3±0.2

Table 5.2: Ultimate and calorific value of biomass

Plant Material	**Ultimate Analysis**					**Calorific Value (MJ/kg)**
	C	**H**	**N**	**S**	**O**	
Maple sawdust	47.5±0.2	6.7±0.1	0.06±0.02	0.01	45.7±0.4	19.0±0.2
pinewood	49.0±0.2	6.4±0.1	0.14±0.01	0.01	44.4±0.4	19.6±0.2

The inorganic elemental composition of ash from the maple sawdust was determined in ppm, the concentration of elements: Mg (16465), Al (2707), Ca (57059), P (7374), Cr (73), Mn (2651), Fe (9123), Co (63), Cu (339), Zn (4956), Sr (351), Sb (8), Ba (842), Pb (464) ppm. The elements such as Sc, Ti, V, Ni, As and W were not detected.

The XRD analysis of cellulose and lignin in the maplewood are presented in Figure 5.1. The intense X-ray diffraction peak was detected at a 2θ value of 20 for both maple sawdust and pure cellulose. The plate count of the biomass was 974015 and 1551389 at 13 and 20 2θ values, respectively. Whereas the plate count for pure cellulose was 189122 and 690750 at 13 and 20 2θ values, respectively. The plate count was related to the crystallinity behaviour of the sample. The crystallinity of

the surface is mainly related to the wax content (high molecular mass hydrocarbons and fatty components) in the biomass [Zhang et al, 2008]. However, the overall crystallinity of biomass depends on wax, cellulose content and on the complex nature of bonding [Meshitsuka et al, 1996] between cellulose, hemicellulose and lignin. Therefore, further study on nature of bonding between major chemical classes in the biomass is necessary to confirm the observations done through XRD.

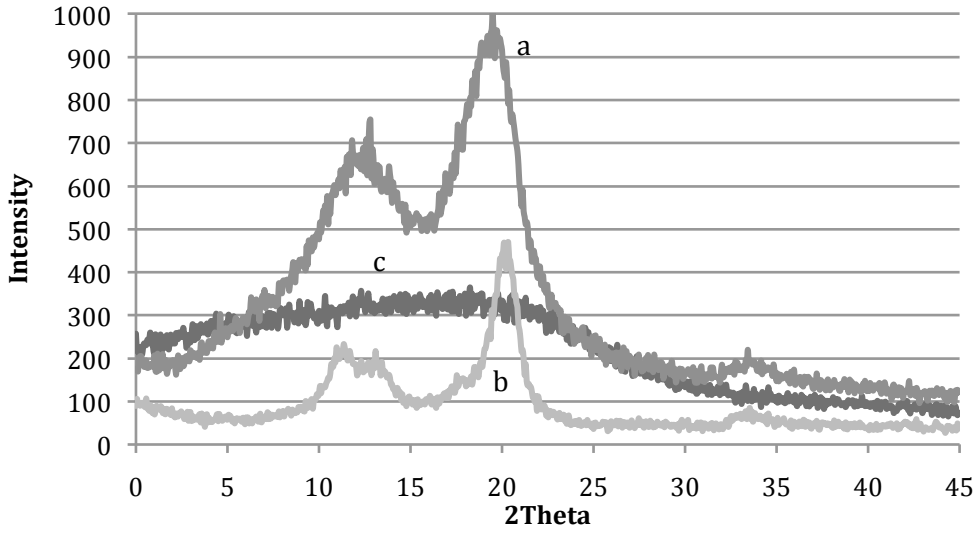

Figure 5.1: XRD analysis of bio-mass samples: a-maple sawdust, b–cellulose, c-lignin.

5.1.2 Chemical properties

The behavior of biomass materials during TGA devolatilization was related to the presence of chemical constituents such as cellulose, hemicellulose and lignin [Raveendran et al, 1996]. The devolatilization behaviors of maple biomass along with cellulose and lignin were presented in Figure 5.2. The onset temperature of devolatilization was in the range of 200-250°C, which corresponds to 5% weight loss with respect to the total weight loss. The bulk of the weight loss ends at 310-

350°C followed by a slow and continuous weight loss. The bulk weight loss was attributed to the primary devolatization, where as the remaining slow continuous weight loss was attributed to the degradation of heavier chemical structures in the solid matrix [Fischer et al, 2002]. Quantitatively, the volatile matter released in the primary devolatilization was more significant than in the secondary devolatilization.

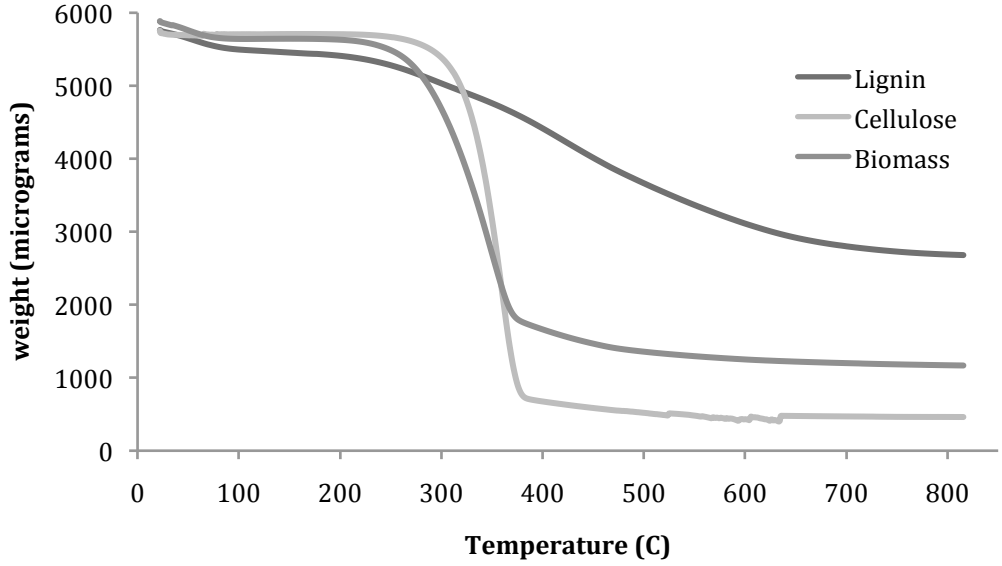

Figure 5.2: Thermogravimetric analysis of maple sawdust biomass, cellulose and lignin

The devolatilization characteristics of cellulose and lignin exhibited during TG analysis were quite different (Figure 5.2). In the case of cellulose, the onset temperature was 319°C, maximum devolatization occurred at 354°C and finally completed at 380°C. The volatiles released after the primary step of devolatization were 79.6%. In the case of lignin, it decomposed in a wider temperature range than cellulose. The lignin bulk weight loss (60%) occurred at 500°C, a much lower temperature than that observed for cellulose. The lignin continued to decompose at

a very slow rate until completion at 800°C. In a similar study, Biagini *et al.* [2006] studied the devolatilization of hemicelluloses using xylan as a standard molecule. The onset temperature was 253°C and maximum weight loss was 299°C. The volatile matter released after primary devolatilization was 76.3% and complete devolatilization occurred around 370°C. The weight loss, as shown in Figure 5.2, can be explained as follows: the weight loss at temperatures less than 100°C is for loss of highly volatile material, the temperature range of 100-130°C accounts for loss of water, 130-250°C for volatile compounds, 250-350°C for hemicellulose, 350-500°C for cellulose and lignin and 500-800°C for lignin. The rate of loss of weight of biomass, cellulose and lignin are presented in figure 5.3. The rate of loss of weight has a maximum value at 300-400°C for biomass and cellulose but lignin followed a wider temperature range from 200-700°C.

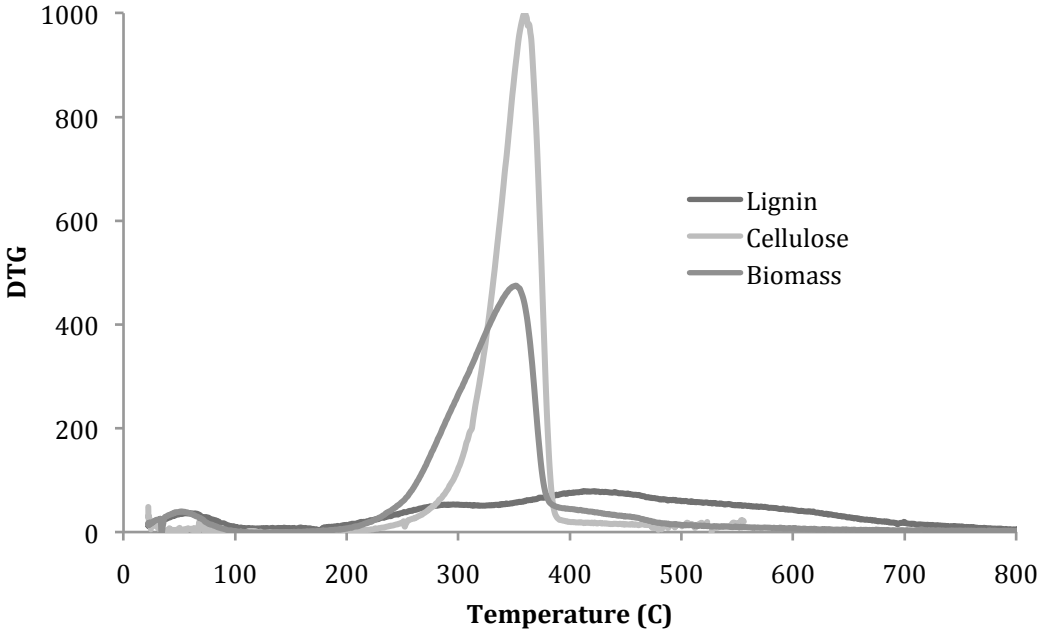

C

Figure 5.3: DTG analysis of wheat-hemlock biomass, cellulose and lignin

The FT-IR studies (Figure 5.4) revealed that the most prominent peaks in the spectrum originate from –OH stretching vibration (3370-3420 cm^{-1}) and CH_2 and CH_3 asymmetric and symmetric stretching vibrations (2935-2915 cm^{-1}). These vibrations are expected from hemicellulose, cellulose and lignin. Very intense peaks in the region 1742-1620 cm^{-1} originate from the stretching mode of carbonyls; mainly ketones and esters [Rout et al, 2009]. Mainly these bands are expected from waxes such as fatty acids, fatty esters, and high molecular mass aldehydes/ ketones. It is interesting to denote that the biomass and bio-oil have very similar IR spectra. Pyrolysis of the biomass only seems to shift the chemical groups towards a higher concentration of ketones and esters, as those are the peaks which become more defined as the biomass is transforms thermochemically to bio-oil.

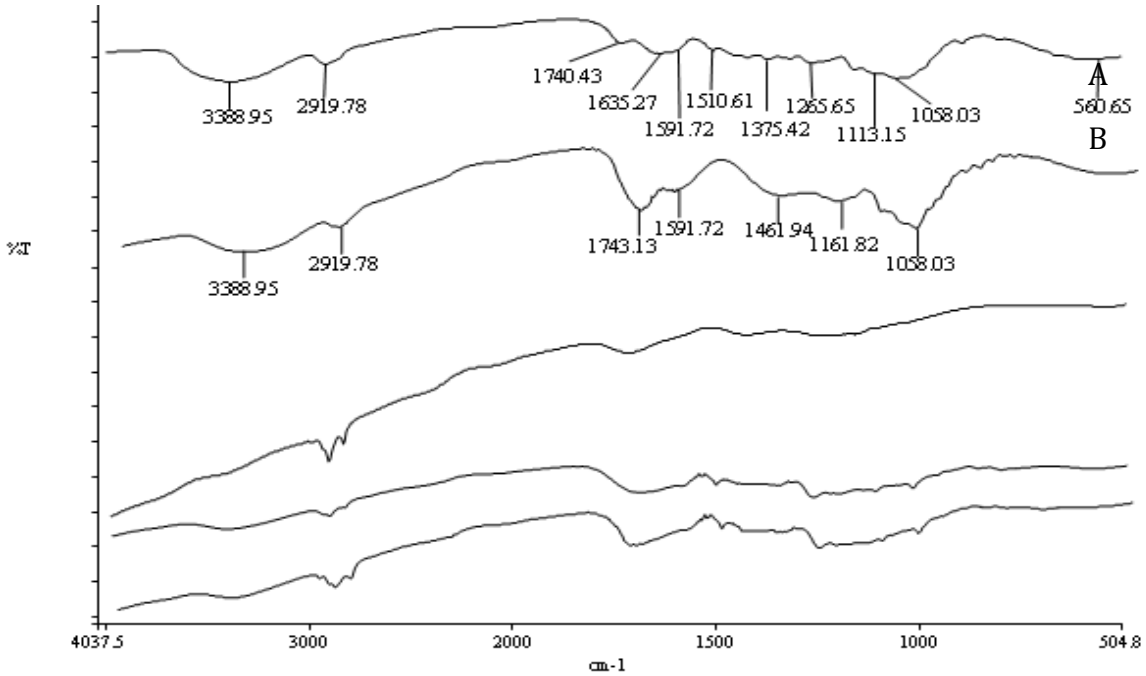

Figure 5.4: FT-IR spectra: a-biomass, b-bio-oil

To determine the total sugar content, the biomass was treated with dilute H_2SO_4. During the process of acid hydrolysis, the sugars brake down into monomers

which can then be detected by HPLC which only detects the sugars in their monomeric forms. The percentage of sugars detected in the biomass was glucose (56.4 %), xylose (6.3 %), galactose (1.9 %), arabinose (31.8 %) and mannose (3.6 %). Cellulobiose was not detected in sugar analysis. The acid insoluble portion of the biomass (lignin) was 21.5 % and with the remaining percentage designated as cellulose and hemicellulose. The maple sawdust also contained wax (2-3 %).

5.2 Characterization of crude bio-oil

The crude bio-oil and its moisture-free derivative were characterized in order to determine their physical properties (or fuel characteristics), approximate elemental composition, and chemical composition. The physical characteristics were determined through bomb calorimetry to determine the heating value, cone and plate viscometer to determine the viscosity, Karl Fischer analysis to quantify the moisture present in the oil, CHNSO analysis for the empirical composition, and furnace methods to determine ash contents. Chemical analysis included FT-IR to identify chemical groups present and GC-FID couples with GC-MS to identify and quantify chemical groups present.

5.2.1 Physical properties

Table 5.3 below summarizes the physical properties of the crude bio-oil. The bio-oil contained a low percentage of C (36.5%) and high percentage of O_2 (55.0%). The low H/C ratio and high H/O ratio suggested the bio-oil contained more oxygen in comparison to carbohydrate, and thus is not suitable for direct application as fuel. Furthermore, the calorific value of the bio-oil is not significantly different than

that of the biomass (19.0 MJ/kg). From this, it can be concluded that fast pyrolysis does little to increase the recoverable energy of the biomass and further reforming is needed. What is most significant is the high moisture content. This contributes to the low heating value and oxygen content. If water could be removed, the bio-oil's energy content would be drastically improved. Furthermore, it would not poison catalysts during upgrading.

Table 5.3: Physical properties of crude bio-oil

Property	**Crude Bio-oil**
Heating Value (MJ/kg)	21.6
Ash Content (wt%)	0.03±0.01
Moisture content (wt%)	30.6±0.6
pH	5.0±0.2
Viscosity (cP)	-
C (wt%)	36.5±0.2
H (wt%)	8.60±0.1
N (wt%)	0.03±0.01
S (wt%)	0.01
O_2 (wt%)	55.0±0.3
H/C ratio	0.23
H/O ratio	0.16

5.2.2 Chemical properties

Through the FT-IR study (Figure 5.4), it was possible to observe the functional groups of bio-oil as well as the biomass feedstock. The O-H stretching

vibrations 3200-3500 cm^{-1} indicate the presence of phenols and alcohols. The broad band in bio-oil indicated many of the chemical groups are involved in hydrogen bonding with water. The peak between 1700-1750 cm^{-1} indicated the presence of ketone and aldehyde groups. The presence of both O-H and C=O stretching vibrations also indicated the presence of acid groups. Symmetrical and asymmetrical C-H stretching vibrations of aliphatic CH_3 and CH_2 groups (2850-2950 cm^{-1}) and C-H bending vibrations between 1350 and 1450 cm^{-1} indicated the presence of alkane groups, where as the peak at 1380 cm^{-1} indicated the presence of CH_3 groups. The peaks between 1450-1550 cm^{-1} represent C=C stretching vibrations that are indicative of both alkanes and aromatics (mono and polycyclic).

It was not possible to analyze the crude bio-oil using GC-MS due to the high moisture content. The column and detector could not handle moisture contents over 2wt%. Therefore, detailed identification of chemical compounds in the crude bio-oil was not possible. Quantification of generalized chemical groupings was possible by comparing retention times of identified model compounds and other identified moisture-free bio-oil samples injected. Table 5.4 below summarizes the quantities of chemical groups found in crude bio-oil. It should be noted that 30.1% of the bio-oil is water.

Table 5.4: Quantification of chemical groups present in crude bio-oil

Chemical group	**wt% present within crude bio-oil**
High MW oxygenates	43.0
Low MW oxygenates	6.8
Hydrocarbons	20.1

5.3 Water removal via solvent extraction

Solvent extraction was explored using three different solvents with varying character; ethanol, chloroform, and benzene. The objective of extraction was to remove water and shift the chemical composition to one with lower oxygen content. The ideal extractive would isolate phenol derivatives, furanoids, benzanoids and other compounds with high H/C ratios and low oxygen contents. Ethanol was chosen for its polarity, benzene for it's non-polar nature, and chloroform for it's slightly polar nature. Variation of polarity was explored due to the complex nature of the bio-oil. Figure 5.5 shows the results from the extraction. Not surprisingly, the solvent with the most versatility, chloroform, which possesses both non-polar and polar characteristics, performed the best. Chloroform produced the highest yield of desirable effluent, 24.0%, in comparison to yields from ethanol, 13.5%, and benzene, 10.9%. Chloroform was successful in producing the most desirable composition (a hydrocarbon mixture with lower overall oxygen content). Chloroform lowered the high MW oxygen content of the crude oil from 43wt% to 30wt% and increased the hydrocarbon content from 20.1wt% to 40.5 wt%. Chloroform was also successful in water removal; the extractive contained <0.02wt% moisture.

Table 5.5 summarizes the physical properties of the moisture-free, chloroform-extracted bio-oil. The extracted fraction contained a higher percentage of C (51.2%) and lower percentage of O_2 (42.1%) when compared to the crude bio-oil. Furthermore, the calorific value of the chloroform extract is significantly higher

at 44.0 MJ/kg. This is comparable to the heating value of gasoline, which is also 42-46 MJ/kg. This drastic change in heating value can be attributed entirely to the

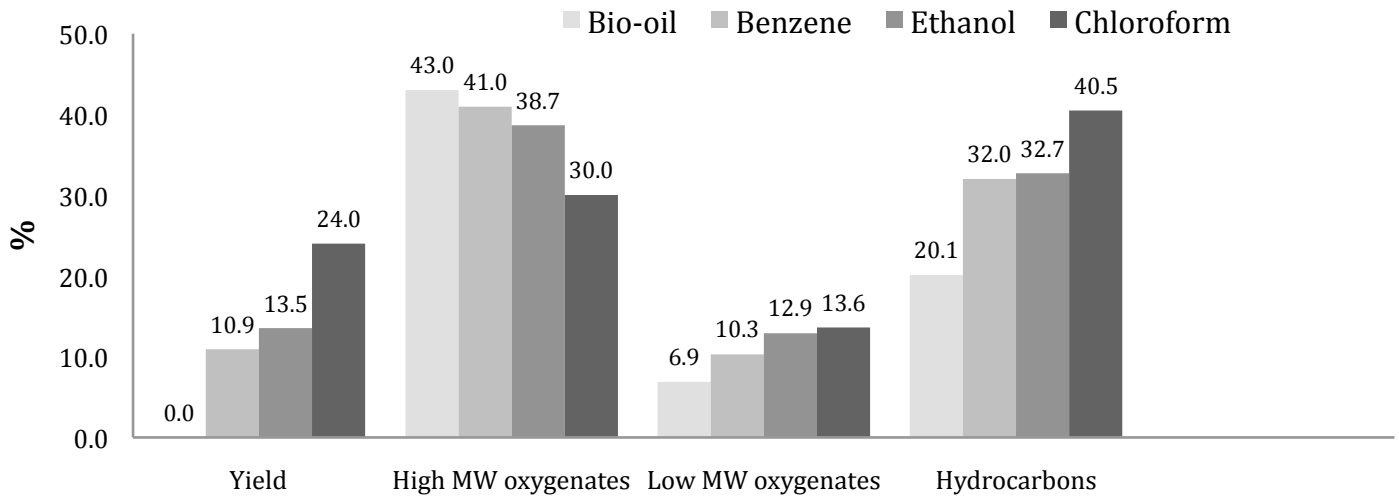

Figure 5.5: Yield and distribution of main chemical groups for each extractive in comparison with crude bio-oil

removal of water, as there is still a significant amount of oxygen in the bio-oil. However, this oxygen is mainly attributed to phenolic compounds, which have a higher energy content than most oxygenates.

Because the water content of the chloroform-extracted bio-oil was negligible, GC-MS was performed, coupled with GC-FID to obtain a detailed composition of the oil. Both the GC chromatogram (Figure 5.6) and a table of the identifiable compounds (Table 5.6) are shown below. In Figure 5.6, it can be see that the hydrocarbons come out first between the retention times of 4-8min. Next, ketone derivatives are grouped between retention times of 10-18min. From 18-30min, phenol and phenol derivates are detected. From 30-40min, bulk aromatics are

identified. From Table 5.6, it can be seen that phenols and ketones comprise the majority of the modified bio-oil with 36.2% and 32.9%, respectively

Table 5.5: Physical properties of chloroform extracted bio-oil compared to crude bio-oil

Property	**Crude Bio-oil**	**Chloroform extract**
Heating Value (MJ/kg)	21.6	44.0
Ash Content (wt%)	0.03±0.01	0.06±0.01
Moisture content (wt%)	30.6±0.6	0.02
pH	5.0±0.2	5.2±0.2
Viscosity (cP)	-	359
C (wt%)	36.5±0.2	51.6±0.3
H (wt%)	8.6±0.1	5.6±0.2
N (wt%)	0.03±0.01	0.05±0.1
S (wt%)	0.01	0.6±0.1
O_2 (wt%)	55.0±0.3	42.1±0.2
H/C ratio	0.23	0.11
H/O ratio	1.51	0.13

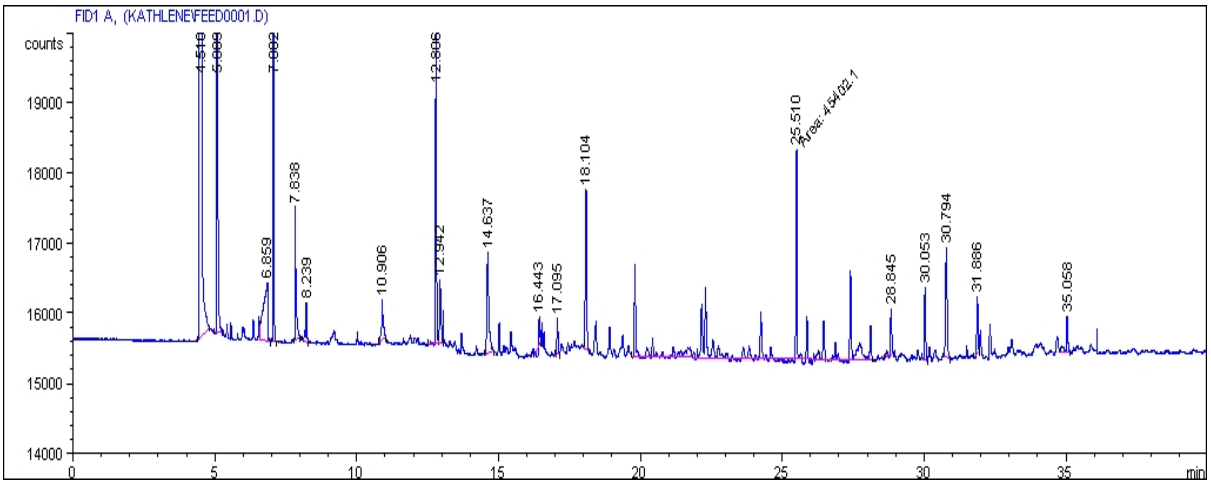

Figure 5.6: GC-FID chromatogram of modified bio-oil obtained over a 40min range using helium as the carrier gas and a split of 50:1.

Table 5.6: Identification and quantification of chemical compounds within moisture-free bio-oil

Retention time (min)	Chemical Compound	Wt%
4.5	Hydrocarbons	16.4
5.9		
6.9		
7.8		
10.9	2,5 dimethyl furan*	3.47
12.8	Propanone	11.63
12.9	Furfural	7.07
14.6	2-furanone*	4.93
16.4	2-cyclopenten-one	3.04
17.1	1,2 cyclopentanedione*	2.76
18.1	Phenol	8.32
19.7	Phenol, 3-methoxy	4.90
22.2	Phenol, 2-methoxy, 4-methyl	5.68
24.4	Phenol, 4-ethyl, 2-methoxy*	2.12
25.5	Phenol, 2,6-dimethoxy	9.89
26.5	Phenol, 2-methoxy, 4-acetate*	1.97
28.8	Phenol, 2,6-dimethoxy, 4,2 propenyl*	3.34
30.1	Benzaldehyde, 4-hydroxy-3,5-dimethoxyphenol*	4.14
30.8	Ethanone 1-(4-hydroxy-3,5-dimethoxyphenyl	5.03
31.9	2-pentanone, 1-(2,4,6-trihydroxyphenol)	3.43
35.1	Not identified	1.88

* not verified with standards, only NIST libraries

5.4 Performance of various aluminosilicates for the upgrading of phenol in a fixed-bed system

Originally, aluminosilicate screenings were conducted with the moisture-free bio-oil fraction obtained from chloroform fractionation. However, these runs needed to be terminated due to excessive lignin-polymerization, coking, and plugging of the reactor. The feed was then switched to phenol to explore the model compound (representing bio-oil) reaction mechanisms under the utilized conditions. Phenol, in particular, was chosen as the model compound because it made up more than 35% of the moisture-free bio-oil fraction and is the most abundant oxygenated compound present in bio-oil, and thus a main constituent in the essential upgrading.

5.4.1 Non-catalytic runs (blank runs)

One run was carried out without catalyst to examine the thermal effects on the phenol. Through this experiment, the effect of the chosen process parameters vs. catalyst became evident. Furthermore, these results can be subtracted from those obtained with catalyst to understand the catalysts role in the upgrading process.

During the non-catalytic run at T=350°C, P=5Mpa, a hydrogen:oil ratio of 1000, and a LHSV of 2.1 h^{-1}, it was observed that some of the xylene in the mixture was converted to ethylbenzene (10.7wt%) and trace amounts of cyclohexane (0.51wt%). Approximately 20% of the xylene was converted to less bulky hydrocarbons. However,

the phenol remained unreacted. The results from the non-catalytic run can be viewed in Table 5.7.

Table 5.7: Products detected after thermoconversion of 1:1 mixture of phenol and xylenes at T=350°C, P=5Mpa, a hydrogen:oil ratio of 1000, and a LHSV of 2.1 h^{-1}

Chemical compound	Weight%
Benzene	0
Cyclohexane	0.51
Ethylbenzene	10.7
p-xylene, m-xylene	29.2
o-xylene	4.98
Phenol	54.4

*0.05% of the mixture was undetectable trace compounds.

5.4.2 Exploration of reaction effects on xylene (without phenol)

Due to the fact that xylene was found to contribute to ethylbenzene formation during the non-catalytic run, one run was carried out to explore xylene's contribution to hydrocarbon formation over ZSM-5 at T=350°C, P=5Mpa, a hydrogen:oil ratio of 1000, and a LHSV of 2.1 h^{-1}. During this run, no new observations were made. Much like the non-catalytic run, approximately 20% conversion of xylene to ethylbenzene occurred with trace amounts of cyclohexane detected. Therefore, it can be predicted that approximately 20% of the xylene dilutant will be lost to ethylbenzene formation in all catalytic runs.

Table 5.8: Products detected from conversion of xylenes over ZSM-5 at T=350°C, P=5Mpa, a hydrogen:oil ratio of 1000, and a LHSV of 2.1 h^{-1}

Chemical compound	Weight%
Cyclohexane	0.5
Ethylbenzene	23.2
P-xylene, m-xylene	64.6
o-xylene	11.3

5.4.3 Catalyst Performance

ZSM-5, HY, beta, γ-alumina, and FCC (commercial fluid catalyst cracking catalyst composed of y zeolite amongst a matrix of silica) catalysts were screened using a feed of phenol dissolved in xylene (1:1 mixture) under the aforementioned conditions. Products formed during this reaction included char, gas, and an organic liquid containing aromatics, phenol derivatives as well as unreacted phenol and xylenes. The catalyst performance was based on benzene formation, as ethylbenzene formation was attributed to thermal degradation of xylene. Aromatic formation detected included benzene, ethylbenzene, and trace amounts of cumeme and toluene. However, the conversion of phenol to benzene was extremely low as can be seen in Figure 5.7.

Although these conversions are low, they are not wholly unexpected. Soltes and coworkers (Soltes et al, 1983 and 1987) conducted studies on the hydroprocessing of tars produced from the pyrolysis of biomass (a very phenolic substance). The tests were carried out under hydrotreating conditions (high pressure and temperature) in a batch reactor with decalin as a hydrogen donor. Various catalysts were screened and hydrocarbon yield varied from 56% on a Pd/alumina catalyst to 3% on silica-alumina. Therefore, it appears that Pd metal impregnation or impregnation of other metals that behave similarly to Pd is necessary to remove oxygen from phenol.

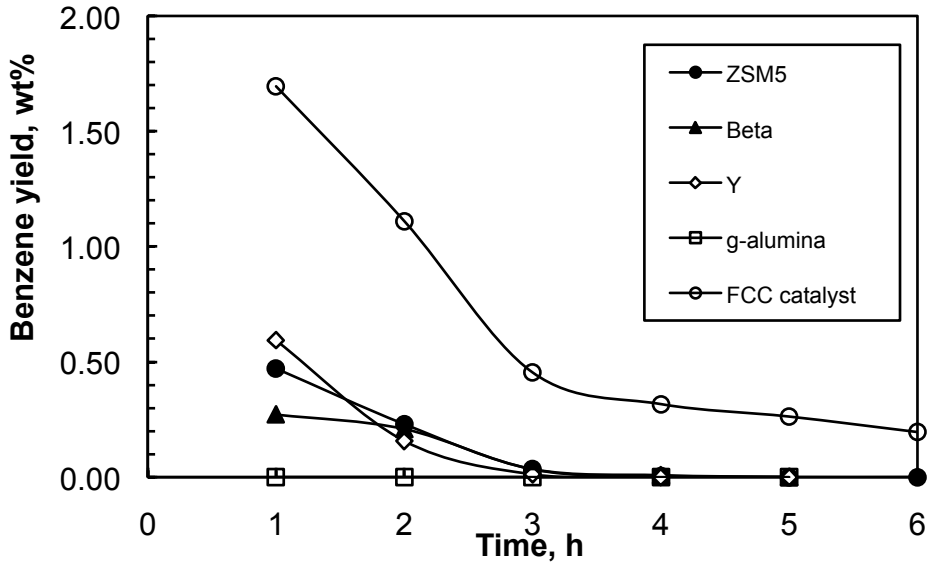

Figure 5.7: Conversion from phenol to benzene over various aluminosilicates at T=350°C, P=5Mpa, a hydrogen:oil ratio of 1000, and a LHSV of 2.1 h^{-1}

The low conversion results presented in this study can also be loosely compared to the model compound upgrading completed by Adjaye [1993]. However, Adjaye's results were obtained utilizing a fixed-bed reactor at a temperature of 330°C, atmospheric pressure, and 3.6 WHSV. HZSM-5 activity was explored over a mixture of model compounds representing bio-oil (propanoic acid, methyl ester of acetic acid, 4-methylcyclohexanol, cyclopentanone, 2-methylcyclopentanone, methoxybenzene, ethoxybenzene, phenol and 2-methoxy-4-(2-propenyl)phenol). The mixture of model compounds contained 14.6wt% phenol which produced 5.1% conversion to benzene. Their low phenol conversions were contributed to phenol's stable nature. It was predicted that isomerization of the original molecule was the main reaction route in their studies. Nonetheless, the conversions obtained in the present study were still 2-5 times lower than those

obtained by Adjaye. This could be due to the difference of reaction conditions. In the present study, a high pressure of 5 MPa was utilized along with a hydrogen:oil of 1000. Adjaye utilized atmospheric pressure and no hydrogen was present.

Furthermore, from the literature reviewed in section 2.7.2 it can be concluded that the conversions obtained using metal-impregnated catalysts at high pressure are significantly higher than those with HZSM-5 at atmospheric pressure. It is notable to observe, that aromatization reactions also take place over zeolites or metal-impregnated aluminosilicates. However, these reactions commonly use a low hydrogen pressure. Therefore, the hydrogen pressure could be promoting aromatization reactions over cracking reactions on the ZSM-5. This would explain the selectivity for benzene observed in the products produced in the present study.

Now, the question arises, do pressure and the presence of hydrogen inhibit the shape-selectivity of the zeolites that allow for cracking and oxygen removal? Zeolites are proven to withstand high pressure with their stable structure. Only mechanical forces have been shown to compromise the structure. Therefore, pressure alone should not affect the reaction. However, hydrogen pressure plays a large role in the formation of products. Based on the results obtained from the present study, as well as the aforementioned results obtained from Adjaye, it would appear that hydrogen pressure lowers the activity of aluminosilicates. This can be explained by examining the basic reaction.

In any deoxygenation reactions (whether with zeolites or hydrotreating catalysts), the oxygen is removed (phenol is converted to hydrocarbons) in the form of CO, CO_2, and H_2O. Zeolites are known to deoxygenate through carboxylation and

dehydration (Adjaye, 1993). When using a zeolite to upgrade bio-oil, phenol, or other oxygenates under atmospheric pressure, the reaction is hydrogen limited (Bridgewater, 1996). Without hydrogen pressure, the oxygen is removed in the form of CO and CO_2 leaving limited hydrogen for hydrocarbon formation. When hydrogen pressure is added, it shifts the reaction, forcing oxygen to leave as water, and hydrogen is consumed. This results in a diminished potential hydrocarbon yield. For example, if a pyrolysis oil (C=52.6%, H=6.5%, O=40.8%) was used as a feed in a perfect hypothetical situation involving zeolites and all the oxygen was eliminated as CO, the hydrocarbon yield could be 27% with an H:C of 4. If the oxygen was eliminated as water, the maximum hydrocarbon yield could be 14% with a H:C of 1.4 (Churin, 1990). Thus, it can be inferred that hydrogen hinders hydrocarbon formation over zeolite catalysts.

The opposite is true when metal catalysts are used for oxygen removal. The reaction pathways used are; hydrogenolysis and hydrogenation, not carboxylation. These reactions are carbon limited. Therefore, when using metal catalysts, the highest hydrocarbon yield is obtained when oxygen is removed through H_20 formation and no C is consumed. Thus, when hydrogen pressure forces oxygen to leave as H_2O, it aids hydrocarbon formation with metal catalysts.

It is difficult to assess the total effect hydrogen pressure has on the present reactions with aluminosilicates. However, from what has already been formulated above, it can be understood that:

1. Hydrogen pressure hinders hydrocarbon formation when using an aluminosilicate without metal impregnation.

2. Hydrocarbon formation can be higher under hydrogen pressure when metal catalysts are employed.
3. Hydrogen pressure can, under the correct conditions with metal catalysts, help destabilize the phenol for higher conversions.

Therefore, all future upgrading work was explored using metal-impregnated zeolites where hydrogen pressure is desirable for high hydrocarbon yields. This work, along with extensive catalyst characterization, served as a means to choose an ideal support and design an appropriate metal-containing hydrotreating catalyst.

5.4.4 Characterization of aluminosilicates

Several characterization techniques were applied to the aluminosilicates explored. Pore size, structure and acidity were all important considerations in choosing an ideal support. The physical properties of the aluminosilicates were explored using x-ray diffraction, N2 adsorption, and thermogravimetric analysis. The acidity of the catalyst was explored through Fourier transform infrared spectroscopy of pyridine as well as the temperature programmed desorption of ammonia.

5.4.4.1 Physical properties of aluminosilicates

The quality and structure of each aluminosilicate was monitored by powder x-ray diffraction patterns. The collected diffractograms of the pure alumina-silicates are shown in Figure 5.8. These patterns confirm that each zeolite and alumina are in their pure forms. Furthermore, that the FCC catalysts possess fajausite Y zeolite

amongst the matrix substance, which is in agreement with the literature [Villanueava Lopez, 2007]. Thermogravimetric analysis of the zeolites (figure not shown) indicated that they were fully converted to the acid forms as no ammonia was released from the zeolites.

The physical properties of the catalysts prepared as described above are laid out in Table 5.9. From the average pore diameter reported, it can be seen that the pore volume varied from 0.25-0.96 cc/g. BETA (the 12-membered ring) was the largest of the zeolites and HY (the 8-membered ring) the smallest. HZSM-5 was moderate in both its pore diameter and surface area. Both HY and BETA zeolites exhibited high surface areas of 896 and 820 m^2/g, respectively. Pure alumina had both low surface area and pore volume. The FCC catalyst's surface area was limited by its matrix, nonetheless, it possessed the largest average pore diameter due to the same matrix.

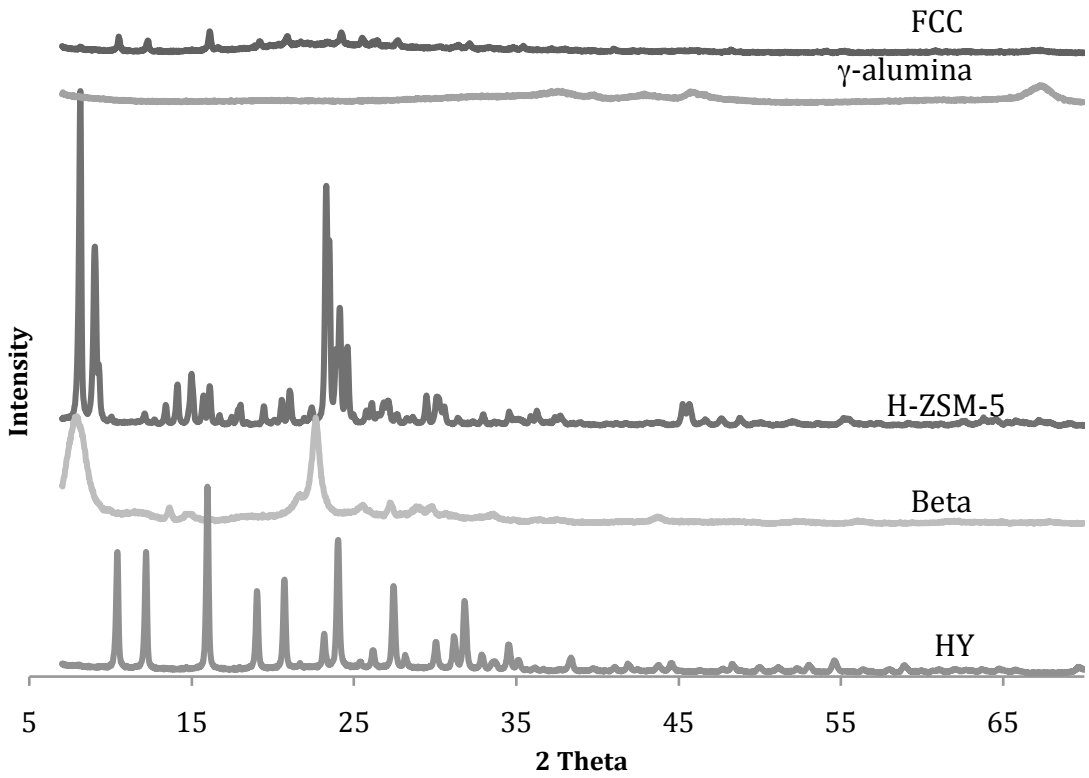

Figure 5.8: Powder X-ray diffraction patterns for pure alumina-silicates.

Table 5.9: Physical properties of aluminosilicates obtained from nitrogen adsorption

Catalyst	BET surface area (m^2/g)	Micropore area (m^2/g)	Micropore Volume (cm^3/g)	Total Pore Volume (cm^3/g)	Average Pore Diameter (4V/A)
H-ZSM-5	524	392	0.17	0.31	24
HY	896	813	0.35	0.47	21
BETA	820	544	0.23	0.96	47
Alumina	198	55	0	0.25	51
FCC	116	91	0.04	-	163

5.4.4.2 Acidity of the aluminosilicates

The nature of the acidity was determined through Fourier transform infrared spectrometry of adsorbed pyridine. The FT-IR spectra are given in Figure 5.9. The band at 1545 cm^{-1} is assigned to the vibrational tension of the C-C bond of the pyridinium ion and indicates the presence of Brønsted sites. The band at 1455 cm^{-1} is assigned to the vibrational tension of the C-C coordinate bond of the pyridine complex, which is an indication of Lewis acidity [Aguayo et al., 2005; Emeis, 2003; Delanney, 1984]. The peak at ~1490 cm^{-1} is a combination of Brønsted and Lewis sites that heavily favors Brønsted sites. The Brønsted/Lewis site ratio (Table 5.10) has been determined from the ratio of the corrected integrated area corresponding to the respective bands by applying the apparent integrated extinction coefficient reported in literature [Aguayo et al., 2005; Emeis, 2003]. In Table 5.10, it can be seen that ZSM-5 and the beta zeolite possessed the most Lewis acid sites after γ-alumina, while HY contained the most Brønsted acid sites after γ-alumina. The higher concentration of Bronsted acid sites for the HY zeolite could be due to its higher alumina content (it possesses the lowest silica to alumina ratio of 5.2). The higher alumina content enables more H protons creating more Bronsted sites. The ZSM-5 and BETA zeolites have higher silica to alumina ratios (50 and 25, respectively) allowing for higher Lewis site (electron pair donor site) concentrations. The FCC catalyst possessed the lowest concentration of acid sites of either type.

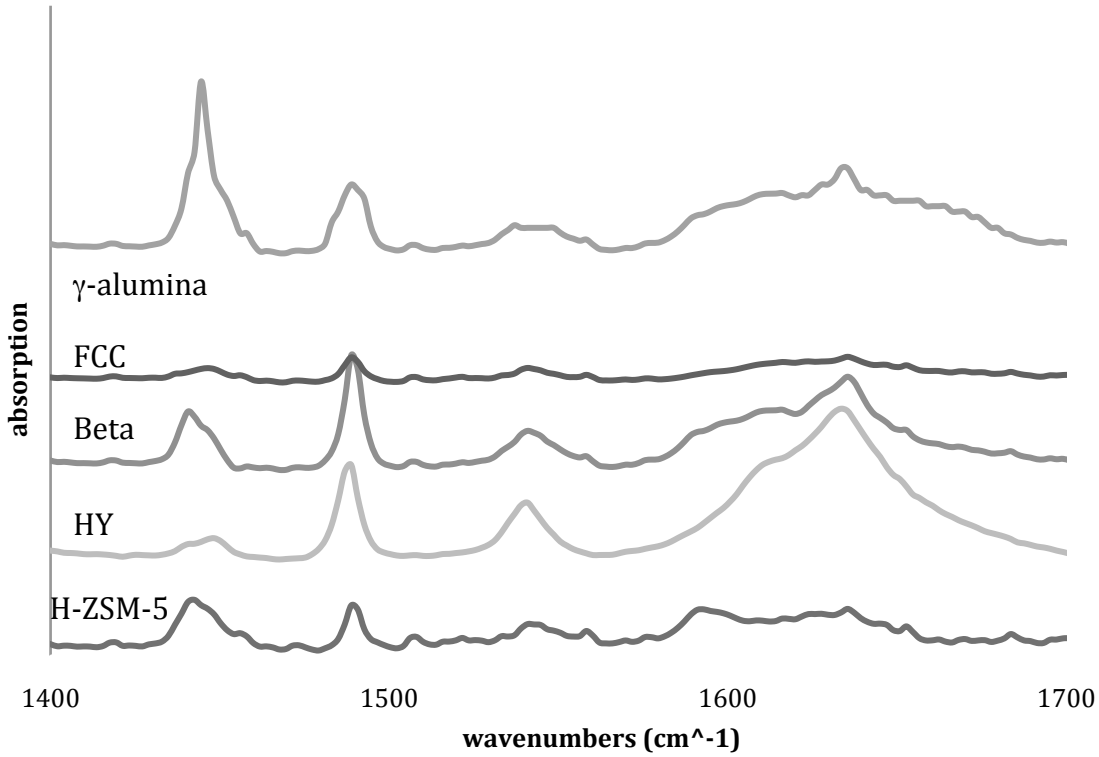

Figure 5.9: Comparison of Lewis (1450 cm^{-1}) and Brønsted (1550 cm^{-1}) acid sites obtained from FT-IR with pyridine for various aluminosilicates.

Table 5.10: Quantity of Lewis and Brønsted acid sites obtained from FT-IR with pyridine

Catalyst	Lewis - integrated area	Lewis - corrected area (μmol)	Brønsted - integrated area	Brønsted - Corrected area (μmol)	B/L
H-ZSM-5	1.37	3.04	0.59	0.98	0.32
Beta	1.12	2.49	1.23	2.05	0.82
HY	0.58	1.29	1.46	2.44	1.89
FCC	0.36	0.81	0.43	0.72	0.89
Alumina	2.13	4.73	1.47	2.45	0.52

Table 5.11 shows the results of total acidity of the catalysts and the maximum temperature achieved in the desorption process. From this table, it can

be concluded that the FCC catalyst possessed the highest total acidity and medium acid strength, closely followed by the ZSM-5. Furthermore, beta zeolite had high acid strength compared to HY zeolite. The lower acid strength of ZSM-5 is due to its higher silica to alumina ratio.

Table 5.11: Total acidity, ammonia adsorption heat and location of NH_3 desorption peaks for the different aluminosilicates obtained from temperature programmed desorption of ammonia

Catalyst	Total acidity (mmol/g cat)	Desorption peak (°C)	
		First peak	Second peak
ZSM-5	0.50	218	394
Beta	0.47	245	389
HY	0.41	213	355
Alumina	0.45	266	-
FCC	1.43	227	-

Figure 5.10 shows the results of the temperature programmed desorption of ammonia. The area under the curve indicates the total amount of ammonia desorbed, which is proportional to the total acidity, whereas the desorption temperature indicates the acid strength of the sites, given that the weaker acid sites require lower desorption temperature. From this figure it may be seen that the zeolites provided two desorption peaks that are characteristic of these catalysts, corresponding to sites of different acid strength. For ZSM-5 and beta, the first peak has a maximum at 210-270 °C corresponding to weak sites, and it is a main peak for the beta zeolite and a minor peak for both ZSM-5 and HY; the second peak appears at higher temperatures (in the 350-400°C) and is indicative of the presence of strong acid sites [Aguayo et al, 2005]. It is observed that the position of this high

temperature peak indicates a great amount of strong acid sites. In Figure 5.10, it is also clear that the area under the high temperature peak is much larger for HY than for ZSM-5, which indicates that the former has a greater amount of strong acid sites. This is in agreement with the aforementioned physical properties, silica to alumina ratios, and calorimetric measurements of acidity.

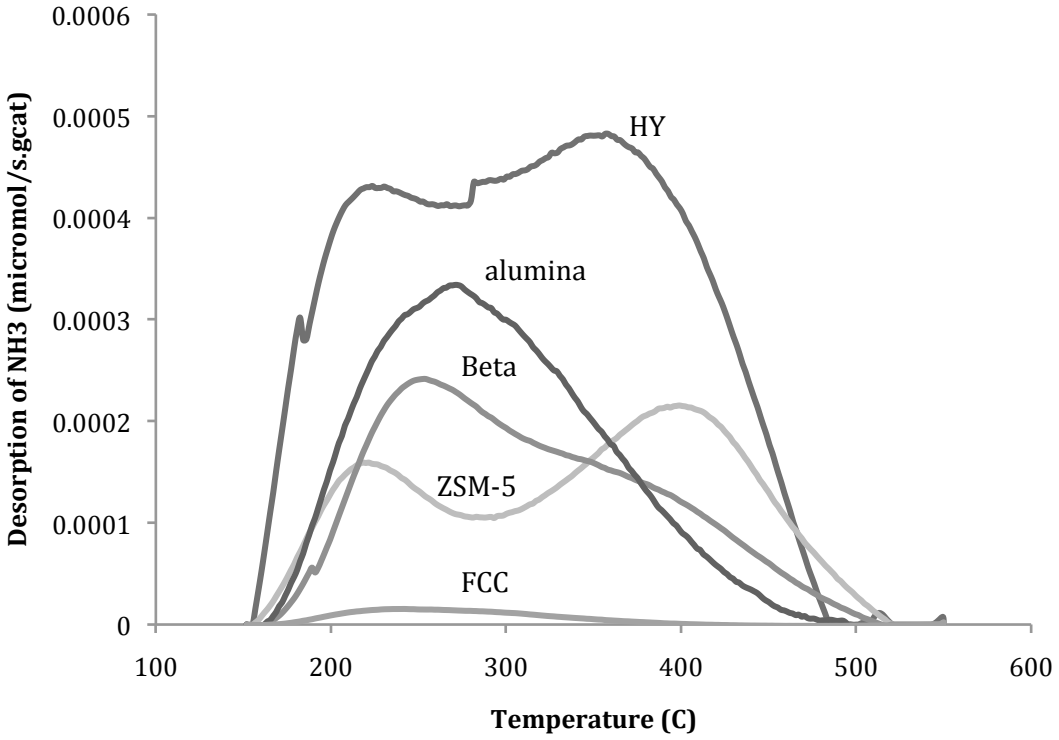

Figure 5.10: Comparison of acid strength determined through temperature programmed desorption of ammonia through various aluminosilicates.

5.4.5 Choosing an aluminosilicate as a support for hydrodeoxygenation experiments

Screening of the various aluminosilicates through model compound upgrading provided little insight for choosing 'the best' aluminosilicate to design a hydrotreating catalyst. The benzene yields were low and there was no significant difference between the activities (Figure 5.7). Therefore, the best catalyst was chosen solely upon its physical and chemical characteristics as well as it's industrial

uses.

Moisture-free bio-oil is a fairly complex mixture with many different sized molecules. However, the majority of the oil is phenolic. A mid-sized pore diameter would be ideal in upgrading phenol. From Table 5.9, it can be seen that H-ZSM-5 had a mid-sized pore diameter and therefore is a candidate for a support. However, the large pore diameter of the beta zeolite could be beneficial in accommodating some of the bulkier-compounds, especially the polynucleic aromatics (PNAs). The pore-diameter of the Y zeolite is too small to accommodate the large molecules of the modified bio-oil.

From the acidity studies, ZSM-5 possessed the most Lewis acid sites; an attribute of high value when designing a hydrotreating catalyst. Furthermore, ZSM-5 possessed a high concentration of strong acid sites in comparison to the beta zeolite. Therefore, these characterization studies suggest that ZSM-5 is the 'best' aluminosilicate to use as a support in a hydrotreating catalyst. Not only does ZSM-5 have an ideal pore diameter (0.54nm) and high Lewis acidity, but, it's known for its ability to remove oxygen in industry. The best example of this is the one in which ZSM-5 was invented for, Mobil's methanol to gas (MTG) process.

5.5 Conversion and performance of various metal-impregnated catalyst for the upgrading of moisture-free bio-oil in a batch reactor system

The bio-oil fraction obtained from chloroform extraction was found to polymerize easily during upgrading in a fixed bed apparatus. This was due to the fraction's highly phenolic nature (phenol is a lignin decomposition product prone to polymerization). Thus, it was necessary to find a method that could stabilize the

moisture-free fraction at high temperatures in order to upgrade further. This was accomplished in a batch system through the introduction of tetralin as a co-feed (used as a hydrogen donor and lignin dilutant) as well as a stabilization step prior to reaction to react the most volatile components at a low temperature of 120°C.

The objective of this phase was to identify the metal catalyst capable of the highest hydrocarbon formation and oxygen removal activities. The metal catalysts were screened in a batch reactor system using identical conditions (T=330°C, P=3MPa, catalyst loading of 2w%, tetralin:oil=4, rpm=500 and a reaction time of 45min) to compare catalyst activity for oxygen removal and hydrocarbon formation. The screening conditions were determined through literature review and primary optimization of both reaction pressure and reaction time. Finally, with the highest activity catalyst, the process was optimized through parameter variation. Temperature, catalyst loading, metal loading on catalyst, and solvent to oil ratio were varied.

5.5.1 Reproducibility experiments

Three runs were completed under identical conditions to ensure the reactor set-up was capable of produce reprocable results. Each run was carried out in the presence of a commercial $NiMo/Al_2O_3$ catalyst reduced in situ (2 hours at 300˚C and 6MPa in the presence of tetralin). All three runs were carried out at T=330˚C, P=3 Mpa, catalyst loading of 2wt%, rpm=500, a reaction time of 1 hour, and a tetralin to oil ratio of 4:1. Through GC and GC-MS, is was concluded that reproducibility was achieved within reasonable limits. From the tabulated results in Table 5.12, it can be observed that the results were reproducible within an error of 3.6wt%. The

largest error (3.6wt%) was found in the calculation of oxygen removal. All other parameters demonstrated smaller error margins.

Table 5.12: Ultimate analysis (wt%) of liquid products obtained during reproducibility experiments at T=330°C, P=3 Mpa, catalyst loading of 2wt%, rpm=500, a reaction time of 1 hour, and a tetralin:oil ratio of 4:1

	C	**H**	**N**	**S**	**O_2**	**Oxygen removal**	**Hydrocarbon yield**
1st run	84.7	8.5	0.01	0.02	6.8	83.8	44.6
2nd run	84.1	8.3	0.02	0.02	7.6	81.9	46.1
3rd run	85.0	8.9	0.01	0.02	6.1	85.5	47.4
Average Value	84.6	8.6	0.01	0.02	6.8	83.7	46.0
Deviation	0.9	0.6	0.01	-	1.5	3.6	2.8

5.5.2 Optimization of pressure

Five runs were completed to fully explore the effects of pressure in the presence of a commercial $NiMo/Al_2O_3$ catalyst reduced in situ (2 hours at 300˚C and 6MPa in the presence of tetralin). One run was carried out at each pressure, 1, 2, 3, 4, and 5 MPa, while holding all other variables constant; T=330˚C, catalyst loading of 2wt%, rpm=500, a reaction time of 1 hour, and a tetralin to oil ratio of 4:1. It was discovered through GC and GC-MS that after 3 MPa, the liquid product composition did not change. However, solid formation increased dramatically after 4 MPa. Therefore, 3 MPa was chosen as the optimum pressure. 85.5% oxygen removal was observed at the optimum pressure. Results are shown in Table 5.13**.**

Table 5.13: Ultimate analysis (wt%) of liquid products obtained during pressure optimization at T=330°C, catalyst loading of 2wt%, rpm=500, a reaction time of 1 hour, and a tetralin:oil ratio of 4:1

Pressure	C	H	N	S	O_2	Oxygen Removal (%)	Main product
1 MPa	81.4±0.7	8.6±0.1	0.01	0.05	10.0±0.2	1MPa	-
2 MPa	83.4±0.8	8.3±0.1	0.03	0.02	8.1±0.2	2MPa	C_{18}-C_{20} aromatics
3 MPa	85.0±0.8	8.9±0.1	0.01	0.002	6.1±0.1	3MPa	C_{18}-C_{20} aromatics
4 MPa	84.4±0.8	8.9±0.1	0.01	0.001	6.6±0.1	4MPa	C_{18}-C_{20} aromatics
5 MPa	84.8±0.8	8.9±0.1	0.01	0.001	6.2±0.1	5MPa	C_{18}-C_{20} aromatics

5.5.3 Optimization of reaction time

One run was carried out where 8 samples were collected (stabilization step, 15, 30, 45, 60, 75, 90, and 105 min) to determine the optimum reaction time in the presence of a commercial $NiMo/Al_2O_3$ catalyst reduced in situ. In the stabilization step (used to stabilize the extracted moisture-free bio-oil by reacting the most volatile components for 30 min at a low temperature=120°C, P=3 MPa, catalyst loading=2wt%, rpm=500, and tetralin:oil of 4:1), minimal conversion of the phenolic feedstock was observed. Furfural found in the feedstock was slightly depleted and a small amount (2.1%) of C_{18}-C_{20} aromatic hydrocarbons were formed (mainly cyclohexane,1,2-diphenyl). After the stabilization step, normal reaction conditions were maintained at T=330°C, P=3 MPa, rpm=500 and a tetralin:oil of 4:1. After 15min of reaction under these conditions, the liquid products collected

appeared similar to those collected in the stabilization step. The 30 min sample began to show almost 100% depletion in the feedstock's highly oxygenated bulky phenols (phenols with more than one hydroxyl group) with an overall oxygen removal of 69.4%. It appeared that the reduction of oxygenated compounds contributed to the formation of more C_{18}-C_{20} aromatic hydrocarbons, 6.9% of the products detected. The liquid products collected after 45 min showed great depletion of all oxygenates present in the feedstock with an overall oxygen removal of 82.4%. Furthermore, the products obtained after 45 min not only demonstrated a 52.3% yield of hydrocarbons, 4.8% of which was attributed to aliphatic hydrocarbons. No further conversion was observed after 45 min, nor was there any excessive solid formation, even after 105 min. Therefore, 45 min was chosen as the optimum reaction time. 85% oxygen removal was maintained. Results from time optimization are shown in Table 5.14

Table 5.14: Ultimate analysis (wt%) of liquid products obtained during reaction time optimization at reactions conditions of T=330C, P=3 MPa, catalyst loading of 2wt% rpm=500 and a tetralin:oil ratio of 4:1

Time	C	H	N	S	O_2	Oxygen Removal (%)	Main Product
Stabilization*	73.2±0.7	7.8±0.1	0.01	0.01	19.0±0.3	54.8±2.0	-
15min	77.7±0.7	8.7±0.1	0.01	0.13	13.5±0.2	67.9±2.4	-
30min	78.3±0.7	8.7±0.1	0	0.002	13.0±0.2	69.4±2.5	Furfural/ C18-C20 aromatics
45min	83.9±0.8	8.7±0.1	0.01	0.001	7.4±0.1	82.4±3.0	C18-C20 aromatics
60min	84.4±0.8	8.9±0.1	0.01	0.001	6.7±0.1	84.1±3.0	C18-C20 aromatics
75min	84.6±0.8	8.8±0.1	0.01	0.001	6.6±0.1	84.3±3.0	C18-C20 aromatics
90min	85.1±0.8	8.7±0.1	0.01	0.001	6.2±0.1	85.3±3.1	C18-C20 aromatics

*The stabilization step is used to stabilize the extracted moisture-free bio-oil by reacting the most volatile components for 30 min at a low temperature 120°C, P=3 MPa, catalyst loading of 2wt%, rpm=500, and tetralin:oil ratio of 4:1

5.5.4 Non-catalytic runs (blank runs)

One run was carried out under screening conditions (T=330°C, P=3 MPa, tetralin:oil=4, rpm=500 and a reaction time of 45 min) in the presence of zero catalyst. This was done to explore the effects of the reaction temperature and pressure on the feedstock as well as further understand the role of the catalyst during reaction. From this run, it was evident that the temperature and pressure play an intrinsic role upgrading the modified bio-oil. The zero-catalyst run was able

to reduce the oxygen content to 5.5wt%, which is equivalent to 87.0% oxygen removal. Furthermore, from the GC-FID chromatogram in Figure 5.11 it can be seen that the non-catalytic run dramatically reformed the chemical composition of the chloroform-extracted bio-oil (chromatogram in Figure 5.6). The hydrocarbon yield was calculated to be 48.3% in the presence of zero catalyst. However, only 2.0% of this yield was aliphatic (11-13.5 min retention times) and the remaining was aromatic. The tetralin can be seen as the largest peak at 13.5 min in Figure 5.11, as it comprises 80% of the solution. The peaks immediately after tetralin from 13.6-17 min represent polynucleic aromatics (PNAs) with only 2 rings such as naphthene and its derivatives (C_{12}-C_{14}). The remaining peaks that appear from 29-37 min are PNAs comprised of 3-4 rings (C_{18}-C_{20} aromatics). Although yield of hydrocarbons is high, it is preferred that the end product hydrocarbons are smaller and aliphatic in order to be viable as transportation fuels.

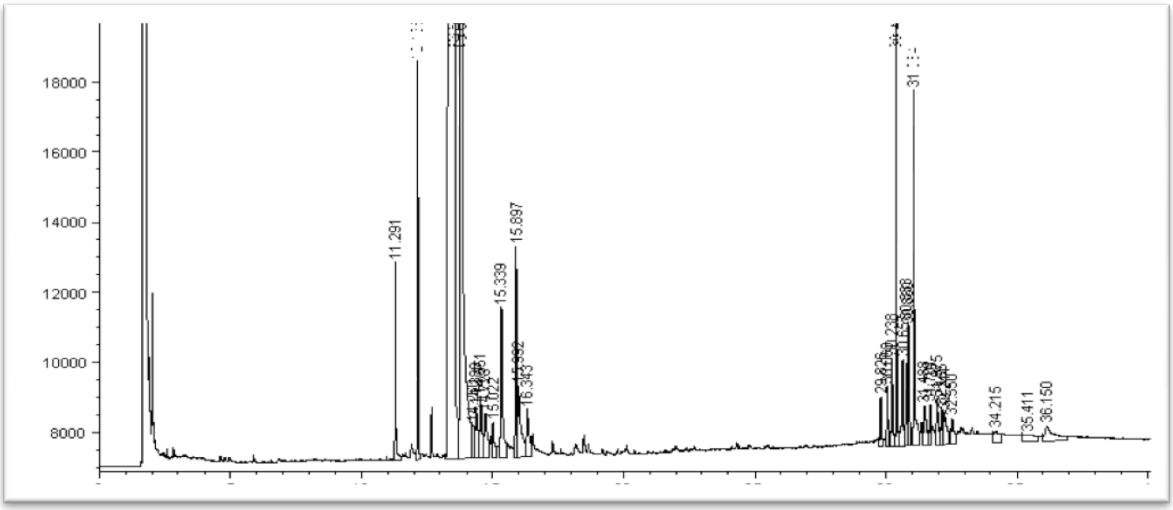

Figure 5.11: GC-FID chromatogram of products obtained from non-catalytic run at T=330°C, P=3MPa, tetralin:oil=4, rpm=500 and a reaction time of 45min

5.5.5 Exploration on effect of tetralin (no bio-oil)

One run was carried out under screening conditions (T=330°C, P=3 MPa, catalyst loading of 2wt% of 2.5% Ni/ZSM-5, rpm=500 and a reaction time of 45 min) with tetralin in the absence of bio-oil. This was done to determine whether or not the hydrogen donor solvent was decomposing under hydrotreating conditions. From this run, it was evident that the tetralin remained stable throughout the entire reaction. It was found that only 3% of the tetralin decomposed to contribute to naphthene formation. This can be seen in the GC-FID chromatogram in Figure 5.12 below.

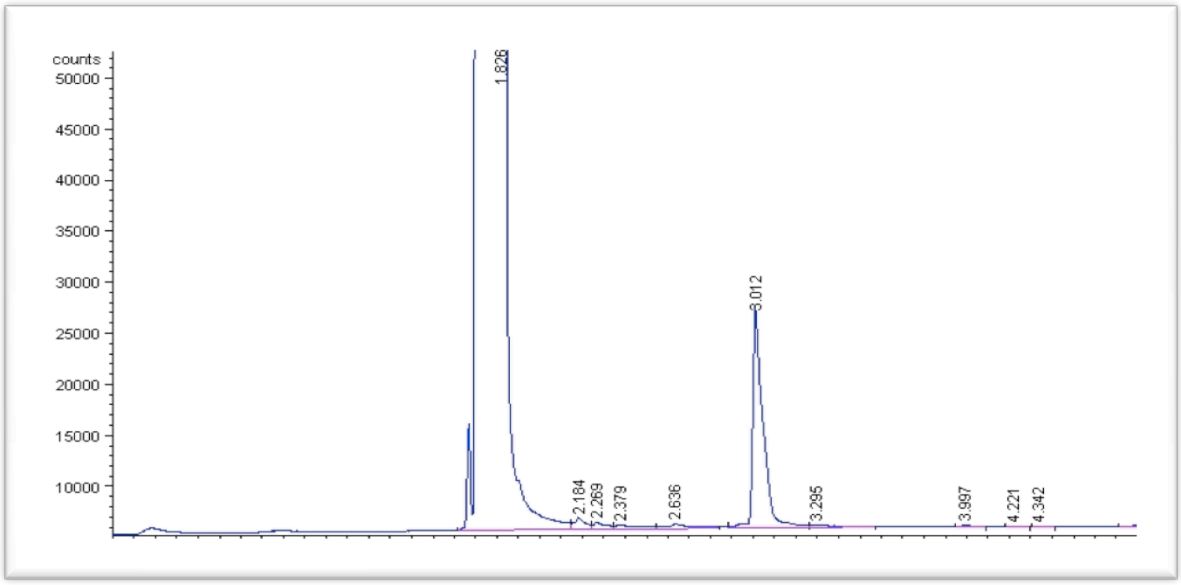

Figure 5.12: GC-FID chromatogram of products obtained from pure tetralin run (no bio-oil) over 7wt% loading of 2.5%Ni/ZSM-5 at T=330°C, P=3MPa, rpm=500 and a reaction time of 45min.

5.5.6 Screening of catalysts

Hydroprocessing of the modified bio-oil was studied using a variety of metal catalysts in a batch reactor. The metals explored were: 8.5% Mo, 13% Mo, 2.5% Ni, 5% Ni, 2.5% Sr, 5% Sr, 5% W, 10% W, CoMo (2.2 wt% Co and 8.5wt Mo) and NiMo (2.5wt% Ni and 13 wt% Mo), which were loaded onto H-ZSM-5 (average pore size, 0.54 nm). All catalysts were screened for optimum activity in oxygen removal and hydrocarbon yield under identical reaction conditions using the procedure shown in Figure 4.5. These conditions were; a temperature of 330°C, pressure of 3 MPa, stirring speed of 500 rpm, catalyst loading of 2wt%, and a tetralin to oil ratio of 4:1. The products obtained consisted of coke/tar, gas, water, and an liquid organic fraction.

Table 5.15 shows the ultimate and proximate analysis of all liquid products from the zero catalyst run and various metal catalyst screenings. From this table it is evident that 2.5% Ni is the superior catalyst in both oxygen removal and hydrocarbon yield. Not only was its hydrocarbon yield high, its yield to aliphatics over aromatics was also the highest at 20%. The next best catalysts were 5% Ni, 5% Sr, and 10% W with a hydrocarbon yield of 69.5%, 58.2%, and 54.3%, respectively. It is not surprising that Ni was successful in oxygen removal and hydrocarbon formation as it is widely known for its hydrogenation and hydrogenolysis abilities. Group VIII metals are the most active in hydrogenation. Besides, activity of the group VIII metals increases across the transition series in the order of Fe < Co < Ni [Satterfield, 1991]. Curiously, the worst catalyst was 2.5% Sr with a hydrocarbon conversion of 24.5%. This was an unexpected result considering that Okado et al

[1988] reported strontium-containing zeolites to have a high activity and stability for oxygen removal in methanol to gasoline reactions.

Table 5.15: Ultimate and proximate analysis of liquid products obtained from reaction with zero catalyst and various metal impregnated ZSM-5 under reaction conditions of T=330C, P=3 MPa, reaction time of 45 min, rpm=500 and a tetralin:oil ratio of 4:1.

Catalyst	Oxygen removal (%)	Hydrocarbon yield (%)	Aliphatic yield (%)	Carbon formation on catalyst (%)	Heating Value (MJ/kg)	Water content (%)
zero catalyst	86±3	47.1±1.3	1.3±0.1	-	44.0±0.4	0.09
2.5% Ni	95±3	89±2.5	20.0±0.6	53±0.3	47.0±0.5	0.07
5% Ni	90±3	69.5±1.9	19.5±0.5	53±0.3	46.8±0.5	0.04
2.5% Sr	89±3	24.5±0.7	2.4±0.1	52±0.3	44.7±0.4	0.03
5% Sr	91±3	58.2±1.6	10.6±0.3	47±0.3	45.1±0.5	0.07
8.5% Mo	88±3	40.8±0.1	2.5±0.1	50±0.3	45.9±0.5	0.05
13% Mo	87±3	56±1.1	6.8±0.2	53±0.3	46.4±0.5	0.05
5% W	89±3	46.9±1.3	4.7±0.1	43±0.3	45.8±0.5	0.05
10% W	89±3	54.3±1.5	6.1±0.2	51±0.3	46.6±0.5	0.05
CoMo	89±3	45.03±1.3	4.8±0.1	51±0.3	47.1±0.5	0.04
NiMo	87±3	51.1±1.4	5.6±0.2	42±0.2	46.7±0.5	0.05

5.5.7 Catalyst performance

The performance of each catalyst screened can be further examined by taking a closer look at each parameter used to evaluate the catalyst's activity; extent

of deoxygenation, hydrocarbon yield and selectivity, coke formation, and the physical properties of the catalyst.

5.5.7.1 Extent of deoxygenation

The extent of deoxygenation was the least informative of the evaluated parameters in differentiating between the activities of the metal catalysts. As can be seen in Table 5.15, the oxygen removal did not vary more than 8% (error margin was 3.6%) for all catalysts screened. Furthermore, not more than 9% increase was seen from the zero catalyst run for any catalyst. Therefore, we can conclude that oxygen removal is a function of temperature and pressure and not a function of the catalyst. As is commonly seen in hydroprocessing reactions, such as thermal cracking, high temperature and pressure alone are able to cleave high-energy bonds and reform chemical compounds [Satterfield, 1985]. Based on the results obtained during catalyst screening, it is hypothesized that the high temperature and pressure of the screening reactions (T=330°C and P=3 MPa), along with the hydrogen donated from the tetralin, were able to cleave the heteroatom bond between oxygen and carbon. The temperature, pressure and tetralin transformed oxygenates into high molecular polynucleic aromatics through direct hydrogenolysis (as shown in the reaction mechanism in Figure 2.3). It must be noted that high temperature and pressure alone would not achieve these yields. Tetralin plays an intrinsic role by readily donating hydrogen needed during hydrogenolysis. This observation was confirmed by the model compound upgrading studies, where little conversion was observed without tetralin.

5.5.7.2 Hydrocarbon yield and selectivity

Hydrocarbon yields varied significantly more than the extent of deoxygenation and played an important role in differentiating between the activities of the various metal catalysts. The catalyst's selectivity in forming aliphatics over aromatics was heavily weighted in choosing the most desirable catalyst. This is because aliphatics are more desired than bulky aromatics as transportation fuels. While a moderate concentration of aromatics can boost octane ratings in gasoline fuel, a high concentration of them can lead to heavy sooting. Aromatics are not desired in diesel fuels [Satterfield, 1985]. From Table 5.16 it is evident that the nickel catalysts are superior in their hydrocarbon yield. Furthermore, they appear to have the highest selectivity for aliphatic hydrocarbon formation.

5.5.7.3 Coke formation

Much like the extent of deoxygenation, the amount of coke formation varied little with different catalysts. As can be seen in Table 5.15, no more than 11% variation was observed over the ten different catalysts. The reason for this consistency could be due to the operating conditions. The high temperature plays a key role in the formation of carbon (coke) on the catalyst. The carbon formation is mainly attributed to degradation of the lignin within the modified bio-oil. The degradation occurs at high temperatures. Another reason that the coke formation is consistent throughout the screenings is the presence of tetralin. The tetralin does

not only act as a hydrogen donor, but also serves to dilute the lignin and decrease the amount of carbon formation and oil polymerization (tar formation).

Table 5.16: Analysis of hydrocarbon formation in liquid products obtained from reaction with zero catalyst and various metal impregnated ZSM-5 under reaction conditions of T=330C, P=3 MPa, reaction time of 45 min, rpm=500 and a tetralin:oil ratio of 4:1

Catalyst	Hydrocarbon Yield (%)	Aliphatic Yield (%)	Aromatic Yield(%)
zero catalyst	47.1	1.30	45.8
2.5% Ni	89.0	20.0	69.0
5% Ni	69.5	19.5	50.0
2.5% Sr	24.5	2.40	22.1
5% Sr	58.2	10.6	47.6
8.5% Mo	40.8	2.50	38.0
13% Mo	56.0	6.80	51.2
5% W	46.9	4.70	42.2
10% W	54.3	6.10	48.2
CoMo	45.0	4.80	40.2
NiMo	51.1	5.60	45.5

5.5.7.4 Product physical properties

Three main products were formed during the hydrotreating reactions; liquid, gas, and coke/tar. The gases formed were mainly carbon monoxide, carbon dioxide, and trace amounts of short chain hydrocarbons. As was stated in the last section, the coke and tar formations found on the catalyst were due to lignin degradation. The coke and tar formation on the catalyst was so severe the recovery

of the catalyst was not possible. The liquid products obtained during hydrotreating were very different from the bio-oil. The naked eye alone could see drastic changes; the liquids were lighter in color (the moisture free bio-oil was dark brown whereas the products were a lighter honey-type color) and less viscous (the moisture free bio-oil was a thick syrup, whereas the upgraded products flowed much more freely). However, some of the change in the viscosity could have been attributed to tetralin dilution.

A summary of the physical characterization of the liquid products obtained is presented in Table 5.17. From this table it can be seen that the heating values increased from the feed's value of 44.0 MJ/kg. The products with the highest heating values were obtained using the catalysts that produced the highest hydrocarbon conversion; 2.5% Ni, 5% Ni, 10% W as well as NiMo and CoMo. Furthermore, the hydroprocessing produced minimal water during reaction and all products remained with less than 0.1% moisture content. The crystallization temperature of the products, identified through differential scanning calorimetry, varied unpredictably in the liquid products. However, all products possessed a crystallization temperature low enough to be used as a transportation fuel. The pH of the liquid products also increased during hydrotreatment. All products exhibited a pH closer to neutral than the value of 5.2 from the modified bio-oil feed. Furthermore, all liquid products, except those obtained via strontium catalysts, were completely miscible with diesel fuel.

Table 5.17: Physical properties of liquid products obtained via hydrotreating using various metal impregnated ZSM-5 catalysts under reaction conditions of T=330°C, P=3 MPa, rpm=500, catalyst loading of 2wt% and a tetralin:oil ratio of 4:1

Catalyst	Heating Value (MJ/kg)	Water content (%)	Crystallization temperature (°C)	pH
2.5% Ni	47.0	0.07	-81.3	6.4
5% Ni	46.8	0.04	-78.8	6.3
2.5% Sr	44.7	0.03	-65.68	5.9
5% Sr	45.1	0.07	-85.52	5.9
8.5% Mo	45.9	0.05	-98.05	6.2
13% Mo	46.4	0.05	-95.70	6.2
5% W	45.8	0.05	-92.45	6.1
10% W	46.6	0.05	-73.75	6.1
CoMo	47.1	0.04	-76.88	6.0
NiMo	46.7	0.05	-77.55	6.2

5.5.8 Characterization of metal catalysts

The metal catalysts were characterized using several techniques. X-ray diffraction was conducted to ensure that the metal impregnation did not affect the structure of the zeolite. The pore size of the catalyst was monitored using N_2 to insure that the metal impregnation did not plug the pores of the zeolite. Transmission electron microscopy was used to further monitor the distribution of the metal over the zeolites. The acidity of the catalyst was explored through Fourier transform infrared spectroscopy of pyridine, as well as the temperature programmed desorption of ammonia.

5.5.8.1 Physical properties of catalysts

The quality and structure of each metal-impregnated ZSM-5 zeolite was monitored by powder X-ray diffraction patterns of all catalysts. From these, it can be concluded that the metal impregnation did not affect the structure of the zeolite (Figure not shown).

TEM images of the metal catalysts can be viewed in Figure 5.13. From these images, it is observed that the metal particles are deposited evenly across the zeolite's surface and have a uniform size.

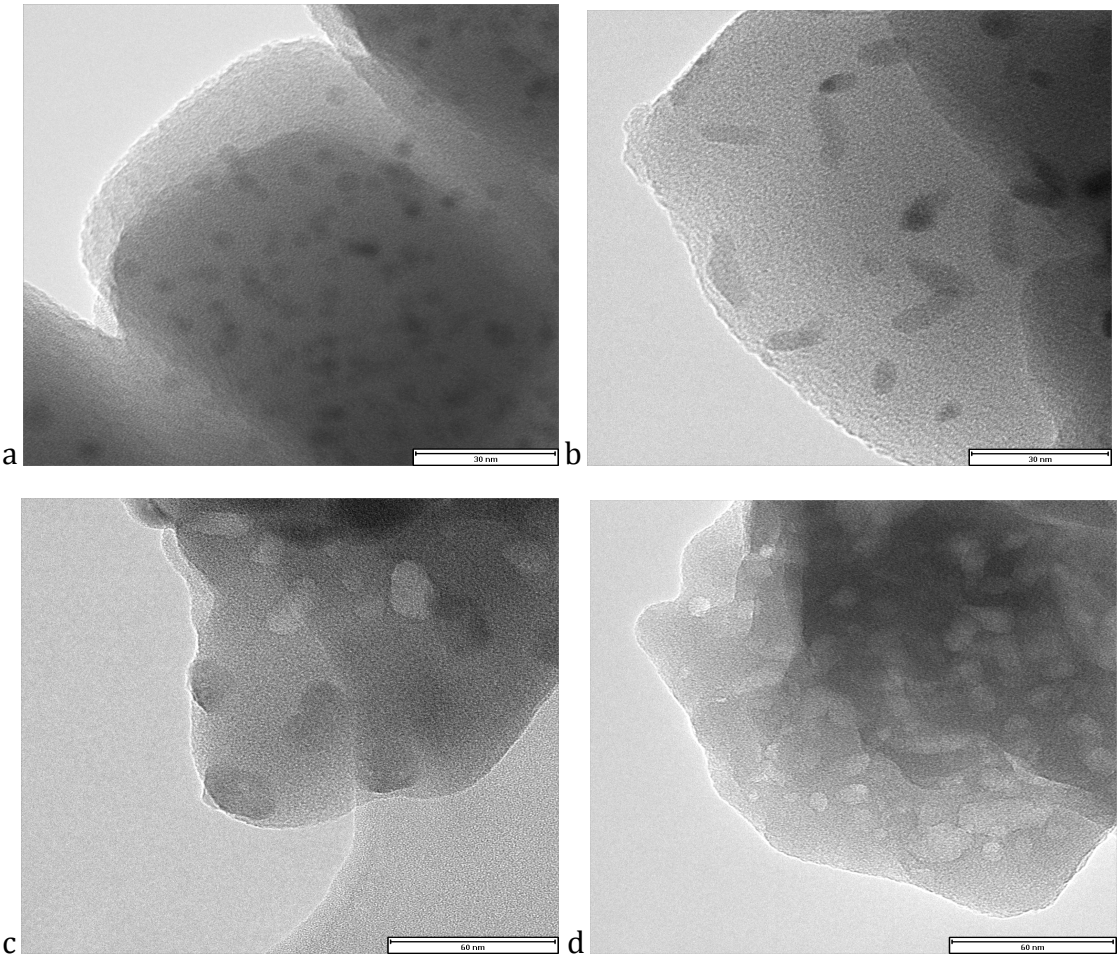

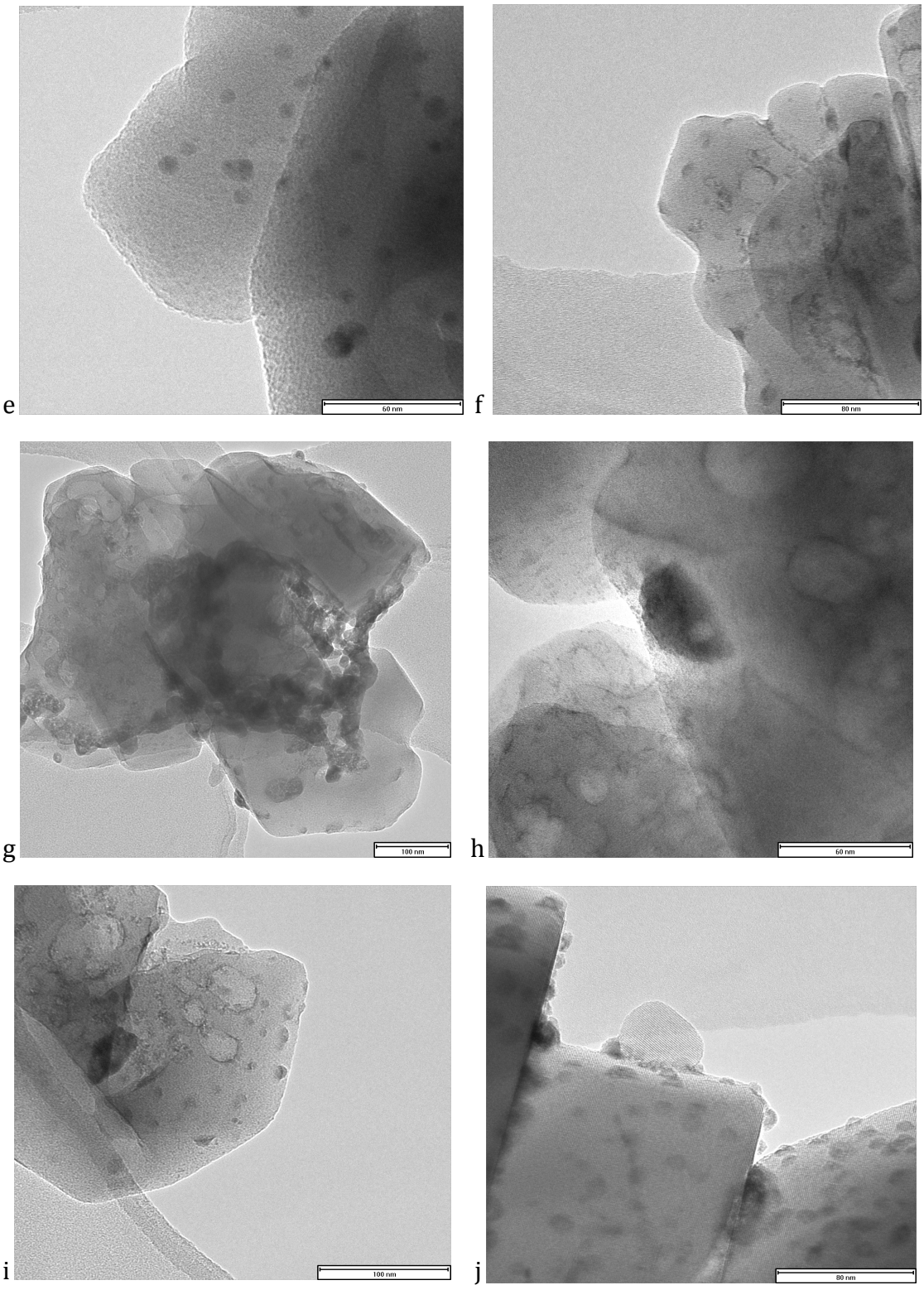

Figure 5.13: TEM images of (a) 2.5%Ni/ZSM-5 (b) 5%Ni/ZSM-5 (c) 2.5%Sr/ZSM-5 (d) 5%Sr/ZSM-5 (e) 8.5%Mo/ZSM-5 (f) 13%W/ZSM-5 (g) 5%W/ZSM-5 (h) 10%W/ZSM-5 (i) CoMo/ZSM-5 (j) NiMo/ZSM-5

The physical properties of the prepared metal catalysts are presented in Table 5.18. From this Table it is evident that both pore volume and surface area are affected by metal impregnation; both decrease. The 2.5%Ni, CoMo, and NiMo impregnations decrease the pore volume and surface area the most. The average pore diameter appears to be relatively unaffected.

Table 5.18: Physical properties of various metal impregnated ZSM-5 obtained from nitrogen adsorption

Catalyst	BET surface area (m2/g)	Micropore area (m^2/g)	Micropore Volume (cm^3/g)	S.P Total Pore Volume (cm^3/g)	Average Pore (4V/A)
H-ZSM-5	524	392	0.17	0.31	24
2.5% Ni	369	284	0.12	0.22	24
5% Ni	437	338	0.15	0.25	23
2.5% Sr	378	421	0.17	0.30	22
5% Sr	477	374	0.16	0.27	23
5% W	514	416	0.18	0.30	22
10% W	504	387	0.17	0.28	22
CoMo	377	310	0.13	0.21	22
NiMo	425	334	0.24	0.23	22

5.5.8.2 Acidic Study of the catalysts

Through the Fourier transform infrared spectroscopy, the Lewis and Brønsted acid sites were identified and quantified using pyridine adsorption. In Figure 5.14, the spectrum produced by each catalyst is present. Table 5.19 presents the quantity of acid sites found. From both Table 5.19 and Figure 5.14, it can be

seen that nickel-impregnated and strontium-impregnated ZSM-5 catalysts possessed the most Lewis acid sites. This was expected, as literature stated that nickel impregnation enhances Lewis acidity [Satterfield, 1991]. Surprisingly, CoMo had a higher concentration of Lewis acid sites than NiMo. The strontium-impregnated zeolite possessed the most Brønsted acid sites, closely followed by the 5% nickel impregnation and 5% tungsten impregnation.

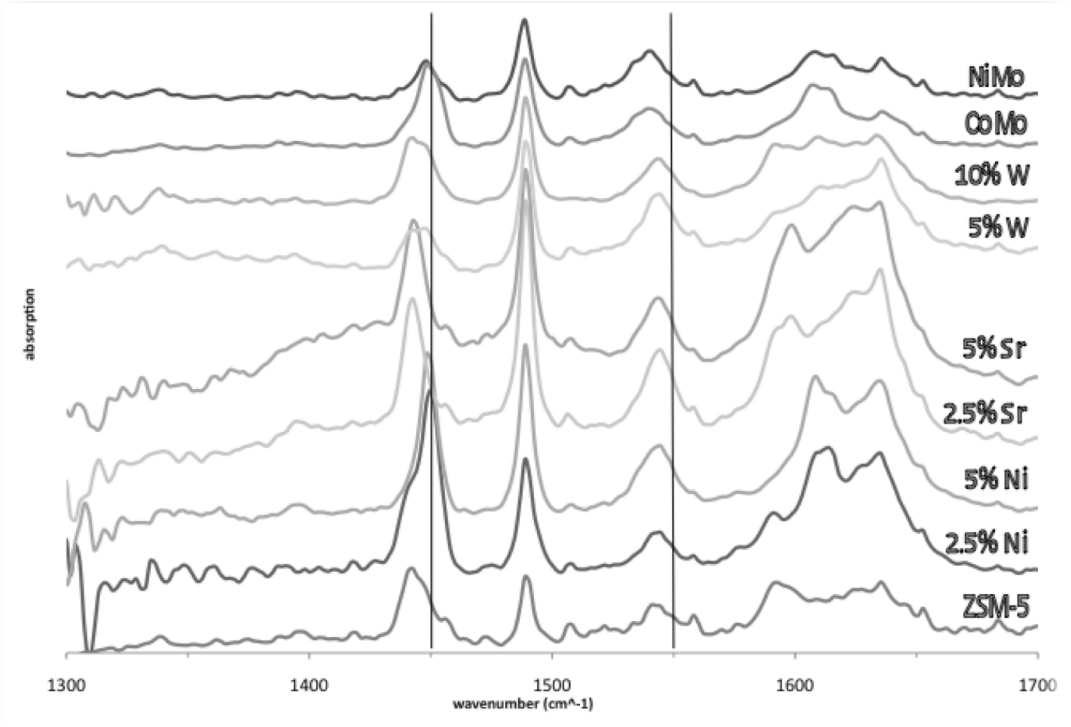

Figure 5.14: Comparison of Lewis (1450 cm^{-1}) and Brønsted (1550 cm^{-1}) acid sites obtained from FT-IR with pyridine for various metal-impregnated catalysts

Table 5.19: Quantity of Lewis and Brønsted acid sites obtained from FT-IR with pyridine

Catalyst	Lewis - integrated area	Lewis - corrected area (μmol)	Bronsted - integrated area	Bronsted - Corrected area (μmol)	B/L
H-ZSM-5	1.37	3.04	0.59	0.98	0.32
2.5% Ni	3.05	6.76	0.66	1.11	0.16
5% Ni	2.08	4.62	1.32	2.21	0.48
2.5% Sr	1.81	4.02	1.46	2.44	0.61
5% Sr	1.62	3.59	1.15	1.92	0.53
8.5% Mo	0.78	1.73	1.02	1.70	0.98
13% Mo	0.64	1.42	0.98	1.64	1.15
5% W	0.85	1.90	1.19	1.99	1.05
10% W	1.31	2.91	0.80	1.33	0.46
CoMo	1.38	3.07	0.91	1.52	0.50
NiMo	0.62	1.38	1.13	1.89	1.37

5.5.9 Choosing the best metal catalyst as a support for hydrodeoxygenation experiments

The metal catalysts were evaluated using a variety of calculated parameters (extent of deoxygenation, hydrocarbon yield and selectivity, coke formation, and the physical properties of the liquid products formed) to choose which catalyst was most appropriate in transforming modified bio-oil into a transportation fuel. However, because some of the parameters (the extent of deoxygenation and coke formation) varied minimally during the screening reactions, they were not considered when choosing a 'best' catalyst. Hydrocarbon yield and selectivity were

the most heavily considered.

Based on this criterion, it is evident that the nickel catalysts were superior. They not only appeared to have the highest hydrocarbon yield, but also exhibited the highest selectivity for aliphatic hydrocarbon formation. This can be seen in Table 5.15. It is not surprising that Ni was successful in oxygen removal and hydrocarbon formation, as it is widely known for its hydrogenation and hydrogenolysis abilities. Group VIII metals are the most active in hydrogenation. Besides, activity of the group VIII metals increases across the transition series in the order of Fe < Co < Ni [Satterfield, 1991]. This hypothesis was confirmed by the catalyst acidity studies. From FT-IR characterization, it can be seen that nickel-impregnated ZSM-5 catalysts possessed the most Lewis acid sites. Furthermore, as can be seen in Table 5.16, the liquid products obtained via 2.5% Ni/ZSM-5 possessed highly desirable properties such as high heating value (47.0 MJ/kg) and a close to neutral pH (6.4). Therefore, 2.5% Ni/ZSM-5 was chosen as the most desirable catalyst and was used for optimization studies.

5.5.10 Optimization of nickel metal loading on ZMS-5

Nickel metal was explored in 3 different impregnation weights, 1wt%, 2.5wt%, and 5wt%. This was done to determine whether a nickel impregnation higher or lower than 2.5wt% would be beneficial in achieving higher hydrocarbon yields and selectivity. All three Ni catalysts were screened under identical conditions similar to the screening of the other metal catalysts; T=330C, P=3 MPa, rpm=500, a tetralin to oil ratio of 4:1, and a reaction time of 45 min. The results

from these experiments are tabulated in Table 5.20. From this table, it is evident that increasing the nickel content from 2.5wt% to 5wt% was not successful in increasing the hydrocarbon yield or selectivity. However, no change in hydrocarbon formation or oxygen removal was observed when decreasing the nickel loading to 1wt%. Furthermore, the physical properties of the products obtained from 1wt% Ni were not more desirable than that of 2.5wt% Ni. Therefore, further investigiation is required to differentiate between nickel loading of 1wt% and 25wt%. 2.5%Ni/ZSM-5 was chosen as the optimum catalyst to be used in optimization experiments.

Table 5.20: Catalyst loading optimization at T=350°C, P=3 MPa, reaction time of 45 min, rpm=500, and a tetralin:oil ratio of 4:1

Catalyst	Oxygen removal (%)	Hydrocarbon Yield (%)	Aliphatic Yield (%)	Carbon formation on catalyst (%)	Heating Value (MJ/kg)	Water content (%)
1% Ni	93±3	87.0±2.4	20.0±0.6	53±0.3	46.8±0.5	0.05
2.5% Ni	95±3	89.0±2.5	20.0±0.6	53±0.3	47.0±0.5	0.07
5% Ni	90±3	69.5±1.9	19.5±0.5	53±0.3	46.8±0.5	0.04

5.5.11 Process optimization

The process optimization was carried out in 17 experiments (3 of which used for reproducibility) using 2.5% Ni/ZSM-5. The object of these experiments was to examine the effects of temperature, catalyst loading and solvent to oil ratio. The conditions for these reactions were generated by statistical design software, Design Expert 6.0, and are shown in Table 4.3. Each experiment used the procedure presented in Figure 4.5. However, reaction parameters were adjusted accordingly.

After the 17 optimization experiments were complete and the products were analyzed for oxygen removal and hydrocarbon formation, that information was entered into the statistical design expert software to generate a predictive model for hydrogen yield (not oxygen removal because it demonstrated little variation). It was found that a quadratic model was the best fit for the data. The relevance of this model was confirmed through a partial sum of squares, F value (lack-of-fit test), and lack of fit analysis. The equation produced was:

$$\mathbf{HC_{yield}} = 0.676T + 20.581C - 0.5124S - 0.0012T^2 - 1.806^2 - 0.914S^2 - 0.029T*C + 0.052T*S + 0.184C*S - 98.460 \quad \text{(Eqn. 1)}$$

Where T=temperature; C=catalyst loading (g); S=solvent to oil ratio

The reliability and restrictions of this generated equation must be discussed. From statistical point of view, three tests are required to evaluate the model; a) Test of significance of factors and interactions, a partial sum of squares, b) R-squared test, and c) The lack-of-fit test. Test of significance means leaving out insignificant factors or terms of a model, which in turn produces a simpler mathematical model and easier interpretation. R-squared is the relative predictive power of a model and is in the range of 0 to 1. If it is much closer to one, the model can better predict real data. The test of lack-of-fit is used to determine whether discrepancies between measured and expected values can be attributed to random or systematic error. The lack-of-fit test compares the residual error to pure error from replicated design points [Lazic, 2004]. From the experimental data, a quadratic model was generated. This model (eqn. 1) passed all statistical tests thus confirming the significance of the

equation. Furthermore, the lack-of-fit test confirmed reproducibility found in earlier experiments.

The statistical software makes two assumptions regarding the data. Firstly, the software assumes the reproducibility confirmed by 3 repeated experiments is applicable over the entire range of conditions (T=250-350°C, catalyst loading=1-5 g, and tetralin to oil ratio = 2-10). However, the repeated experiments occur at the center of the range and may not apply to the extremes of the conditions. Nevertheless, at the beginning of hydroprocessing experiments, 3 experiments were conducted outside of the experimental design under different conditions. Both sets of repeated experiments confirmed reproducibility within 3.6% (see section 5.5.1) under different conditions. Thus, it can be assumed that reproducibility is relevant throughout the entire range of conditions. The second assumption made by the design software is that a maximum of two factors affect the reaction at any given point in time. More investigation would be required to confirm this assumption made by the design software in generating equation 1.

The experimental values obtained for all 17 experiments are shown below in Table 5.21. From this table it can be observed that the runs with the highest tetralin to oil ratio of 10 coupled with a high temperature of 350°C and moderate catalyst loading had the highest hydrocarbon yield (90-93%). Aside from this observation, little can be deduced from these results alone. Therefore, the effect of each parameter must be examined separately using the predictive model (Eqn. 1).

Table 5.21: Experimental results obtained for optimization experiments conducted at P=3MPa, rpm=500, and a reaction time of 45min.

Run	Temperature (°C)	Catalyst loading (g)	Solvent: Oil	Oxygen removal (%)	Experimental hydrocarbon yield(%)
1	350	1.0	10	95	62.6±1.8
2	250	5.0	2	83	51.6±1.4
3	216	3.0	6	85	55.0±1.5
4	350	1.0	2	76	26.3±0.7
5	250	1.0	2	67	17.7±0.5
6	350	5.0	10	93	90.8±2.5
7	250	1.0	10	77	32.9±0.9
8	300	3.0	12.7	88	82.4±2.3
9	250	5.0	10	80	52.3±1.5
10	300	3.0	6	87	82.6±2.3
11	300	3.0	6	87	83.3±2.3
12	350	5.0	2	72	28.3±0.8
13	300	0.0	6	86	78.5±2.2
14	384	3.0	6	93	93.7±2.6
15	300	3.0	6	79	83.2±2.4
16	300	6.4	6	81	56.8±1.6
17	300	3.0	1	77	12.0±0.3

5.5.11.1 Effect of catalyst loading

The effect of catalyst loading was studied using the predictive model (eqn. 1). The value of catalyst loading was increased stepwise while the other parameters were held constant. Three graphs were generated from this data: one at a temperature of 250°C and a solvent to oil ratio of 10, one at a temperature of 300°C and a solvent to oil ratio of 10, and one at a temperature of 350°C and a solvent to oil ratio of 10. The solvent to oil ratio of 10 was chosen based on the initial observation that hydrocarbon yield increases with an increase in solvent concentration. From this, a maximum hydrocarbon yield is observed at each

temperature. At 250°C (Figure 5.15), a maximum hydrocarbon yield of 59.9% occurs at a catalyst loading of 4.25g. At 300°C (Figure 5.16) a maximum hydrocarbon yield of 80.5% occurs at a catalyst loading of 3.75g. At 350°C (Figure 5.17) a maximum hydrocarbon yield of 95.3% occurs at a catalyst loading of 3.5g. Therefore, at high temperature, the optimum catalyst loading is 3.5g or 7wt%.

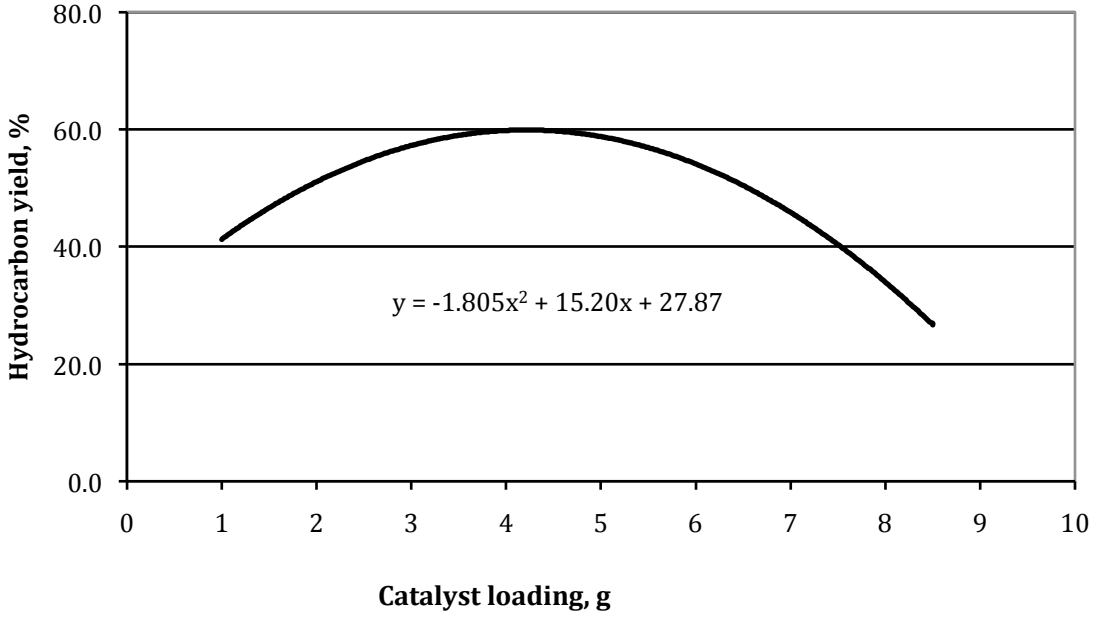

Figure 5.15: Catalyst loading optimization at T=250°C, P=3MPa, reaction time of 45min, rpm=500 and solvent to oil ratio of 10 using predictive model

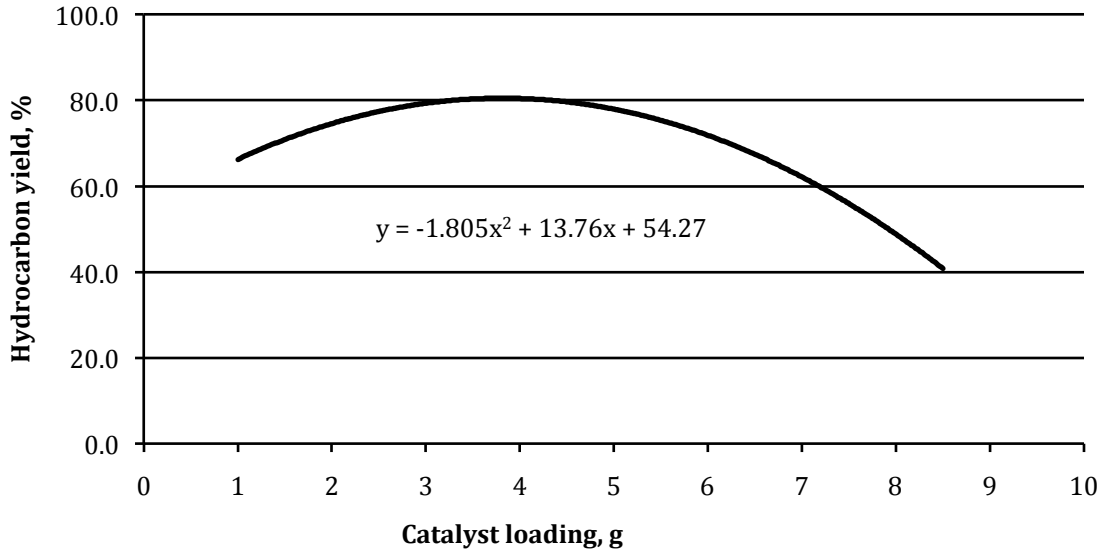

Figure 5.16: Catalyst loading optimization at T=300°C, P=3MPa, reaction time of 45min, rpm=500 and solvent to oil ratio of 10 using predictive model

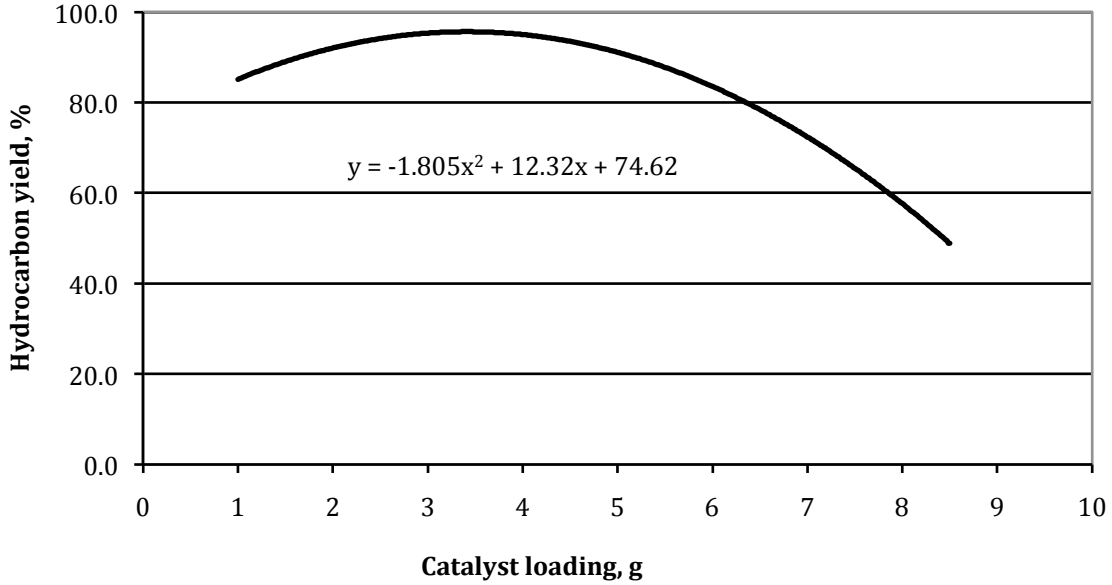

Figure 5.17: Catalyst loading optimization at T=350°C, P=3MPa, reaction time of 45min, rpm=500 and solvent to oil ratio of 10 using predictive model

5.5.11.2 Effect of temperature

The effect of temperature was also studied, much like catalyst loading, by using the predictive model (eqn. 1). A graph was generated by increasing the temperature stepwise while holding the other two variables constant at a catalyst loading of 5g and a tetralin to oil ratio of 10. The graph generated is presented in Figure 5.18. From this, we can see the model appears to be linear when only temperature is taken into account. However, this figure only truly represents the trend to some extent. Much of the literature had shown that after 400°C there was a drastic and detrimental increase in solid formation [Adjaye, 1993; Baldauf et al, 1992; Chen et al, 1988; Churin et al, 1988; Mahfud, 2009; Sharma et al, 1991; Soltes et al, 1987; Wildshut, 2009; Zhang et al, 2005]. The literature, catalyst loading results, and the limitations of the batch reactor apparatus (maximum operating temperature of 350°C) led to the conclusion of the optimum operation temperature being 350°C.

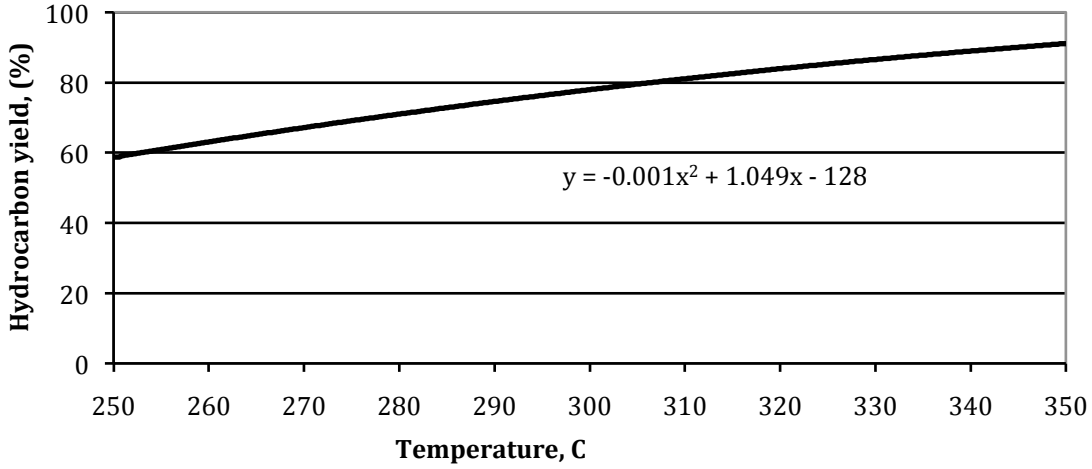

Figure 5.18: Temperature optimization at catalyst loading of 5g, P=3MPa, reaction time of 45min, rpm=500 and solvent to oil ratio of 10 using predictive model

5.5.11.3 Effect of tetralin to oil ratio

The effect of the tetralin to oil ratio was also studied by using the predictive model (eqn. 1). The ratio's effect was observed by increasing its value stepwise and holding the other two variables constant at a temperature of 350°C and a catalyst loading of 5g. The generated graph is presented in Figure 5.19. From this graph it, it can be observed that the hydrocarbon yield begins to plateau at a ratio of 9 (89.7%). The maximum hydrocarbon yield of 89.9% is reached at solvent to oil ratio of 9.7. The same hydrocarbon yield was achieved using a solvent:oil ratio of 10. It was concluded that the optimum tetralin to oil ratio was 10.

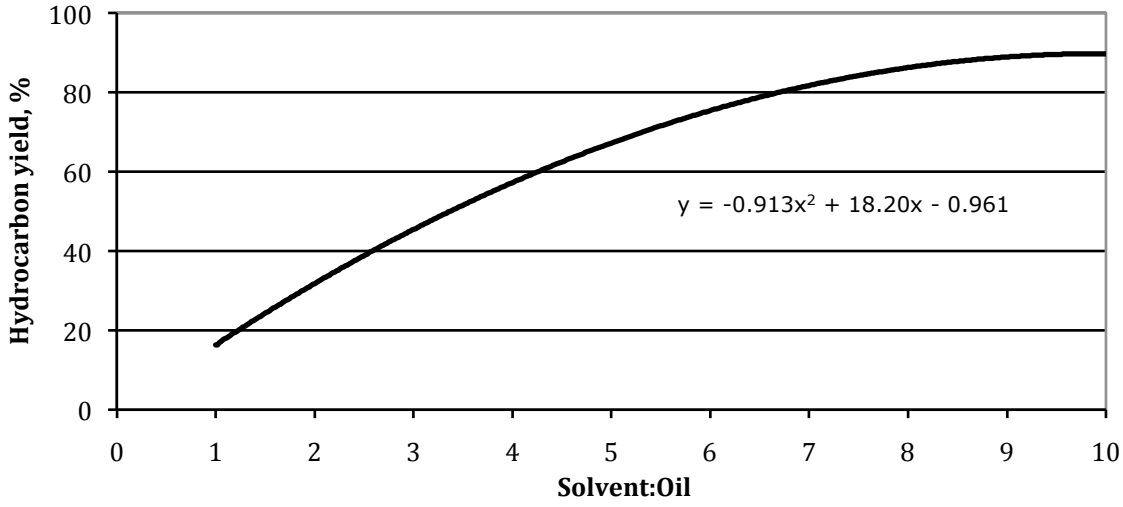

Figure 5.19: Solvent:oil optimization at temperature of 350°C, P=3MPa, reaction time of 45min, rpm=500 and a catalyst loading 5g using predictive model

5.5.11.4 Discussion on optimization study

The optimum conditions were found to be T=350°C, catalyst loading=3.5 g (7 wt%), and a solvent to oil ratio of 10:1. This was further confirmed by the surface

plot of the predicted results shown in Figure 5.20. Furthermore, one experiment was carried out at the optimum conditions to see if the predicted hydrocarbon yield of 95.3% could be achieved. The experiment resulted in a hydrocarbon yield of 94.3% with an oxygen removal of 95% producing liquid products with 22wt% aliphatic hydrocarbons and only 2.1wt% oxygen. Promisingly, the liquid products also exhibited a high heating value of 47.3 MJ/kg, a low moisture content of 0.07wt%, a close-to-neutral pH of 6.4, and a crystallization temperature of -88.4°C. These characteristics are comparable to both gasoline (44 MJ/kg, pH of 7, and freezing point of -40°C) and No. 2 diesel (47 MJ/kg, pH of 7, and freezing point of -40°C). Therefore, the liquid products produced in the present dissertation are viable candidates for transportation fuels. The characteristics of the optimized products can be viewed in Table 5.22. Comparing these results to the summarized literature on bio-oil hydrotreating in Table 2.7, it is evident that the optimum conditions found were quite similar to those determined in other studies. However, the extent of oxygen removal and hydrocarbon formation obtained is considerably higher for the nickel catalysts. This could be attributed to the lack of moisture in the feed as well as the use of tetralin as a hydrogen donor.

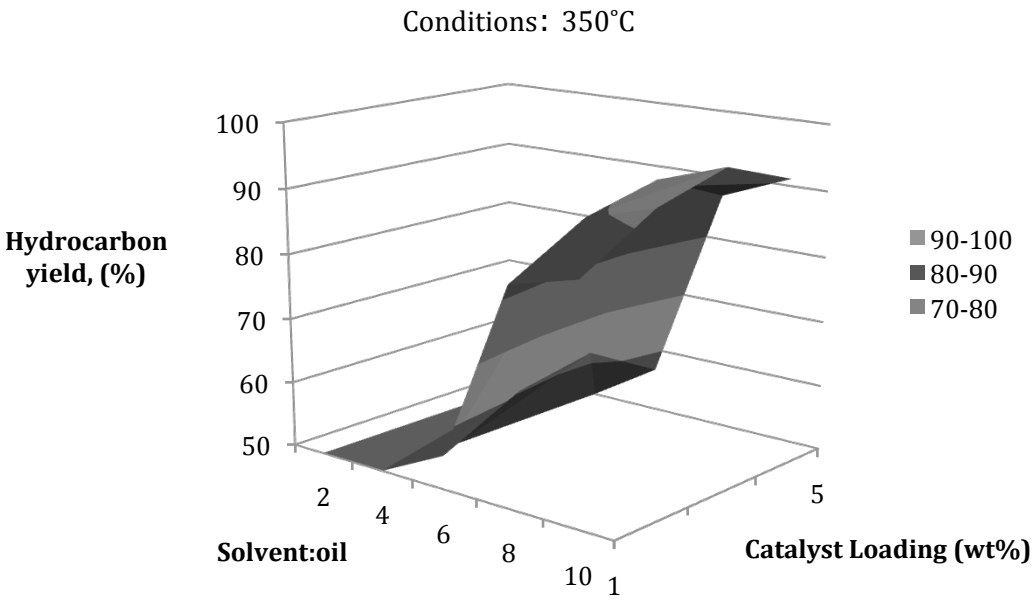

Figure 5.20: Surface plot of the theoretical yield produced from the hydrotreatment of bio-oil over 2.5% Ni/ZSM-5 at P=3MPa, rpm=500, reaction time of 45min and varying temperature, solvent:oil, and catalyst loading

Table 5.22: Properties of products obtained under optimum conditions of T=350°C, P=3Mpa, catalyst loading of 7wt%, solvent:oil=10, rpm=500, and a reaction time of 45min

Product Property	Products
Hydrocarbon yield (%)	94.3±2.6
Aliphatic hydrocarbon yield (%)	22.0±0.6
Extent of deoxygenation (%)	95±3
Carbon formation on catalyst (%)	42±0.2
Heating Value (MJ/kg)	47.3±0.2
Water content (%)	0.07
Crystallization temperature (°C)	-88.4±1.8
pH	6.4±0.3

6 Conclusions and recommendations

6.1 Conclusions

From all the results obtained in the present project, it can be seen that waste biomass has great potential for conversion to transportation fuels through fast pyrolysis and subsequent upgrading processes.

Through biomass characterization, the maple sawdust was found to have a heating value of 19.0 MJ/kg, an oxygen content of 45.7% and a moisture content of 6.6%. Bio-oil from fast pyrolysis of the maple sawdust was found to have heating value to 21.6 MJ/kg as well as increased oxygen and moisture contents of 55.0% and 30.6%, respectively. Both increased values are attributed to the degradation of lignin during pyrolysis [Elliot, 1983]. Furthermore, the oil contained a large amount of high molecular weight oxygenates and a minimal amount of hydrocarbons.

Water removal from the bio-oil via chloroform extraction was able to reduce the water content to <0.02%, decrease the amount of high molecular weight oxygenates, and increase the amount of hydrocarbons in the oil. After extraction, the remaining fraction had more than doubled the heating value (21.6MJ/kg to 44.0 MJ/kg) and consisted mainly of phenolic compounds.

Through extensive characterization of various aluminosilicate supports, it was found that ZSM-5 would serve as an ideal support for bio-oil upgrading. Its uniform structure (0.54nm pore size), acidic nature, and use in industry were the bias upon which it was chosen.

Subsequently, various metal impregnated ZSM-5 catalysts were screened for optimum activity in oxygen removal and hydrocarbon formation. From the 10 different catalysts studied, 2.5% Ni demonstrated the highest level of oxygen removal and hydrocarbon yield at 95% and 89.0%, respectively. The hydrodeoxygenation products obtained from reaction with 2.5%Ni/ZSM-5 possessed a heating value of 47.0 MJ/kg, a crystallization point of 81.3°C, and were completely miscible with diesel fuel.

Optimization of the process utilizing statistical design software and 2.5% Ni/ZSM-5 catalyst yielded an experimental hydrocarbon yield of 94.3% (predicted value of 95.3%). The optimum conditions were found to be T=350°C, P=3MPa, catalyst loading=3.5g (7 wt%), solvent to oil ratio of 10, rpm=500, and a reaction time of 45min. The liquid product obtained under optimum conditions contained 22wt% aliphatics. The physical properties of the liquid product included a high heating value of 47.3 MJ/kg, a low moisture content of 0.07wt%, a close-to-neutral pH of 6.4, and a crystallization temperature of -88.4°C. This proves optimistic for the product to be used as a transportation fuel. The major outcomes from this thesis are summarized in Appendix D.

6.2 Recommendations

Future work in this area should explore methods for both water removal via solvent extraction and hydroprocessing of bio-oils. To improve solvent extraction, solvent exploration is required to find one that is capable of increasing yield and possesses fewer human health concerns. Furthermore, applications for the aqueous

raffinate phase should be examined. Such applications could include ethanol production from the cellulose and hemicellulose present in the raffinate phase.

Future work in the area of hydroprocessing bio-oil should include methods for removal of the hydrogen donor solvent from the liquid products, as well as exploration of alternative hydrogen donor solvents. Furthermore, exploration of reactor design would be beneficial. A series of reactors with increasing catalyst activity (increase in activity as flow progresses through reactors) could potentially improve the chemical configuration of products. Exploration on the effect of catalyst extrudites and shapes would also increase the commercial value of the process. A kinetic study using model compounds (a mixture to represent pyrolysis oil) would be beneficial in determining the true reaction pathways during upgrading.

Further engine testing is required and the following questions should be answered. 1) How does the high aromatic content affect engine performance? Is there an increase in sooting? 2) How does the remaining oxygen content affect the engine performance? 3) What are the cloud and flash points of the fuel? Are they within acceptable limits? 4) How do the viscosity, density, and lubricity affect engine performance? An economical analysis would be helpful in identifying other areas, which require improvement to make this process profitable. The results in the present dissertation prove that great potential lies in the conversion of wastes to transportation fuels. As this is a budding new field, the possibilities for future research are abundant.

7 References

Adjaye, John Deheer. Catalytic conversion of biomass-derived oils to fuels and chemicals. Saskatoon; The University of Saskatchewan. 1993.

Adnanes E. and Holmen A. Catalysis Letters. 34 (1995) 269.

Aguayo A.T., A.G. Gayubo, R. Vivanco, M. Olazar, and Bilbao J. Role of acidity and microporous structure in alternative catalysts for the transformation of methanol into olefins. Applied Catalysis A: General. 283 (2005) 197.

Amin N.A.S. and Anggoro D.D. Optimization of direct conversion of methane to liquid fuels over Cu loaded W/ZSM-5. *Fuel.* 83 (2003) 487.

Anon, Survey of energy resources, In: World energy council, 20th Edition, Elsevier Ltd, Oxford, 2004, p. 267.

Anon, National Renewable Energy Laboratory, In: Biomass feedstock composition and property database, U.S.A., 2005.

Anon, The Canadian encyclopedia, historical foundation of Canada. In: Forestry (accessed 2008).

ASTM D 3173-87, Standard method for determination of moisture content in biomass, In: Am. Society for testing materials, International, Philadelphia, PA, 2003.

ASTM D 3174-04, Standard method for ash in the analysis sample of coal and coke, In: Am. Society for testing materials, International, Philadelphia, PA, 2004.

ASTM D 3175-07, Standard method for volatile matter in the analysis sample of coal and coke, In: Am. Society for testing materials, International, Philadelphia, PA, 2007.

Baker E.G. and Elliot D.C. Catalytic hydrotreating of biomass-derived oils. Pyrolysis Oils from Biomass. Eds. E.J. Soltes and T.A. Milne. American Chemical Society. Washington, D.C. 1988.

Baldauf, W. and Balfanz, U. Upgrading of pyrolysis oils from biomass in existing refinery structures; final report JOUB-0015, Veba Oel AG: Gelsenkirchen, 1992.

Baldauf, W, Balfanz U. Upgrading of fast pyrolysis liquids at Veba Oel AG. *Biomass Gasification and Pyrolysis* - State of the Art and Future Prospects. Kaltschmitt, M, and Bridgewater, A, Eds; CPL Press: Newbury, UK, 1997; p. 392-398

Bataille F., Lemberton J. L., Perot G., Leyrit P., Cseri T., Marchal N., and Kasztelan S. Sulphided Mo and CoMo supported on zeolite as hydrodesulphurization catalysts: transformation of dibenzothiophene and 4,6-dimethyldibenzothiophene. Applied Catalysis A: General. 220 (2001) 191.

Biagina E., Barontini F., and Togonotti L. *Ind. Eng. Chem. Res*. 45 (2004) 4486.

Boateng A.A., Hicks K.B., Vogel K.P. Pyrolysis of switchgrass harvested at several stages of maturity. Journal of Analytical Applied pyrolysis . 75 (2006) 53.

Bockrath, B.C., "Chemistry of hydrogen-donor solvents", in Coal Science, M. L. Gorbaty, J. W. Larsen and (eds.) Academic Press, New York, 2, 65-120, (1983).

Bonelli P.R., Della Rocca P.A., Cerrella E.G., Cukierman A.L. Effect of pyrolysis temperature on composition, surface properties and thermal degradation rates of Brazil nut shells. Bioresource Technology. 76 (2001) 15.

Bridgewater, A.V. Production of high grade fuels and chemicals from catalytic pyrolysis of biomass. Catalysis Today. 29 (1996) 285.

Chantal P.D., Kaliaguine S., and Grandmaison J.L. Reactions of phenolic compounds over HZSM-5. Appl. Catal., 18 (1985) 133.

Chen N.Y., Walsh D.E. and Koenig L.R. “Fluidized bed upgrading of wood pyrolysis liquids and related compounds” in Pyrolysis Oil from Biomass: Producing, Analyzing and Upgrading, E.J. Soltes and T.A. Milne (eds), ACS Symposium Series 376, Washington, DC. 277-289. 1998.

Che, N.Y, Garwood W.E., and Dwyer F.G. Shape Selective Catalysts in Industrial Applications, Marcel Dekker Inc. 155-196, 1989.

Chen G., Andries J., Spliethoff H. Experimental investigation of biomass waste (rice straw, cotton stalk, an pine sawdust) pyrolysis characteristics. *Energy Sources*. 25 (2003) 331.

Chiaramonti D.. Bonini A., Fratini E., Tondi G., Gartner, K. and Bridgwater, A.V. Development of Emulsions from Biomass Pyrolysis Liquid and Diesel and Their use in Engines - Part 2: Tests in Diesel Engines. Biomass Bioenerg. 2003, 25 (1) 101.

Churin E., Maggi R., Grange P., and Delmon B. Characterization and Upgrading of bio-oil produced by pyrolysis of biomass. Research in Thermochemical Biomasss Conversion; Bridgewater, A.V., Kuester, J.L., Eds., Elsevier Science Publishers, LTD. Barking, England.: 1988; pp 898-909.

Debdoubi A., El amarti A., Blesa M.J., and Hajjaj L.H. The effect of heating rate of yields and compositions of oil products from esparto pyrolysis. International Journal of Energy Research. 30 (2006) 1243.

Delannay E.F. Acidity and Infrared (IR) Spectroscopy. “Characterization of Heterogeneous”. Mareal Dekker Inc; New York, 1984. Chapter 8: The measurement of surface acidity.

Dermibas, A. Kinetics for non-isothermal flash pyrolysis of hazelnut shells. Bioresource Technology. 66 (1998) 247.

Demirbas, A. The influence of temperature on the yields of compounds existing in bio-oils obtained from biomass samples via pyrolysis. Fuel Processing Technology. 88 (2007) 591.

Dietz, W.A. Response factors for gas chromatographic analysis. Esso Research and Engineering Company, Analytical Research Division. Linden, New Jersey. 1968.

Elliot D.C. Hydrodeoxygenation of Phenolic Compounds of Wood-derived oil. Prepr. Pap. – Am. Chem. Soc., Div. Pet. Chem. 28 (1983) 667.

Elliott D.C., Baker E G. Upgrading Biomass Liquefaction Products through hydrodeoxygenation. Biotechnol. Bioeng. Symp. 14 (1984) 159.

Elliott D.C., Beckman D, Bridgewater AV. Developments in direct thermochemical liquefaction of biomass: 1983–1990. Energy & Fuels. 5 (1991) 399.

Elliott D.C., and Neuenschwander, G.G. Liquid Fuels by Low-Severity Hydrotreating of Biocrude. Bridgwater, A.V. and Boocock, D.G.B.; Eds. Developments in Thermochemical Biomass Conversion Vol. 1. Blackie Academic & Professional: London, 1996, 611.

Elliot D.C. Historical Developments in Hydroprocessing Bio-oils. Energy and Fuels. 21 (2007): 1792.

Emeis, C.A. Determination of integrated molar extinction coefficients for infrared absorption bands of pyridine absorbed on solid acid catalysts. J. Catal., 141 (1991) 347.

Euzen P., Raybaud P., Kroskidis X., Toulhaot H., le Laorer J.L., Jolivet J.P. and C. Fridefond in: F. Schuth, K. S. Sing, J. Weitkamp (eds), Handbook of Porous Solids, vol. 2, 2002.

Erica C. de O., Cleo T.G.V.M.T.P., and O.P. Heloise J. Braz. Chem. Soc. 17 (2006) 16.

Farag H., Whitehurst D.D. and Mochida I. Ind. Eng. Chem. Res. 37 (1998) 3533.

Fisher T., Hajaligol M., Waymack B. and D. Kellogg, Pyrolysis behaviour and kinetics of biomass derived materials, J. Anal. Appl. Pyolysis 62 (2002) 331.

Fisk C.A., Morgan T., Yaying J., Crocker M., Crofcheck C., Lewis S.A. Bio-oil upgrading over platinum catalysts using in situ generated hydrogen. Applied Catalysis A: General. 358 (2009) 150.

Ferdous D., Dalai A.K., and Adjaye J. Comparison of product selectivity during hydroprocessing of bitumen derived gas oil in the presence of NiMo/Al2O3 catalyst containing boron and phosphorus. Fuel. 85 (2006) 1286.

Fonseca A., Zeuthen P and Nagy J.B. ^{13}C NMR quantitative analysis of catalyst carbon deposits. Fuel. 75 (1996), 1363.

Furimsky E. and Massoth F.E. Deactivation of Hydrotreating catalysts. Catalysis Today. 52 (1999) 381.

Garcia-Perez M., Chaala A., Pakdel H., Kretschmer D., and Roy C. Characterization of bio-oils in chemical families. Biomass and Bioenergy. 31 (2007) 222.

Grainger, L. and J. Gibson, "Liquefaction of coal", in Coal Utilization, Technology« Economics and Policy, Kings English Book Printers, 211-218, (1981).

Grange P, Laurent E, Maggi R, Centeno A, and Delmon B. Hydrotreatment of pyrolysis oils from biomass: reactivity of the various categories of oxygenated compounds and preliminary techno-economical study. Catalysis Today. 29 (1996) 297.

Gregg S.J., Sing K.S.W. Adsorption, Surface Area and Porosity. London: New York: Academic Press, 1967.

Gregory, Alicia P. Green Energy. Odyssey. Univeristy of Kentucky. Date updated: Jan. 23, 2007. Date accessed: Jan. 10. 2011.

Guo X., Shen J.-P., Sun L., Song C., and Wang X. Shape-selective methylation of 4-methylbiphenyl to 4,4'-dimethylbiphenyl over zeolite HZSM-5 Modified with metal oxides of MgO, CaO, SrO, BaO, and ZnO. Catalysis Letters. 87 (2003) 1.

He R., Ye X.P., English B.C., and Satrio J.A. Influence of pyrolysis condition on switchgrass bio-oil yield and physiochemical properties. Bioresource Technology. 100 (2009) 5305.

Hilmen A.M., D. Schanke D., Hanssen K.F., and Holmen A.M.E. Dry, Catal. Lett. 7 (1990) 204.

Hubbard W., Scott D. and G. Waddington, In: F. Rossini (Eds.), Experimental thermochemistry, Interscience publ., 1956, Chapter 5.

Huber G.W., Iborra S., and Corma A. Synthesis of transportation fuels from biomass: chemistry, catalysts, and engineering. Chemical review. 106 (2006) 4044.

Imamura S., Nakai T., Kanai H., and Ito T. Titanium sties of titania-silica mixed oxides for epoxidation activity and Lewis acidity. Catalysis Letters. 28 (1994) 277.

Jones, Matthew R. " Biomass for Energy." *Biomass Handbook* Ed. Osamu Kitani and Carl W. Hall. New York : Gordon and Breach Science Publishers, 1989. 97-106

Junming X., Jianchun J., Yunjung S., and Yanju S. Bio-oil upgrading by means of ethyl ester production in reactive distillation to remove water and to improve storage and fuel characteristics. Biomass and Bioenergy. 32 (2008) 1056.

Kallury R.K.M.R. and Tidwell T.T. High temperature catalytic hydrogenolysis and alkylation of anisole and phenol. Canadian Journal of Chemistry. 62 (1984) 2540.

Kang C.C., Nongbri G., and Stewart N. "The effect of the solvent in the solvent refined coal process", in Liquids Fuels from Coal, Academic Press, 1-18, (1976).

Kobayashi S., Kushiyama S., Aizawa, R., Koinuma Y., Imoue K., Shimizu Y. and K. Egi. Kinetic study on the hydrotreating of heavy oil. 2. Effect of catalyst pore size. Ind. Eng. Chem. Res. 26 (1987) 2245.

Kumaran G.M., Garg S, Kumar M., Viswanatham, N, Gupta J.K., Sharma L.D. and Dhar G.M. Origin of hydrocracking functionality in β-zeolite supported tungsten catalysts. Energy and Fuels. 20 (2006) 2308.

Krishnamurthy S. and Shah Y.T. Interations between dibenzothiophene, 7, 8 benzoquinoline and oxygen compounds during heteroatom removal. Chemical Engineering Communications. 16 (1982) 109.

Laurent E. and Delmon B. Influence of oxygen-, nitrogen-, and sulfur-containing compounds on the hydrodeoxygenation of phenols over sulphided cobalt molybdenum/.gamma.-alumina and nickel-molybdenum/.gamma.-alumina catalysts Ind. Eng. Chem. Res. 32 (1993) 2516.

Laurent E. and Delmon B. Study of the hydrodeoxygenation of carbonyl, carboxylic and guaiacol groups over sulphided CoMo/γ-Al2O3 and NiMo/γ-Al2O3 catalysts: I. Catalytic reaction scheme. Applied Catalysis. 109 (1994a) 31.

Laurent E. and Delmon B., in: B. Delmon, G.F. Froment (Eds.), Catalyst Deactivation, Elsevier, Amsterdam, 1994b, p. 459.

Lazic Z. R., Design of experiments in chemical engineering, Wiley-VCH Verlag GmbH, Weinheim, 1st ed., 2004, Chapter 2.

Luengnaruemitchai A. and Kaengsilalai A. Activity of different zeolite-supported Ni catalysts for methane reforming with carbon dioxide. Chemical Engineering Journal. 144 (2008) 96.

Li J., Xu L., Keogh R.A., and Davis B.H., ACS Div. Petr. Chem.Preprints 45 (2000) 253.

Lipsch J.M.J.G. and Schuit G.C.A. The CoO---MoO3---Al2O3 catalyst : III. Catalytic properties. Journal of Catalysis. 15 (1969) 179.

Lopez Juste G. and Salva Monfort JJ. Preliminary test on combustion of wood derived fast pyrolysis oils in a gas turbine combustor. *Biomass and Bioenergy* 19 (2000) 119.

Mahfud F.H. Exploratory Studies on Fast Pyrolysis Oil Upgrading. RIJKSUNIVERSITEIT GRONINGEN. 1975

Masalska A. Ni-loaded catalyst containing ZSM-5 zeolite for toluene hydrogenation. *Applied Catalysis A: General.* 294 (2005) 260.

Mauchausse C., Kural E., Trimm D.L., Cant N,W. Optimization of tungsten-based catalysts for the hydrotreatment of coal-derived liquids. Fuel. 71 (1992) 203

Meshitsuka G. and Isogai A. Chemical structures of cellulose, hemicellulose and lignin, (Eds.), D.N. Hon. Chemical modification of lignocellulosic materials, Marcel Dekker Inc., New York, 1996, pp. 11-34.

Michio I., Maria S., and Ed H. Emulsification of pyrolysis derived bio-oil in diesel fuel. Biomass and Bioenergy. 24 (2003) 221.

Mohan, Dinesh. Pyrolysis of Wood/Biomass: A Critical Review. Energy & Fuels. 20 (2006) 848.

Myers T.E., Le F.S., Myers B.L., Fleisch T.H. and Zajac G.E., AIChE Symposium Series. 85 (1989) 32.

Oasmaa A. and Czernik S. Fuel oil quality of biomass pyrolysis oils-state of the art for the end-users. Energy Fuels. 13 (1991) 914.

Oasmaa, A. Fuel Oil Quality Properties of Wood Based Pyrolysis Liquids. PhD thesis, University of Jyväskylä, Finland 2003a.

Oasmaa, A., Kuoppala, E., and Solantausta, Y. Fast Pyrolysis of Forestry Residue. 2. Physicochemical Composition of Product Liquid. Energ. Fuel. 17 (2003b) 433.

Okado H., Sano T., Suzuki K., Okabe K., and Takaya H. The long-term testing of ZSM-5-type zeolite containing strontium for the high-temperature conversion of methanol to olefin. Bull. Chem. Soc. Jpn. 61 (1988) 3383.

Onay O. Influence of pyrolysis temperature and heating rate on the production of bio-oil and char from safflower seed by pyrolysis, using a well-swept fixed-bed reaction. Fuel Processing Technology. 88 (2007) 523.

Raveendran K., Ganesh A., and Khilar K.C. Pyrolysis characteristics of biomass and biomass components, Fuel 75 (1996) 987.

Renaud M., Chantal P.D., and Kaliaguine S. Anisole production by alkylation of phenol over ZSM-5. Can. J. Chem. Eng. 64 (1986) 787.

Rout P.K., Naik M.K., Naik S.M., Goud V.V., Das L.M., and Dalai A.K. Supercritical CO_2 Fractionation of Bio-oil Produced from Mixed Biomass of Wheat and Wood Sawdust. Energy & Fuels. 23 (2009) 6181.

Roy A.H., Broudy R.R., Auerbach S.M., Vining W J. Teaching materials that matter: An interactive, multi-media module on zeolites in general chemistry. The Chemical Educator. 4 (1999) 1.

Saidina Amin N.A. and D.D. Anggoro. Optimization of direct conversion of methane to liquid fuels over Cu loaded W/ZSM-5 catalyst. Fuel. 83 (2004) 487.

Sanderson M.A., Agblevor F., Collins M., and Johnson D.K. Compositional analysis of biomass feedstocks by near infrared reflectance spectroscopy. Biomass and Bioenergy. 11 (1996) 365.

Satterfield C.N. Heterogeneous Catalysis in Industrial Practice. ; McGraw-Hill. 1991.

Satterfield C.N., Smith C.M., Ingails M. , Industrial and Engineering Chemistry Process Design and Development. 24 (1985) 1000.

Schanke D., Hilmen A.M., Bergene E., Kinnari K., and Rytter E. Applied Catalysis. 186 (1999) 169.

Scholze B. and Meier D. Characterization of the water-insoluble fraction for pyrolysis oil (pyrolytic lignin) Part I. PY-GC/MS, FTIR and functional groups. *J Anal Appl Pyrol*, 60 (2001) 4.

Scott D.S., Piskorz J., and Radlein D. Liquid products from the continuous flash pyrolysis of biomass. Ind. Eng. Chem. Proc. Des. Dev. 24 (1985) 581.

Senol O.I., Ryymin E.-M., Viljava T.-R., and Krause A.O.I. Effect of hydrogen sulfide on the hydrodeoxygenation of aromatic and aliphatic oxygenates on sulphided catalysts. Journal of Molecular catalysis A: Chemica.l 277 (2007) 107.

Sensoz S. and Angin D. Pyrolysis of safflower seed press cake in a fixed bed reactor: Part 2. Structural characterization of pyrolysis bio-oils. *Bioresource Technology*. 99 (2008) 5498.

Sharma R.K. and Bakhshi N.N. Upgrading of wood-derived pyrolytic oils over HZSM-5. Biores. Tech. 35 (1991) 57.

Sheu, Y.-H.E. and Anthony R.G. Kinetic Studies of Upgrading Pine Pyrolytic Oil by Hydrotreatment. Fuel and Processing Technology, 19 (1988) 31.

Soltes E.J., Lin S-C.K., and Sheu Y-H.E. Catalyst specificities in high pressure hydroprocessing of pyrolysis and gasification tars. Amer. Chem. Soc., Div. Fuel Chem., Prepts. 32 (1987) 229.

Sundaramurthy V., Dalai A.K., and Adjaye J. Effect of phosphorus addition on the hydrotreating activity of NiMo/Al2O3 carbide catalyst. Catalysis Today. 125 (2007) 239.

Su-Ping Z., Yong-Jie Y., Zhengwei R., and Tingchen L. Study of hydrodeoxygenation of bio-oil from the fast pyrolysis of biomass. Energy Sources. 25 (2003) 57.

Topsoe H. and Clausen B.S., *Catal. Rev.-Sci. Eng.* 22 (1981) 401.

Vichi S., Santini C., Natali N., Claudio R., Lopez-Tamames E., and Buxaderas S. Volatile and semivolatile components of oak wood chips analyzed by accelerated solvent extraction (ASE) coupled to gas chromatography-mass spectrometry (GC-MS). Food Chem. 102 (2007) 1260-1269.

Villanueva Lopez, I. Proyecto de Prepacion y caracterizacion de catalizadores bifuncionales de hydrocraqueo. Final career project report. 2007.

Vogelzang M.W., Lee C.-L. , Schuit G.C.A., Gates B.C. , Petrakis L. Hydrodeoxygenation of 1-naphthol: Activities and stabilities of molybdenum and related catalysts. Journal of Catalysis. 84 (1983) 170

Weiksner J.M., Crump S.L., and White T.L. Understanding Biodiesel Fuel Quality and Performance. Contract No. DE-AC09-96SR18500, 2005.

Wildschut, J. Pyrolysis Oil Upgrading to Transportation Fuels by Catalytic Hydrotreatment. University of Groningen. 2009.

Yang Y., Quan C.T.T. and Smith K.J. Influence of MoS2 catalyst morphology on the hydrodeoxygenation of phenols. Catalyst communications. 9 (2008) 1364.

Ye X.P., Lui L., Hayes D., Womac A., Hong K., Sokjansanj S. Fast classification and compositional analysis of cornstover fractions using Fourier transform near-infrared techniques. *Bioresource Technology*. 99 (2008) 7323.

Zhang L.H., Dong L., Wang L-J., Wang T-P., Zhang L., Chen X-D., Mao Z-H. Effect of steam-explosion on biodegradation of lignin in wheat straw, Bioresour.Tech. 99 (2008) 8512.

Zhang S.P, Yan Yongjie, and Li T. Upgrading fuel from the pyrolysis of biomass. Bioresource Technology. 96 (2005) 545.

Zhang Q., Chang J., Wang J., Wang T., and Xu J. Review of biomass pyrolysis oil properties and upgrading research. Energy and Conservation Management. 48 (2007) 87

Appendix A: Structures of Relevant Chemical Compounds

Many chemical compounds were discussed in the present thesis. This appendix attempts to present the chemical structure of these relevant compounds.

Biomass consists of three main constituents; cellulose, hemicellulose, and lignin. Figure A1-3 displays these chemical compounds.

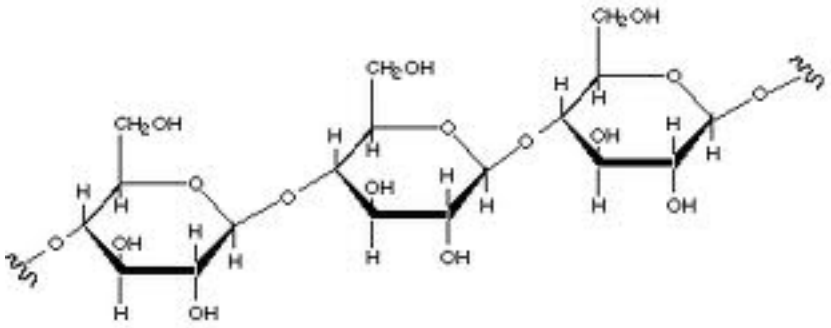

Figure A1: Chemical Structure of monomers that compose cellulose chain (Elliot, 2007)

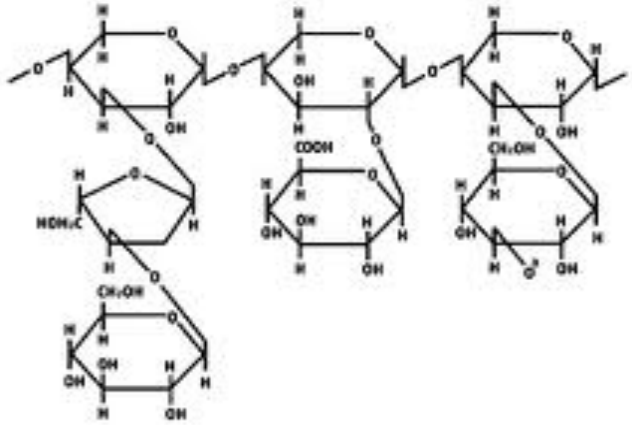

Figure A2: Chemical Structure of monomers that compose hemicellulose (Elliot, 2007)

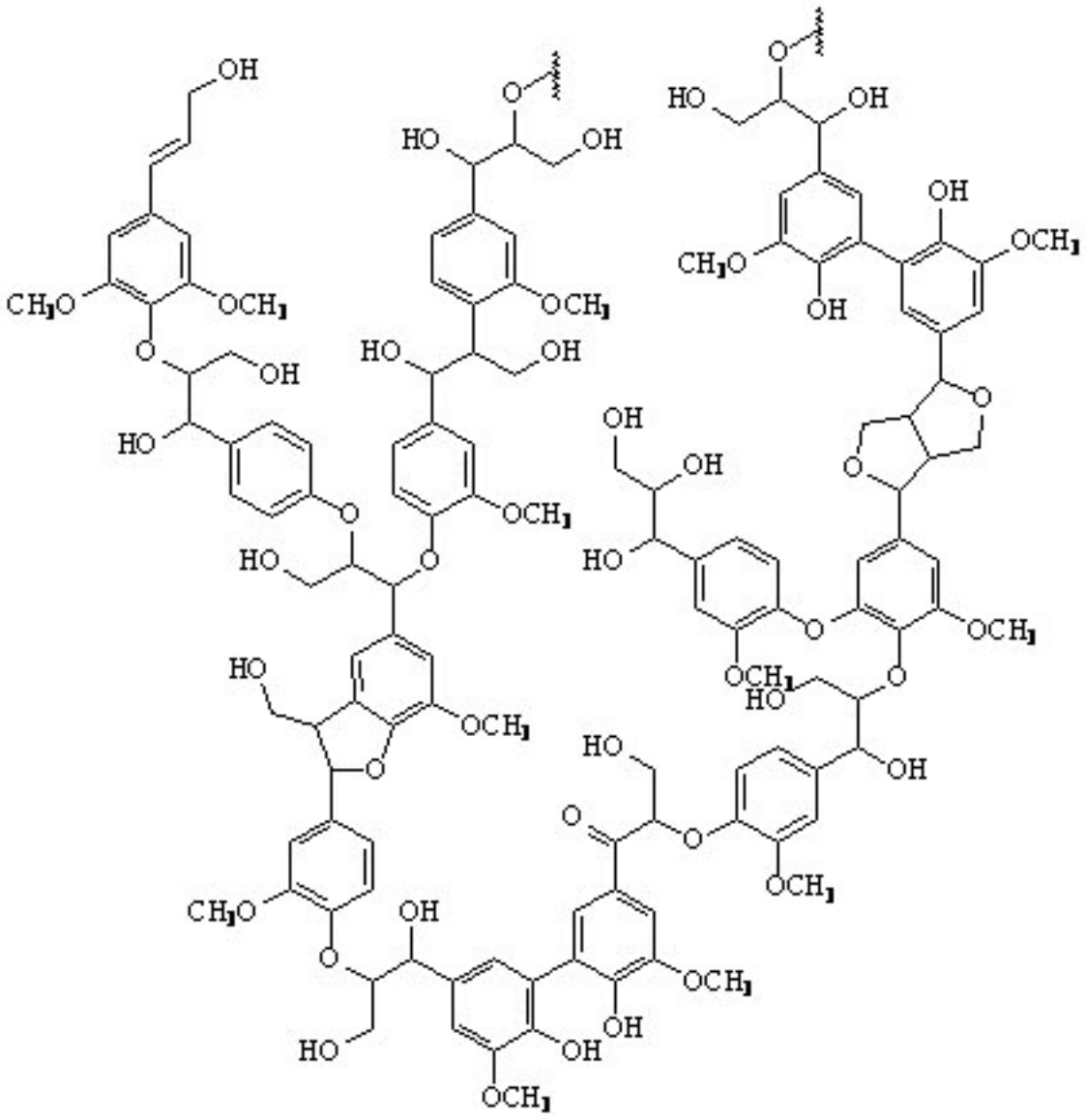

Figure A3: Chemical structure of lignin [Gregory, 2007]

The composition of bio-oil can vary significantly depending on the biomass pyrolyzed as well as the pyrolysis conditions. However, bio-oil composition can be generally classified as containing acids, ketones, aldehydes, furans, phenols, benzenoids and other miscellaneous acids. Examples found of these identified in the bio-oil studied can be view in Figure A4-17

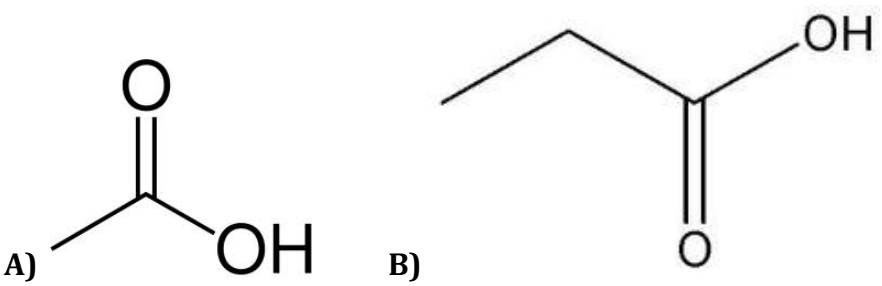

Figure A4: Chemical structure of acids present in bio-oil derived from maple sawdust A) Acetic acid and B) Propanoic acid

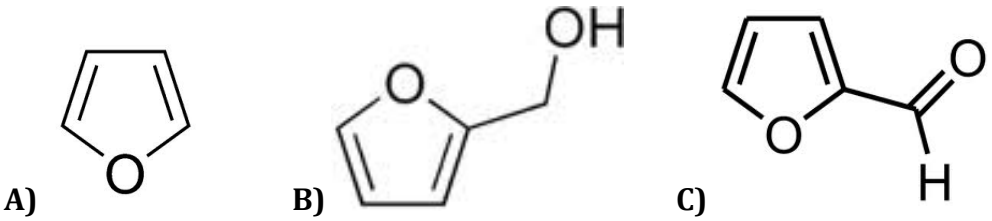

Figure A5: Chemical structure of furans present in bio-oil derived from maple sawdust. A) Furan, B) Furfurol (furfuralcohol), and C) Furfural (furfuraldehyde)

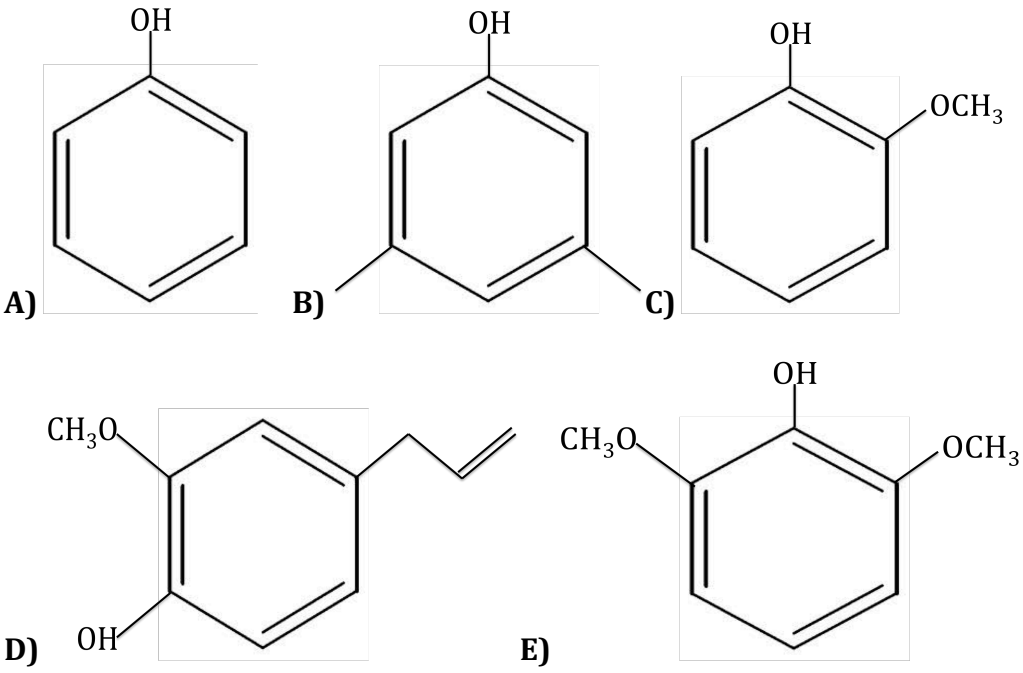

Figure A6: Chemical structure of phenolic compounds present in bio-oil derived from maple sawdust. A) Phenol, B) Dimethyl phenol, C) Guaiacol, D) Eugenol, and E) Syringol

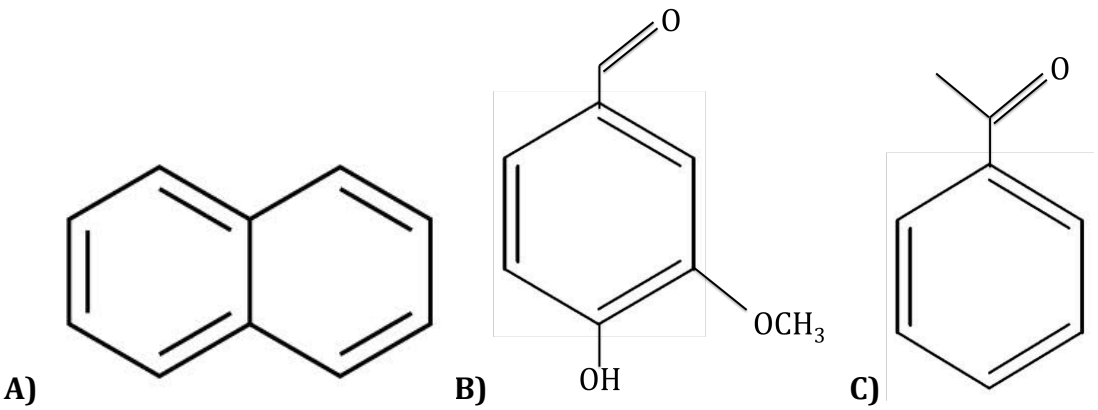

Figure A7: Chemical structure of benzenoids present in bio-oil derived from maple sawdust. A) Naphthalene, B) Vanillin, and C) Benzaldehyde

Aside from chemicals commonly found in bio-oil, there were two other chemicals often discussed in the present dissertation, the organic solvents used for water removal and hydrogen donation. The chemical structures for chloroform and tetralin are shown in Figure A8.

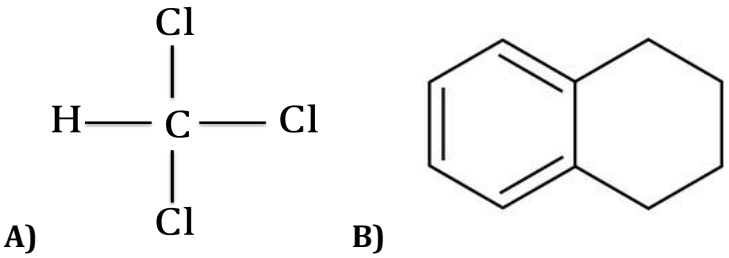

Figure A8: Chemical structure of organic solvents used for water removal and hydrogen donation A) Chloroform and B) Tetralin

Appendix B: Sample Calculations

$$\text{Hydrocarbon Yield (\%)} = \frac{\text{\% Hydrocarbon formed during reaction}}{\text{\% of biooil in feed}} \times 100\%$$

$$\text{Oxygen Removal (\%)} = 1 - \frac{\text{\% oxygen in product}}{\text{\% oxygen in feed}} \times 100\%$$

Appendix C: GC Chromatograms from screening reactions and original bio-oil

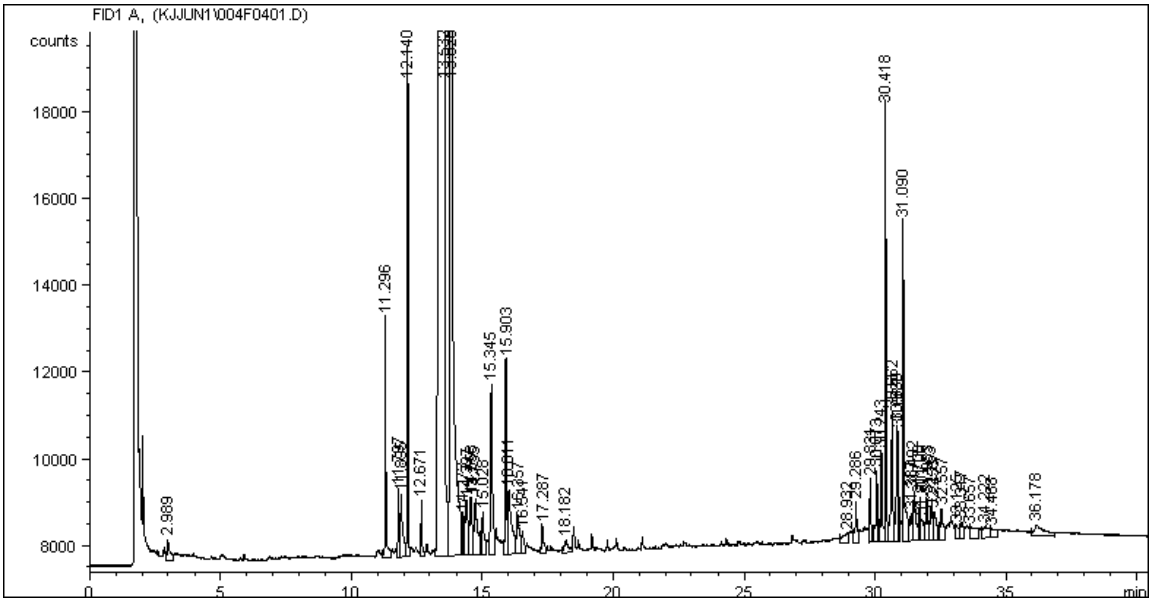

Figure C1: GC-FID chromatogram of products obtained the screening of 8%Mo/ZSM-5 at 7wt% catalyst loading, T=330°C, P=3 MPa, rpm=500 and a reaction time of 45 min.

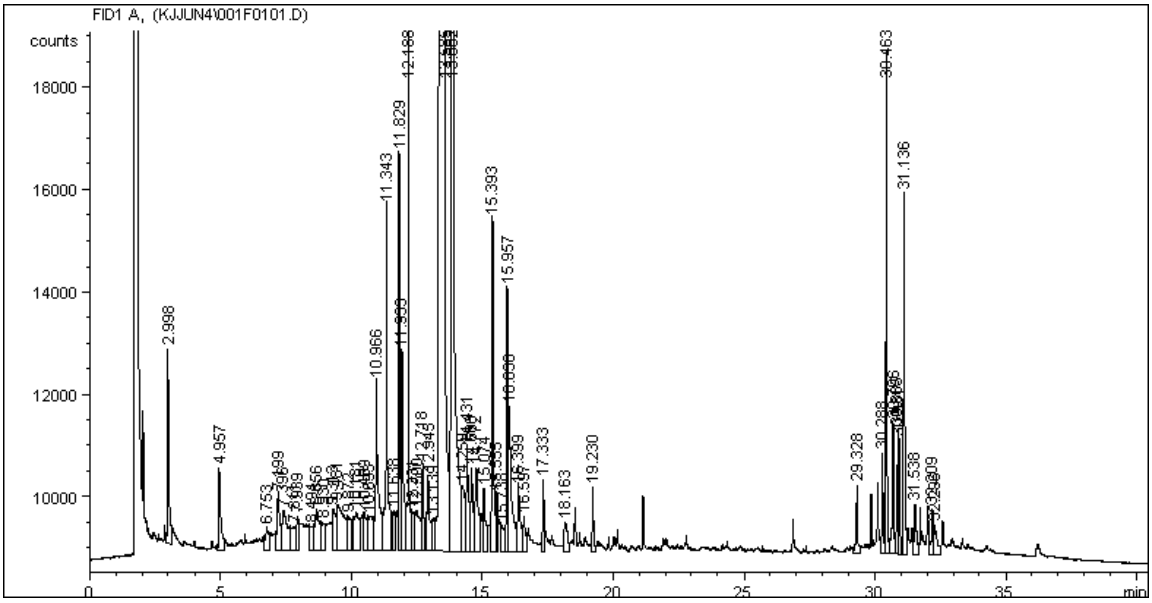

Figure C2: GC-FID chromatogram of products obtained the screening of 13%Mo/ZSM-5 at 7wt% catalyst loading, T=330°C, P=3 MPa, rpm=500 and a reaction time of 45 min.

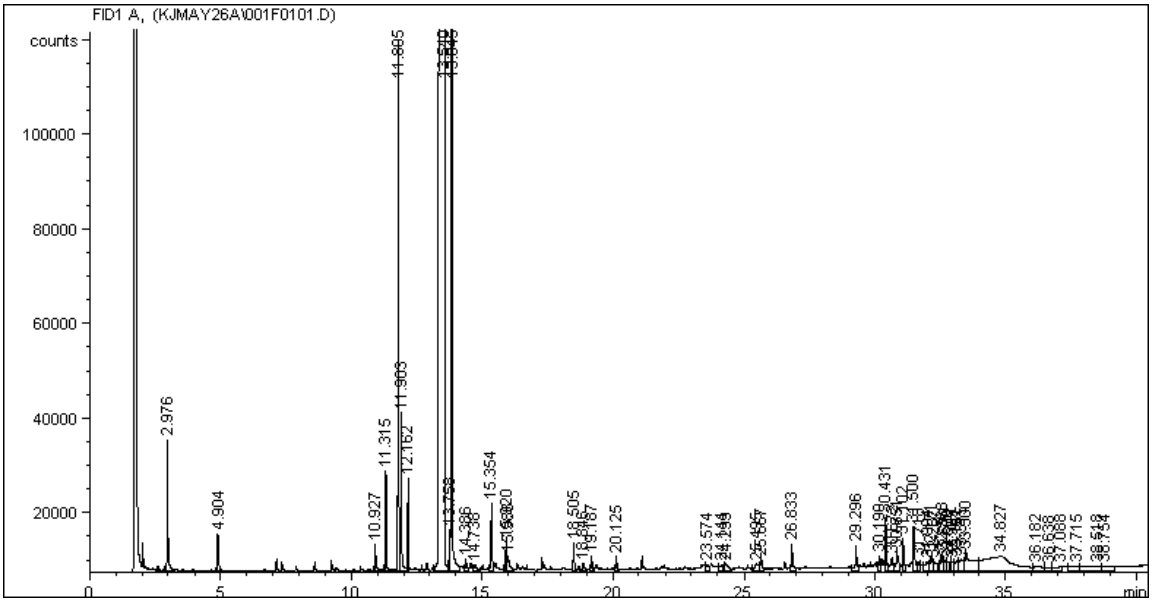

Figure C3: GC-FID chromatogram of products obtained the screening of 2.5%Ni/ZSM-5 at 7wt% catalyst loading, T=330°C, P=3 MPa, rpm=500 and a reaction time of 45 min.

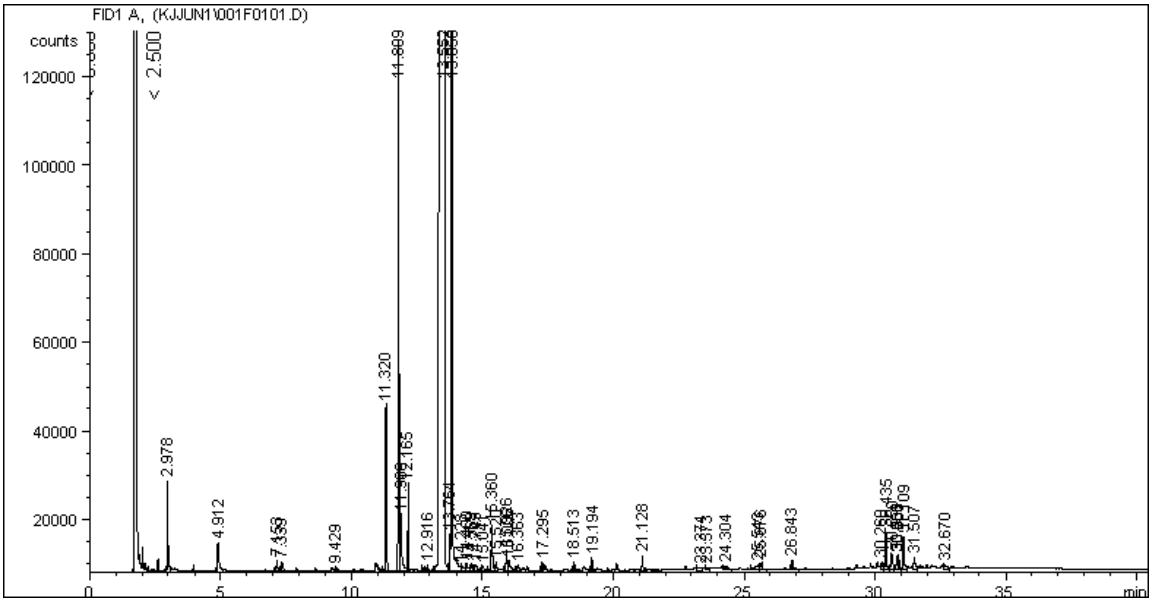

Figure C4: GC-FID chromatogram of products obtained the screening of 5%Ni/ZSM-5 at 7wt% catalyst loading, T=330°C, P=3 MPa, rpm=500 and a reaction time of 45 min.

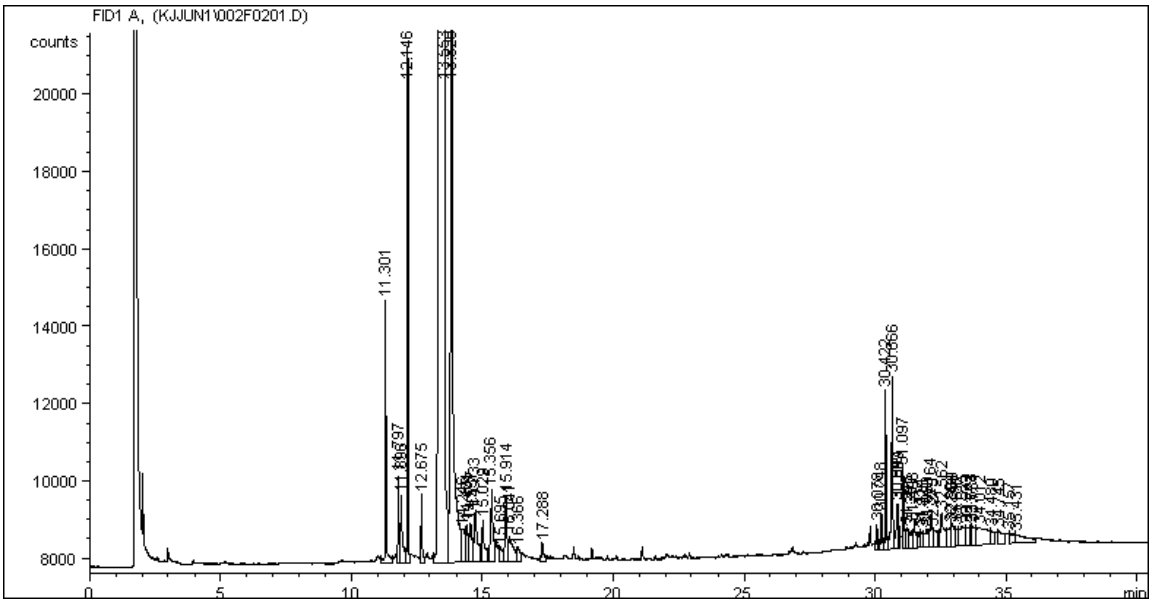

Figure C5: GC-FID chromatogram of products obtained the screening of 2.5%Sr/ZSM-5 at 7wt% catalyst loading, T=330°C, P=3 MPa, rpm=500 and a reaction time of 45 min.

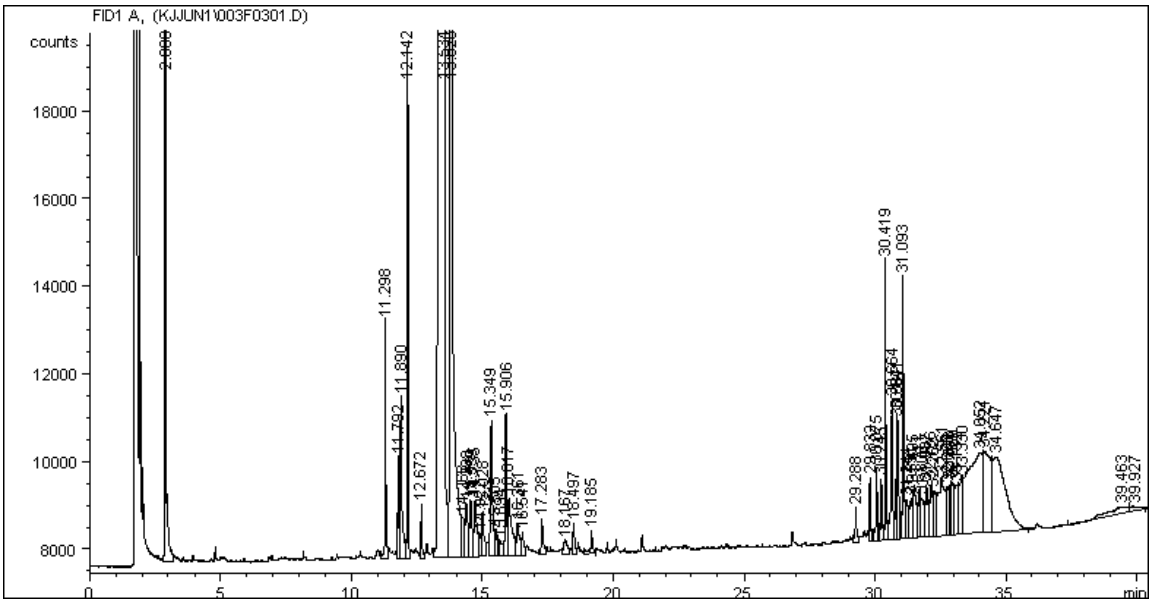

Figure C6: GC-FID chromatogram of products obtained the screening of 5%Sr/ZSM-5 at 7wt% catalyst loading, T=330°C, P=3 MPa, rpm=500 and a reaction time of 45 min.

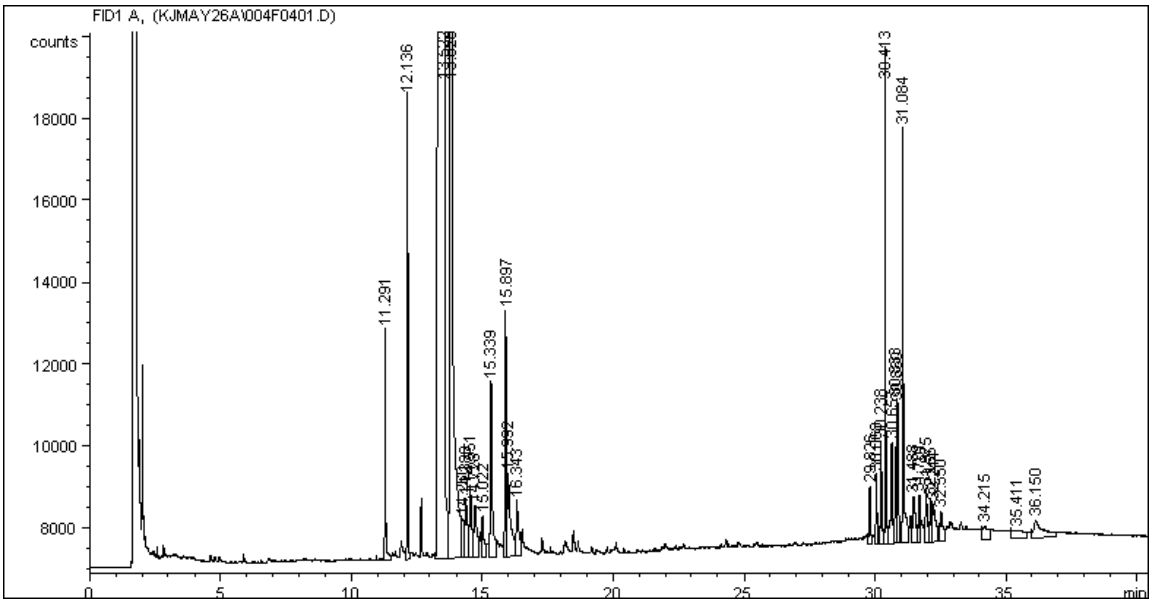

Figure C7: GC-FID chromatogram of products obtained the screening of 5%W/ZSM-5 at 7wt% catalyst loading, T=330°C, P=3 MPa, rpm=500 and a reaction time of 45 min.

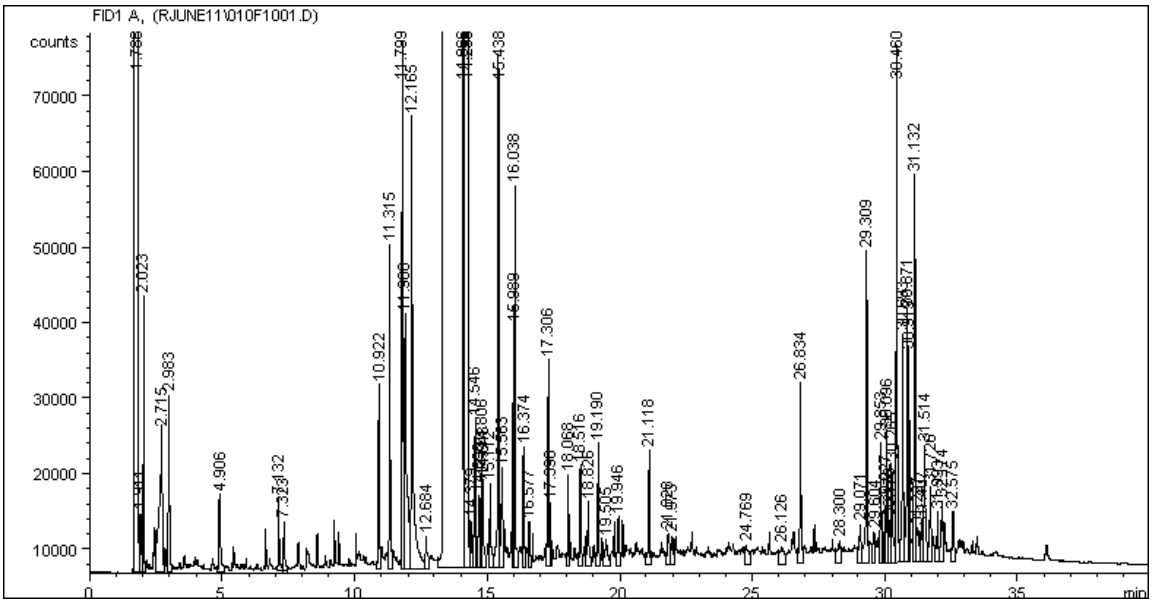

Figure C8: GC-FID chromatogram of products obtained the screening of 10%W/ZSM-5 at 7wt% catalyst loading, T=330°C, P=3 MPa, rpm=500 and a reaction time of 45 min.

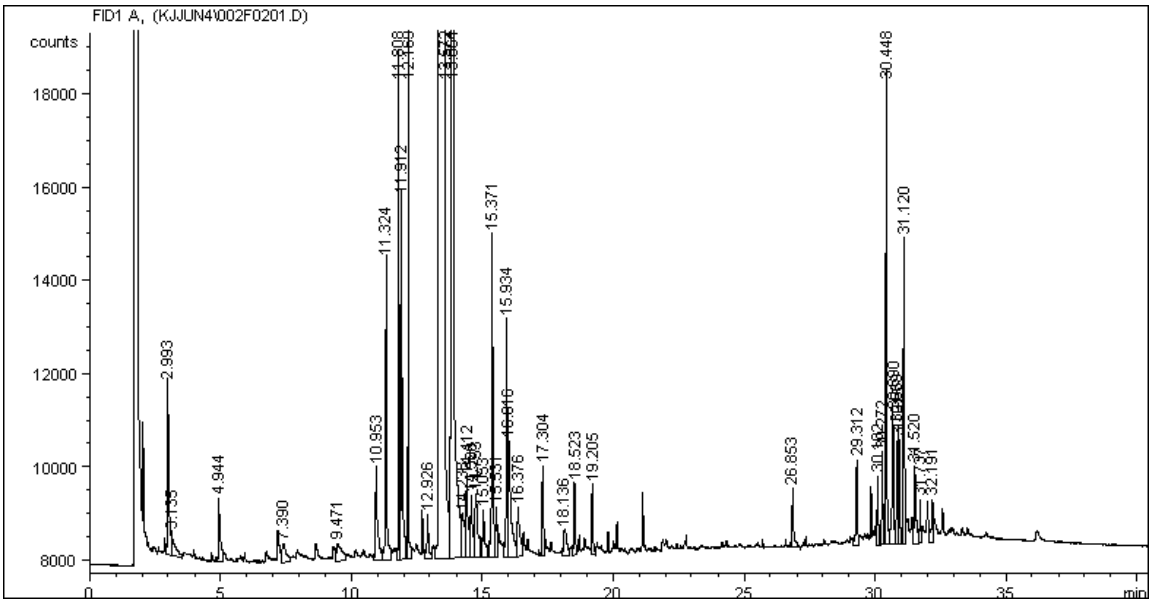

Figure C9: GC-FID chromatogram of products obtained the screening of CoMo/ZSM-5 at 7wt% catalyst loading, T=330°C, P=3 MPa, rpm=500 and a reaction time of 45 min.

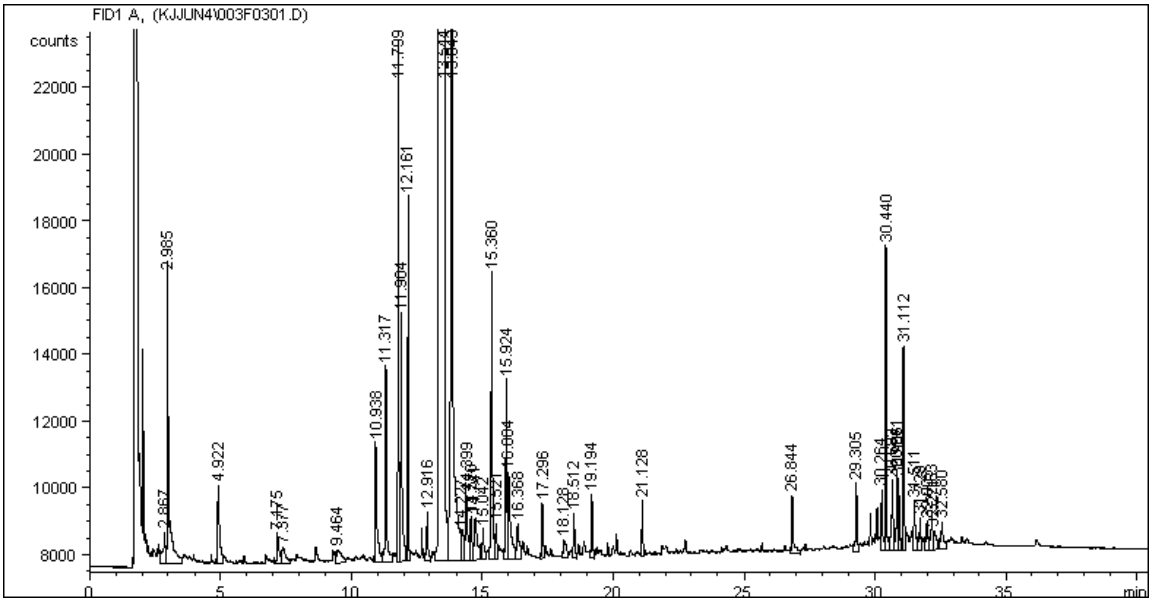

Figure C10: GC-FID chromatogram of products obtained the screening of NiMo/ZSM-5 at 7wt% catalyst loading, T=330°C, P=3 MPa, rpm=500 and a reaction time of 45 min.

Appendix D: Contributions from thesis work

Publications

F. Berruti, J. Berthorsen, C. Briens, A. K. Dalai, D. Levin, A. Ragauskas, and K. Jacobson, Marie-Rose S., Lavoie J-M, J. Chaouki, R. Azargohar and Bassem Hallac. Lignocellulose Conversion, Combustion and Utilization for Biofuel Production. (In progress)

Kathlene Jacobson and Ajay K. Dalai. Catalytic upgrading bio-oil from pyrolysis of biomass: A review. (In progress)

Kathlene Jacobson and Ajay K. Dalai. Valorization of bio-oil from Maple Sawdust. Canadian Journal of Chemical Engineering. Under Review.

Satyanarayan Naik, Vaibhav V. Goud, Prasant K. Rout, Kathlene Jacobson, Ajay K. Dalai. Characterization of Canadian biomass for alternative renewable biofuel. Renewable Energy. 35 (2010) 1624-1631.

Refereed Conference Presentations/Posters

Kathlene Jacobson and Ajay K. Dalai. Hydrotreatment of bio-oil to obtain transportation fuels. Poster and oral presentation at the Bioenergy III Conference: Present and new perspectives on biorefineries. Lanzorote, Canary Islands, Spain. May 22-27, 2011.

Kathlene Jacobson, Ramin Azargohar, and Ajay K. Dalai. Transportation fuels and value-added chemicals from maple sawdust bio-oil. Poster presentation at the ABIN 2011 Conference in London, Ontario. Jan 9-11, 2011.

Kathlene Jacobson and Ajay K. Dalai. Valorization of bio-oil from maple sawdust. Oral Presentation at the CSChE 2010 Conference in Saskatoon, SK

Kathlene Jacobson, Majak Mapiour, Ramin Azargohar, and Ajay K. Dalai. 2nd generation fuels from waste biomass. Poster presentation at the AUTO21 2010 Conference in Windsor, Ontario.

Awards

First place in Auto21's annual poster competition, 2010.